SECTION

COUCHES LIMITES TURBULENTES

TURBULENT BOUNDARY LAYERS

Présidents : Professeur H. W. LIEPMANN, Professeur H. SCHLICHTING

INCOMPRESSIBLE TURBULENT BOUNDARY LAYERS

Ing. J. C. ROTTA
Aerodynamische Versuchsanstalt Göttingen

SOMMAIRE

Une brève vue d'ensemble des connaissances actuelles sur les couches limites turbulentes en écoulement incompressible bidimensionnel est donnée. En particulier, l'attention est portée vers les différents comportements de l'écoulement près de la paroi et dans la partie externe de la couche. L'utilité de la conception d'une couche à deux régions est examinée et le problème de la prédétermination de la couche limite turbulente dans un champ de pression arbitraire est discuté.

SUMMARY

A brief outline of the present knowledge of turbulent boundary layers in twodimensional incompressible flow is given. In particular, the attention is directed towards the different behaviour of the flow near the wall and in the outer part of the layer. The applicability of the two-layer conception is reviewed and the problem to predict the development of the turbulent boundary layer in an arbitrarily given pressure field is discussed.

Contents :

1. Introduction.
2. The two-layer conception.
3. Boundary layer on a flat plate.
4. Equilibrium boundary layers.
5. Boundary layers in arbitrary pressure distribution.
6. Non-separating boundary layers in very severe pressure gradients.
7. Concluding remarks.
8. References.

1. Introduction

One field, in which the knowledge about turbulent flow is most urgently needed, is the turbulent boundary layer. There is certainly no other type of turbulent flow than the boundary layer, which encounters in so many engineering problems and is subjected to such a great variety of conditions. A vast number of experimental and theoretical investigations on this subject has been published. Nevertheless, the basic problem of the turbulent boundary layer in an incompressible fluid is still far from being solved. In

the course of time the range of interest in boundary layers has immensely increased. Modern developments in engineering sciences have raised many new questions, for instance what happens to the turbulent boundary layer, when at high speeds the friction causes heavy temperature variations, when fluid is removed or injected through the surface, and when many other changes are imposed on the boundary layer.

My paper confines itself to a rather small part of the wide field of turbulent boundary layer problems. It deals with the turbulent boundary layer in a steady, incompressible, two-dimensional flow on plane, impermeable walls. There is no doubt but the treatment of any more complex case profits from the knowledge, which is available for the simple case.

Although further attempts which could promote the understanding of the flow phenomena are still highly important, relatively little fundamental research work, which is within the scope of my presentation has actually been published recently. Thus I am not in a position to offer basically new ideas to the problem. The purpose of my paper is rather to recall some essential aspects and thus to provide a basis for the subsequent discussion. Since our final goal is to be able to predict the characteristics of the boundary layer, which develops in a given environment, I will refer to some conceptions which have proved useful in this respect and point out, where gaps in our knowledge prevent further refinements of the existing calculation methods.

Before beginning with the real subject I will give an illustration of the turbulent boundary layer. *Fig. 1* represents a spark shadow graph of a turbulent boundary layer on a hollow circular cylinder in supersonic flow taken at NASA Ames Research Center. This pictures shows clearly the irregular but distinct boundary between fluid in turbulent motion inside the boundary layer and non-turbulent fluid outside the layer. This sharp outline of the turbulent part is a feature which the turbulent boundary layer has in common with the turbulent wake and jet flow, and which has already been discussed by Profs. LIEPMANN and COLES during the session on free turbulence.

2. The two-layer conception

While the early experimental investigations had been confined to the measurement of mean velocity distributions, later using the hot wire technique and the necessary electrical equipment, the research has been extended to measure diverse statistical quantities, like velocity fluctuations, velocity derivative fluctuations, several mean values of velocity fluctuation products, frequency spectra, and space and time correlation functions etc. These efforts have very much promoted the understanding of the mechanics of the turbulent boundary layer. Many relations, which earlier have been suspected only, have been confirmed later by more detailed measurements and could finally be supported by a sound physical picture.

Very extensive and careful measurements of space time correlation functions of the velocity fluctuations in a boundary layer on a flat plate have been made by Prof. FAVRE et. al. [1, 2] here in Marseille. As a starting point of the subsequent representation I will show two diagrams from these measurements. *Fig. 2* gives longitudinal space-time correlations. The first curve is the so called auto-correlation function, which defines the mean product of velocity fluctuation components, observed at the same position of

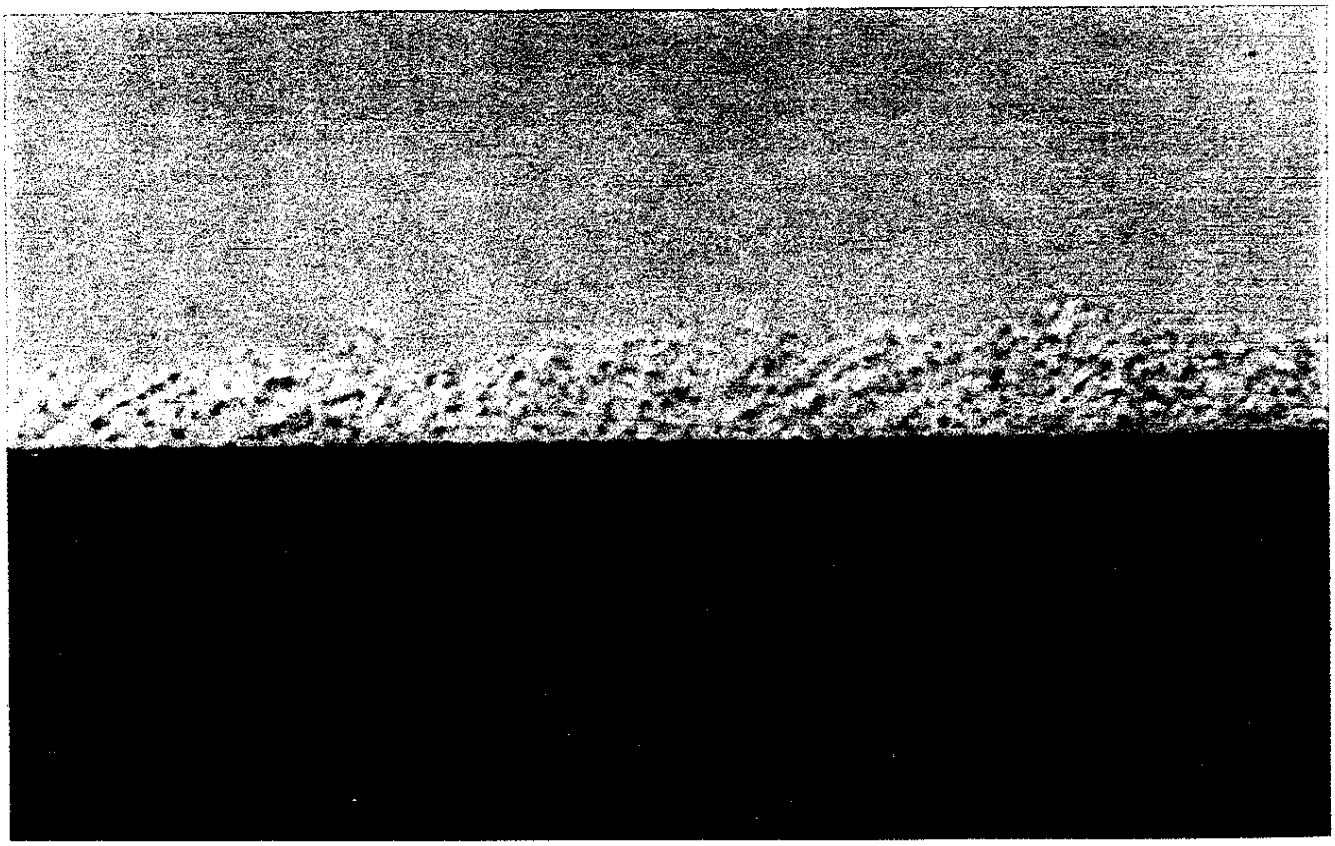

Fig. 1. — Shadowgraph of a turbulent boundary layer on a hollow circular cylinder at Mach number 3. 1. Direction of flow from left to right. (Courtesy of NASA Ames Research Center).

space at different times. The other curves represent the time correlation function for the velocity fluctuation components at two different points at distance r_x. The longitudinal space time correlation functions shown in *Fig. 2* give some information on the

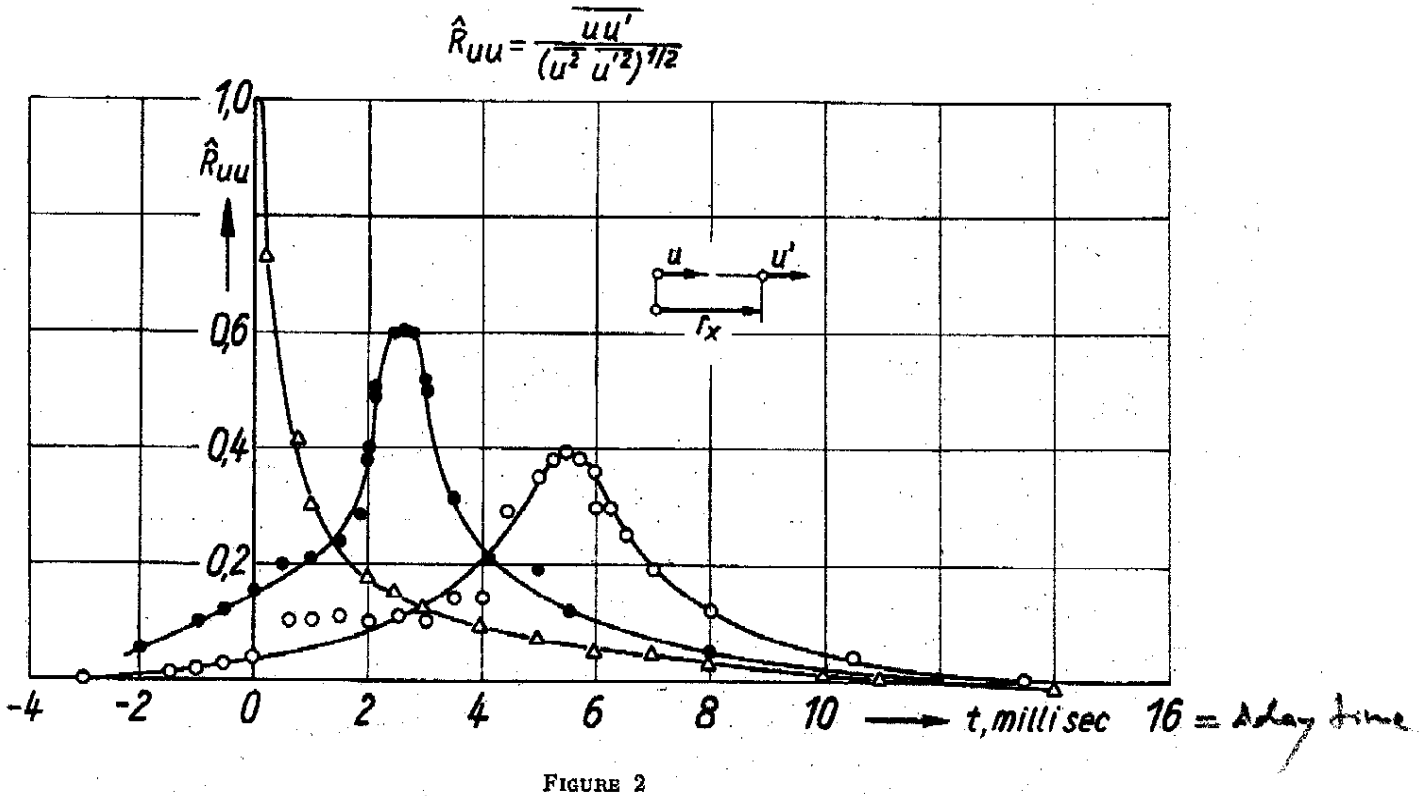

FIGURE 2

Longitudinal space-time correlations in the boundary layer on a flat plate after FAVRE, GAVIGLIO, DUMAS [1], $y/\delta = 0.24$,
$U_\infty = 12.0$ m/sec, $\delta = 16.8$ mm, $r_y \sim 0$, $r_z = 0$.

△	$r_x = 0$	
•	$r_x = 25.4$ mm	$\frac{r_x}{t_m U_\infty} = 0.81$
○	$r_x = 50.8$ mm	$= 0.79$.

life history of the eddies. Each correlation curve has a maximum at a delay time t_m, which increases at a rate proportional to the distance r_x. The ratio $\frac{r_x}{t_m\, U_\infty} \sim 0.8$ indicates that the eddies travel in the flow direction with a velocity of about $0.8\, U_\infty$. It is generally taken for granted that any individual eddy has a limitted duration of life. This is shown by a decrease of the maximum value of the correlation as r_x grows. The envelope of the curves gives the correlation for optimum delay time t_m. When r_x is given, the space-time correlation $R_{uu}(r_x, r_y, 0, t_m)$ with optimum delay t_m reaches a maximum maximorum for one value of r_y. Corresponding values of r_x and r_y form a line of maximum correlation with optimum delay. The corresponding correlation functions are presented in *Fig. 3* for three different distances from the wall. As seen from these Figs., the correlation coefficient with optimum delay time retains high values for consi-

derable distances $\frac{r_x}{\delta}$ along the mean flow upstream and downstream. On the average, the passage of a large eddy can be identified over a distance about one order of magnitude larger than the boundary layer thickness.

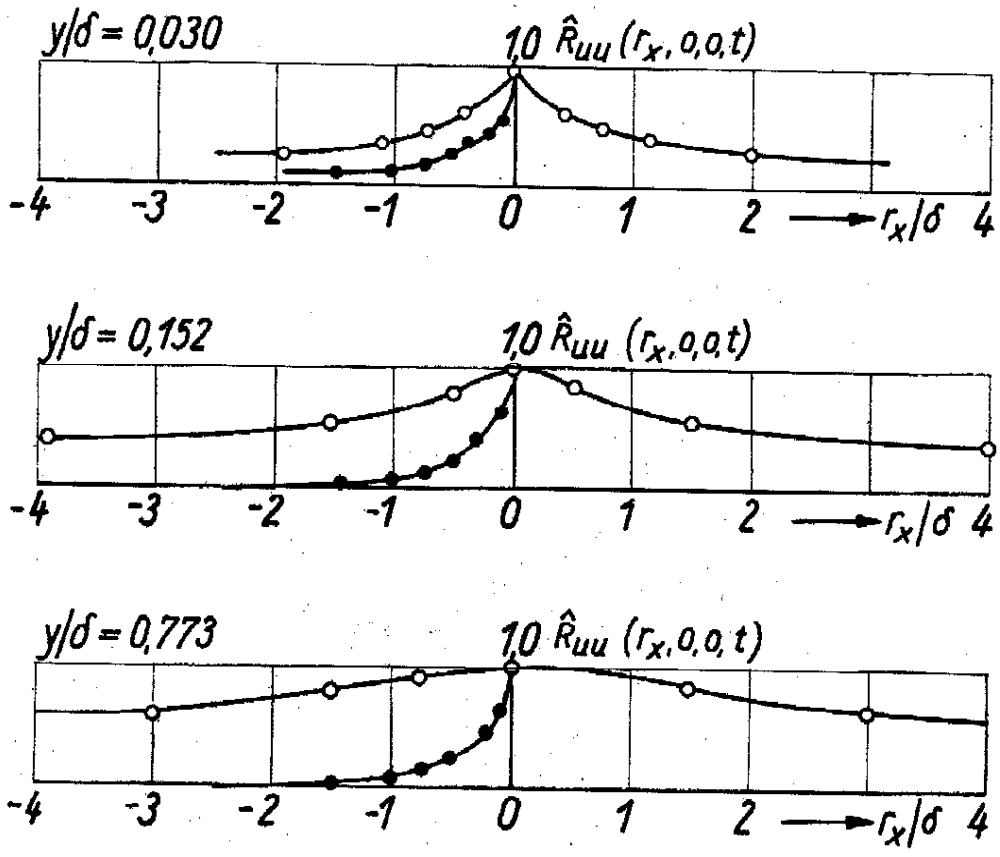

FIGURE 3

Space-time correlations in the boundary layer on a flat plate ($r_z = 0$) after FAVRE, GAVIGLIO, DUMAS [2].

○ Along the line of maximum correlation with optimum delay t_m for given r_x.

• Along a mean stream line with zero delay.

A most remarkable feature of this figure is the increase of extension of the maximum correlation function with distance from the wall, which indicates that the eddies nearer to the wall have a shorter average duration of life than the eddies further away from the wall.

One conception which has widely found application in turbulent boundary layer theory is the so called two-layer concept. It is based on the notion that the flow in the layer near the wall is ruled by local parameters only, like wall shear stress, distance from the wall, and local surface conditions (roughness) and, of course, the fluid properties (density and viscosity), whereas the flow is affected to a great extent by the upstream conditions at greater distance from the wall. This idea is physically supported by the shorter life duration of the eddies near the wall, as shown by the aforementioned sample of correlation function.

Another striking illustration for the different behaviour of turbulent flow near the solid wall and at greater distances is provided by an older experiment, made by W. JACOBS [3] at Göttingen in 1938. Here turbulent flow in a rectangular channel passes from a rough surface to a smooth one and vice versa. *Fig. 4* shows the shearing

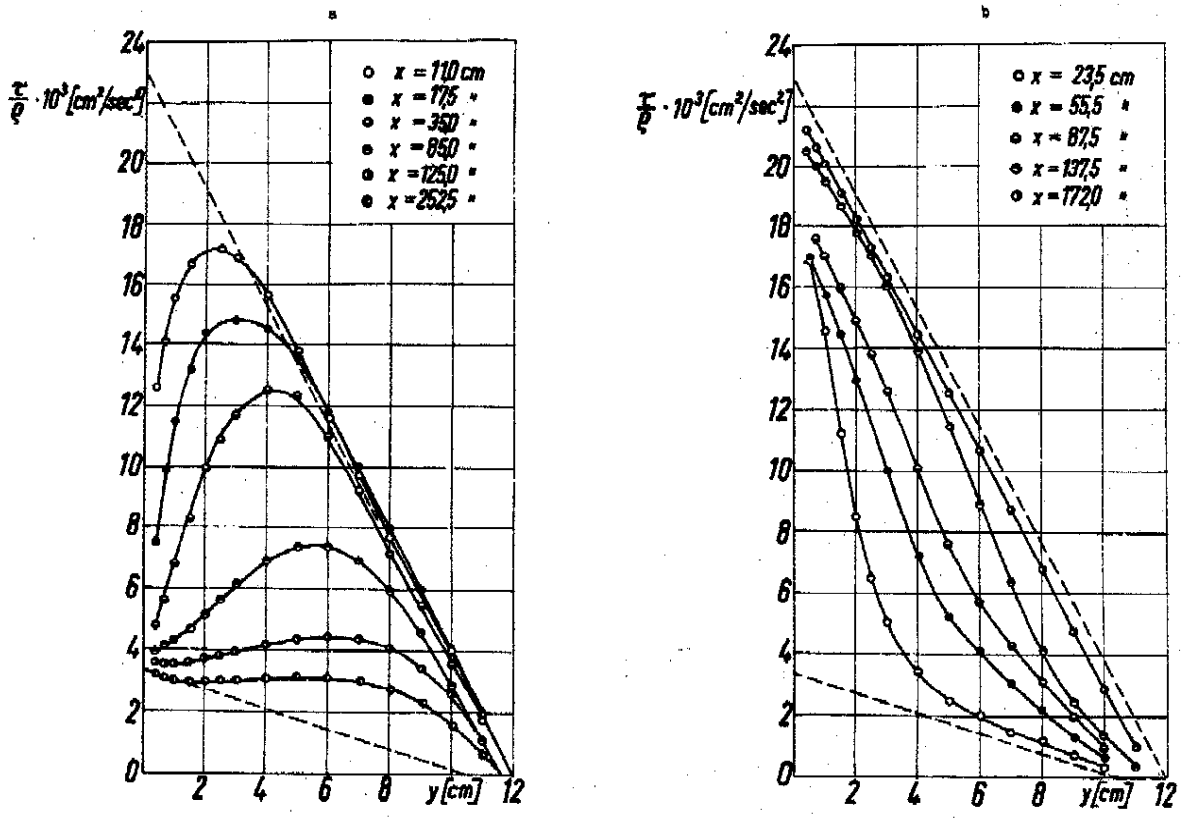

FIGURE 4

Variation of the shearing stress distribution in turbulent flow through a rectangular channel, after W. JACOBS [3].

a. passing from rough to smooth surface
b. passing from smooth to rough surface
x = distance from the border of rough surface
— — — — shearing stress distribution for fully developed channel flow.

stress distributions as calculated from the measured velocity distributions with the use of the equation of mean motion. It is seen from the diagram that in both cases the shearing stress near the wall assumes very rapidly the new value corresponding to the local surface conditions, while at layers away from the wall the shearing stress, which equals to the Reynolds stress $\tau = -\rho\overline{uv}$ here, changes very slowly. In fact, a new state of equilibrium is established only at rather long distances x measured from the border of the rough surface. Although the present experiment has been made for channel flow it is beyond any doubts that the basic phenomenon applies also to boundary layers.

Usually the law of the wall is based on the assumption that the shearing stress is constant throughout its region

$$\frac{\tau}{\rho} = -\overline{uv} + \nu \frac{\partial U}{\partial y} = \frac{\tau_w}{\rho} \tag{1}$$

and that mean velocity distribution can be expressed by the similarity relation

$$U = u_\tau f\left(\frac{y u_\tau}{\nu}\right), \tag{2}$$

where

$$u_\tau = \sqrt{\frac{\tau_w}{\rho}}$$

is the shear stress velocity, and f is a universal function of $\frac{y u_\tau}{\nu}$ which is seen from *Fig. 5*. Outside the viscous sublayer the differential quotient of the velocity distribution can be written as

$$\frac{dU}{dy} = \frac{u_\tau}{\kappa y} \tag{3}$$

which is derived from dimensional arguments, where κ is a dimensionless constant ($\kappa = 0.4$). Eq. (3) gives upon integration for large values of $\frac{y u_\tau}{\nu}$ the wellknown semilogarithmic velocity distribution

$$U = u_\tau \left[\frac{1}{\kappa} \ln \frac{y u_\tau}{\nu} + C\right]. \tag{4}$$

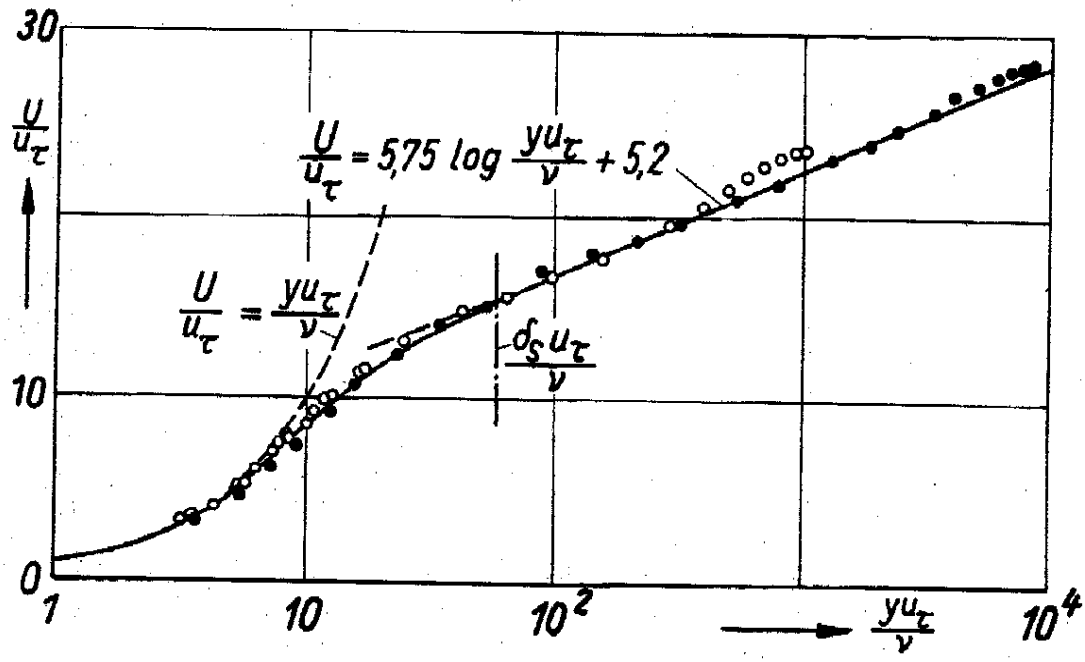

FIGURE 5
Semilogarithmic plot of mean velocity distribution in the vicinity of a smooth wall. Experimental points for a smooth circular pipe after LAUFER.
○ Reynolds number = 50.000
• = 500.000

The value of C is for smooth surface a universal constant. Furthermore it is known that outside the sublayer, the effect of surface roughness manifests itself merely as a shift of the velocity profile in the semilogarithmic plot. That means the roughness distribution affects only the value of the constant C.

A very important contribution to our knowledge on turbulent boundary layer flow has been made by LUDWIEG and TILLMANN [4] by whom the existence of the universal law of wall flow has been experimentally verified in boundary layers with non-zero pressure gradients. The experimental data of various boundary layers coincide near the wall, when $\frac{U}{u_\tau}$ is plotted versus $\log \frac{y u_\tau}{\nu}$, thus confirming the general validity of the similarity relations Eqs. (2) and (4). This result has led to a number of new approaches to the calculation of turbulent boundary layers and is now generally accepted as a constituent part of the theory.

Theoretically an influence of the pressure gradient is anticipated since an additional term $y \frac{dP_\infty}{dx}$ will appear in Eq. (1) and this invalidates the underlying supposition of a constant shear stress. In this connection an estimate of the shear stress distribution near the wall is in order here. With the assumption that the universal velocity distribution is valid, COLES [5] has calculated the shear stress distribution by introducing the velocity distribution according to Eq. (2) into the equation of mean motion which gives upon integration

$$\tau = \tau_w + y \frac{dP_\infty}{dx} + \nu\varrho \frac{du_\tau}{dx} \int_0^{y u_\tau/\nu} \left(\frac{U}{u_\tau}\right)^2 d\left(\frac{y' u_\tau}{\nu}\right). \tag{5}$$

The integral can readily be evaluated using the universal velocity distribution. Numerical values have been given by COLES. As is seen from Eq. (5) the variation of the shear stress is affected by the derivative of the shear stress velocity and the pressure gradient. Both terms are of the same order of magnitude. While the variation of shear stress is small in the flat plate boundary layer, considerable changes occur if there are external pressure gradients. A rough estimate may be made with the assumption of a constant local skin friction coefficient $c_f = 2\left(\frac{u_\tau}{U_\infty}\right)^2$.

Some results computed by means of these relations are given in a dimensionless form in *Fig. 6* and show that the variation of the shearing stress depends on the value of c_f and is usually much smaller than is expected from the wall constraint $\frac{\partial \tau}{\partial y} = \frac{dP_\infty}{dx}$ alone. This may help to explain why an influence of the pressure gradient on the velocity distribution near the wall is not observed with most of the experiments. However, this will very probably not hold up to arbitrarily high values of

$$\left[\frac{\nu}{\tau_w u_\tau}\right] \frac{dP_\infty}{dx}.$$

In particular, the universal velocity distribution will certainly not apply when the region of separation is approached, where the wall shear stress tends to zero. A theoretical attempt to estimate the effect of $\frac{dP_\infty}{dx}$ on the velocity distribution, has been made by

SZABLEWSKI [6] on the basis of the mixing length concept; the variation of the wall shear stress in mean flow direction was, however, neglected. Consequently these results are useful only if

$$\rho \int_0^y \left(U \frac{\partial U}{\partial x} + V \frac{\partial U}{\partial y} \right) dy \ll y \frac{dP_\infty}{dx}. \tag{6}$$

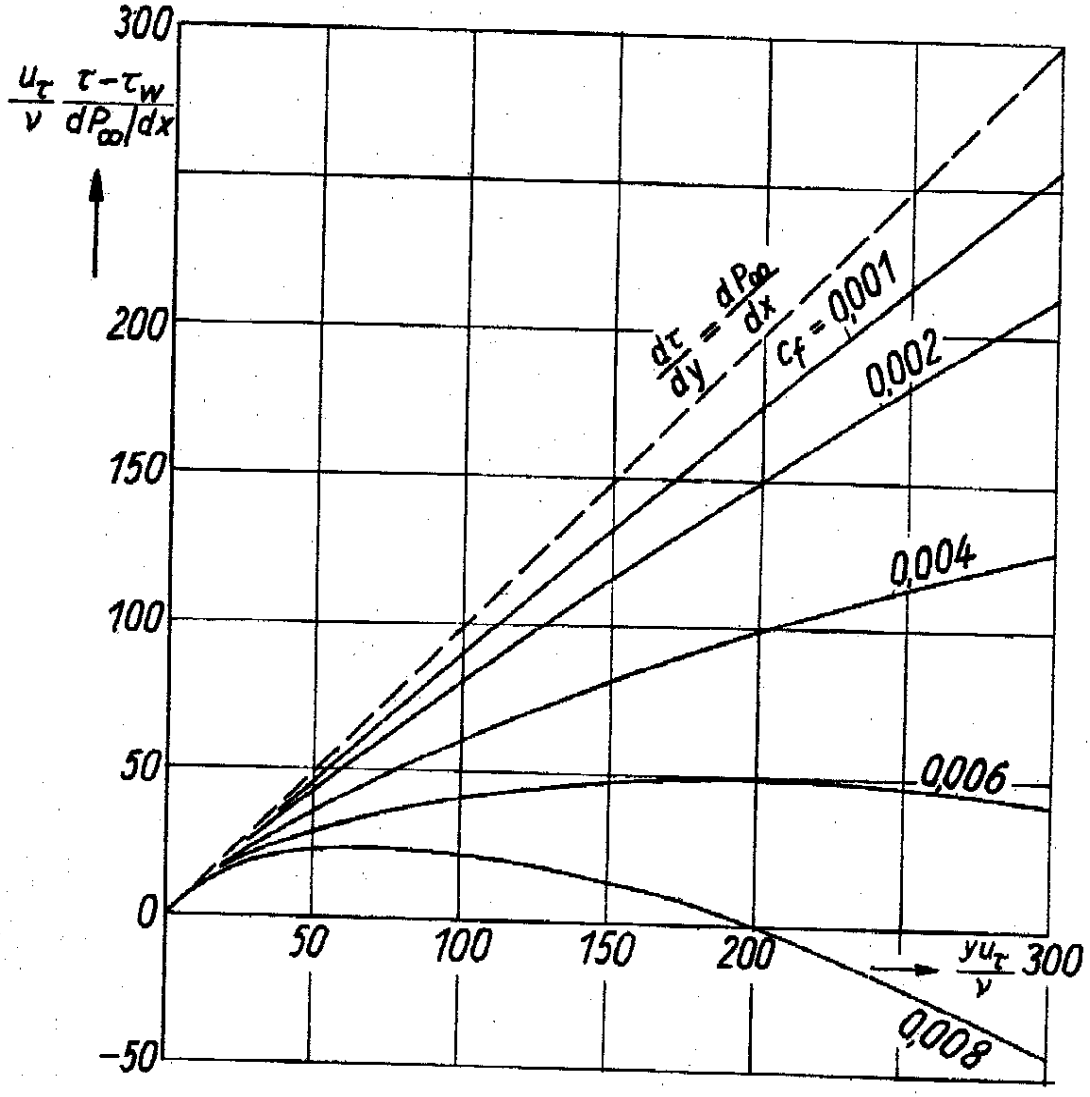

FIGURE 6
Variation of the shearing stress near the wall due to an external pressure gradient according to Eq. (5). Local skin friction coefficient $c_f = \text{const.}$

SZABLEWSKI's investigations include also the limiting case of zero wall shearing stress, for which the velocity distribution may be expressed by

$$U = \left(\frac{\nu}{\rho} \frac{dP_\infty}{dx} \right)^{1/3} f_0 \left(\frac{1}{\rho} \frac{dP_\infty}{dx} \frac{y^3}{\nu^2} \right), \tag{7}$$

as has been shown by STRATFORD [7]. In the fully turbulent part of the flow, the relative motion is again independent of the viscosity and, instead of Eq. (3), we obtain

$$\frac{dU}{dy} = \frac{1}{\kappa_0}\sqrt{\frac{1}{\rho}\frac{dP_\infty}{dx}}\frac{1}{y}. \tag{8}$$

This gives upon integration

$$U = \frac{2}{\kappa_0}\sqrt{\frac{1}{\rho}\frac{dP_\infty}{dx}}\,y + \left(\frac{\nu}{\rho}\frac{dP_\infty}{dx}\right)^{1/3} C_0. \tag{9}$$

The constant κ_0 is expected to be of the same order of magnitude as κ in Eq. (3), TOWNSEND [9] suggested a slightly higher value, viz. $\kappa_0 = 0.5$. The constant of integration C_0 may be of the order 1 or 2. After substituting the distribution of Eq. (9) into the relation (6) and putting C_0, we have

$$y\frac{d}{dx}\log\left(\frac{1}{\rho}\frac{dP_\infty}{dx}\right) \ll \frac{3}{2}\kappa_0 \tag{10}$$

as the condition that the inertia terms in the equation of motion are negligible. Some experimental verification of Eq. (9) is given by STRATFORD [8]. But it is felt that much more experiments are required before a reliable prediction of the effect of pressure gradient on the law of the wall is possible.

3. Boundary layer on a flat plate

The fact that there is a thin layer, in which the velocity distribution is determined by local parameters only, simplifies the problem of the outer part of the boundary layer in so far as the viscosity and surface conditions enter only as boundary conditions, without having a major effect on the overall flow pattern. In other respects, however, any theoretical approach to the problem is confronted to the entire complexity of turbulent flow. Therefore, we will confine the discussion to some characteristic types of boundary layers for a while.

The simplest case of a turbulent boundary layer occurs on a flat plate at zero incidence. The velocity outside the layer is $U_\infty = \text{const}$. Thus the external pressure gradient is zero along the plate. This case is to some extent representative of all turbulent boundary layer flow, and the results can be applied with some degree of approximation to the estimation of the skin friction drag of ships, airplane bodies, lifting surfaces etc. In absence of an adequate theory describing the turbulent mechanism, it is necessary to establish a sound basis, on which available experimental results can be compared.

It may be recapitulated that the velocity profile of the laminar boundary layer on a flat plate has a similar shape at all distances from the leading edge of the plate, if a dimensionless coordiate $\eta = y\sqrt{\frac{U_\infty}{\nu x}}$ is introducted. A similarity of such kind does not exist for the turbulent boundary layer, although a crude consideration suggests such a similarity since both types of layers are subject to the same basic boundary layer concepts. The classical theoretical treatments by V. KÁRMÁN [10] and PRANDTL [11] presumed in fact a complete similarity of the velocity profile. This assumption relied

however on measurements covering only a narrow range of Reynolds numbers. More careful measurements show that this supposition can not be retained over a large range of Reynolds numbers. Nevertheless a similarity in the turbulent boundary layer velocity profile can be assumed with a fair degree of approximation, but the similarity is of a more complex nature.

The basis of the similarity is the observation that under ordinary circumstances the velocity profile can be sufficiently described by the local conditions. The specification " ordinary circumstances " means here that there are no severe disturbances produced by obstacles etc. upstream of the point of observation, so that a normal development of the boundary layer is secured. An experimental investigation by KLEBANOFF and DIEHL [12] shows that disturbances produced by rods, screens and surface roughnesses in a turbulent boundary layer cause considerable alterations in the velocity profile which are, however, obliterated in the downstream direction quite soon. At a certain distance downstream of the disturbing obstacle the same velocity profile is observed as would be expected under normal conditions with the same local parameters. These experimental facts justify one in postulating a local similarity for the turbulent velocity profile of the flat plate boundary layer, according to which the mean velocity distribution $U(y)$ at any plane $x = \text{const}$ may be taken to depend solely on 4 local parameters, viz. free stream velocity U_∞, thickness of the layer δ, kinematic viscosity ν and the representative length scale k_r of the surface roughness distribution. This behaviour of flow entered the literature also under the title " self-preservation of developing flow ".

Provided that the wall flow according to Eq. (4) exists, the similarity for the outer part of the layer can best be described in terms of the velocity defect $U_\infty - U$. It can be shown that the parameters ν and k_r may be substituted by the local skin friction coefficient $c_f = 2\left(\frac{u_\tau}{U_\infty}\right)^2$. Then the similarity relation for outer part can be written as

$$\frac{U_\infty - U}{u_\tau} = F'\left(\frac{y}{\delta}, \frac{u_\tau}{U_\infty}\right). \tag{11}$$

The validity of this universal velocity defect law extends right into the region of the wall flow provided that the thickness of the sublayer is sufficiently small compared with the total thickness of the boundary layer. As the wall layer is approached, the velocity distribution tends to obey Eq. (3), from which the asymptotic form of the velocity defect law is obtained upon integration. Hence,

$$\text{for} \quad \delta_s \ll y \ll \delta: \qquad \frac{U_\infty - U}{u_\tau} = -\frac{1}{\kappa}\ln\frac{y}{\delta} + K'\left(\frac{u_\tau}{U_\infty}\right), \tag{12}$$

where K' is a constant of integration depending on $\frac{u_\tau}{U_\infty}$.

The postulated similarity of the velocity defect could be checked simply by plotting $\frac{(U_\infty - U)}{u_\tau}$ versus $\frac{y}{\delta}$ as is done by many authors. Since the boundary layer thickness δ is a quantity which cannot be exactly defined, I proposed to introduce the dimensionless wall distance $\frac{y u_\tau}{(\delta^* U_\infty)}$ instead of $\frac{y}{\delta}$ [13, 14]. The absissa scale is thereby fixed so that the area enclosed by the curve and the coordinate axes is equal to unity,

$$\int_0^\infty \frac{U_\infty - U}{u_\tau}\, d\left(\frac{y u_\tau}{\delta^* U_\infty}\right) = 1\,, \tag{13}$$

as can be seen from the definition of the displacement thickness, $\delta^* = \int_0^\infty \left(\frac{U_\infty - U}{U_\infty}\right) dy$.

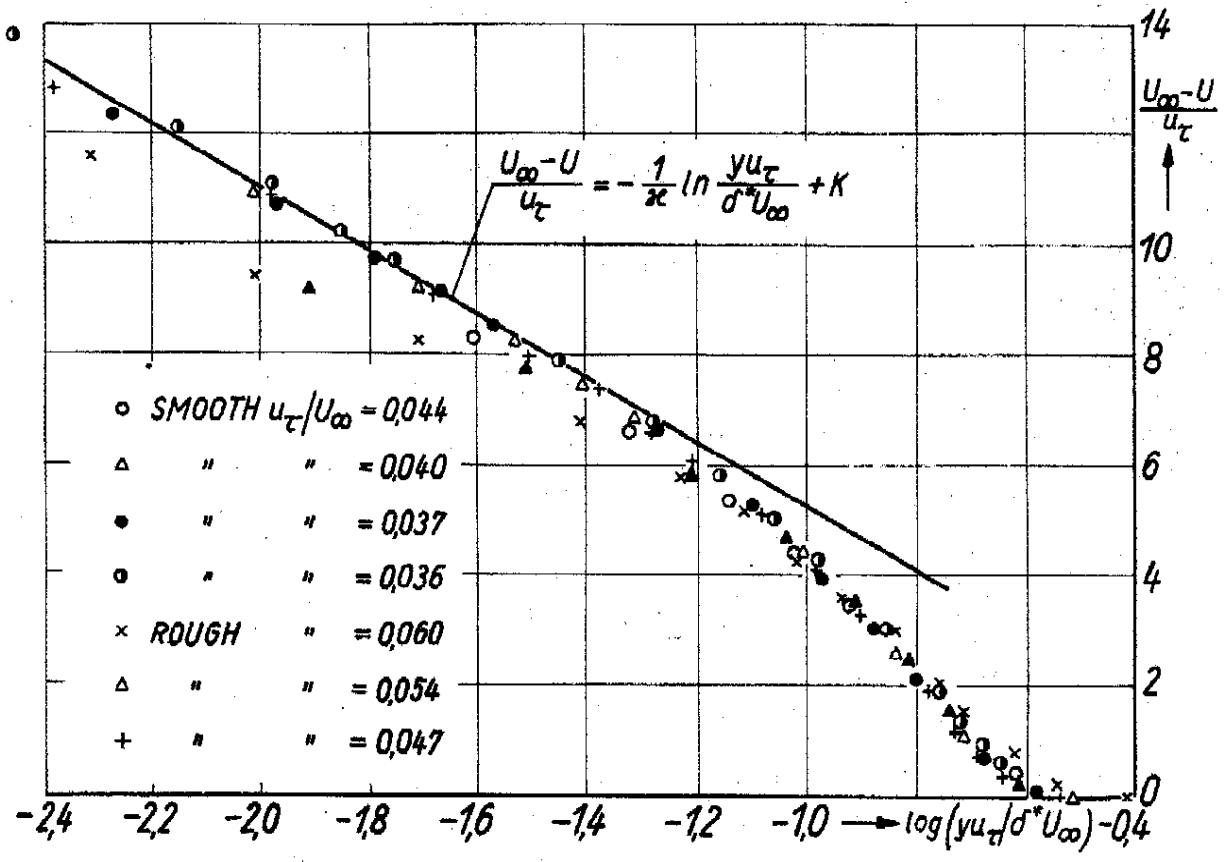

FIGURE 7

Velocity defect profile of the turbulent boundary layer on a flat plate without external pressure gradient according to measurements on a smooth wall by SCHULTZ-GRUNOW [15], and on a rough wall by TILLMANN.

In *Fig. 7* the values $\frac{U_\infty - U}{u_\tau}$ for a flat plate layer without external pressure gradient are plotted against $\frac{y u_\tau}{\delta^* U_\infty}$ in a semilogarithmic diagram. The test points of the smooth plate according to measurements by SCHULTZ-GRUNOW [15] show that the profiles within the investigated Reynolds number range may be represented with sufficient accuracy by a single curve. Nevertheless, a detailed consideration seems to indicate a small systematic influence of the parameter $\frac{u_\tau}{U_\infty}$. The test points of the rough plate according to TILLMANN show somewhat larger deviations due to the greater variation of $\frac{u_\tau}{U_\infty}$.

This comparison confirms the conjecture that the theoretically indicated influence of $\frac{u_\tau}{U_\infty}$ is only a weak one. The effect of $\frac{u_\tau}{U_\infty}$ is quantitatively not yet disclosed. It must be admitted that a small error enters with the definition of Eq. (13), if the displacement thickness δ^* is computed from the experimental profiles. This error caused by the thickness of the sublayer decreases inversely with the Reynolds number and is about 1 % when $\frac{U_\infty \delta^*}{\nu} = 7\,000$.

With the concept of local similarity, some quantities of the boundary layer can be determined, which on the one hand are used in boundary layer calculation and on the other hand can serve for further examination of the similarity. Perhaps the most important quantity is the local skin friction coefficient. When δ is replaced by $\frac{\delta^* U_\infty}{u_\tau}$, Eq. (12) may be written as

$$\frac{U_\infty - U}{u_\tau} = -\frac{1}{\kappa} \ln \frac{y u_\tau}{\delta^* U_\infty} + K\left(\frac{u_\tau}{U_\infty}\right), \tag{14}$$

which applies to the fully turbulent part near the wall, $\delta_s \leqslant y \leqslant \delta$. The local skin friction coefficient $c_f = 2\left(\frac{u_\tau}{U_\infty}\right)^2$ is deduced from this relation, if $\frac{U}{u_\tau}$ is eliminated by means of Eq. (4). This gives

$$\sqrt{\frac{2}{c_f}} = \frac{U_\infty}{u_\tau} = \frac{1}{\kappa} \ln \frac{U_\infty \delta^*}{\nu} + C\left(\frac{k_r u_\tau}{\nu}\right) + K\left(\frac{u_\tau}{U_\infty}\right). \tag{15}$$

Values of $\frac{U_\infty}{u_\tau}$ measured by SCHULTZ-GRUNOW and SMITH and WALKER [16], are plotted versus $\log\left(\frac{U_\infty \delta^*}{\nu}\right)$ in *Fig. 8*. If the surface of the plate is hydraulically smooth ($C\left(\frac{u_\tau k_r}{\nu}\right) = \text{constant}$) and if the magnitude of K does not depend on the value of $\frac{u_\tau}{U_\infty}$, then Eq. (15) gives a straight line. In fact the deviations of the measurements from the straight line

$$\frac{U_\infty}{u_\tau} = 5.75 \log \frac{U_\infty \delta^*}{\nu} + 3.7$$

remain within the limits of a few percent. More precisely, however, the measurements seem to lie on a slightly bent curve. This is possibly a consequence of a continuous variation of the velocity defect with the parameter $\frac{u_\tau}{U_\infty}$. But it can be stated that this plot demonstrates conclusively the applicability of the said conception.

The momentum thickness θ is

$$\theta = \int_0^\infty \frac{U}{U_\infty}\left(1 - \frac{U}{U_\infty}\right) dy = \int_0^\infty \left(1 - \frac{U}{U_\infty}\right) dy - \int_0^\infty \left(1 - \frac{U}{U_\infty}\right)^2 dy, \tag{16}$$

and may also be written as

$$\theta = \delta^* \left(1 - \frac{u_\tau}{U_\infty} I\right), \tag{17}$$

$$I\left(\frac{u_\tau}{U_\infty}\right) = \int_0^\infty \left[\frac{U_\infty - U}{u_\tau}\right]^2 d\left(\frac{y u_\tau}{\delta^* U_\infty}\right) \tag{18}$$

is expected to be approximately a constant for the flat boundary layer. The ratio $H = \frac{\delta^*}{\theta}$ as calculated from various measurements is plotted versus $\frac{U_\infty}{u_\tau}$ in *Fig. 9* and compared with Eq. (17). This diagram which has been taken from HAMA's paper [17] provides another confirmation of the usefulness of the similarity concept.

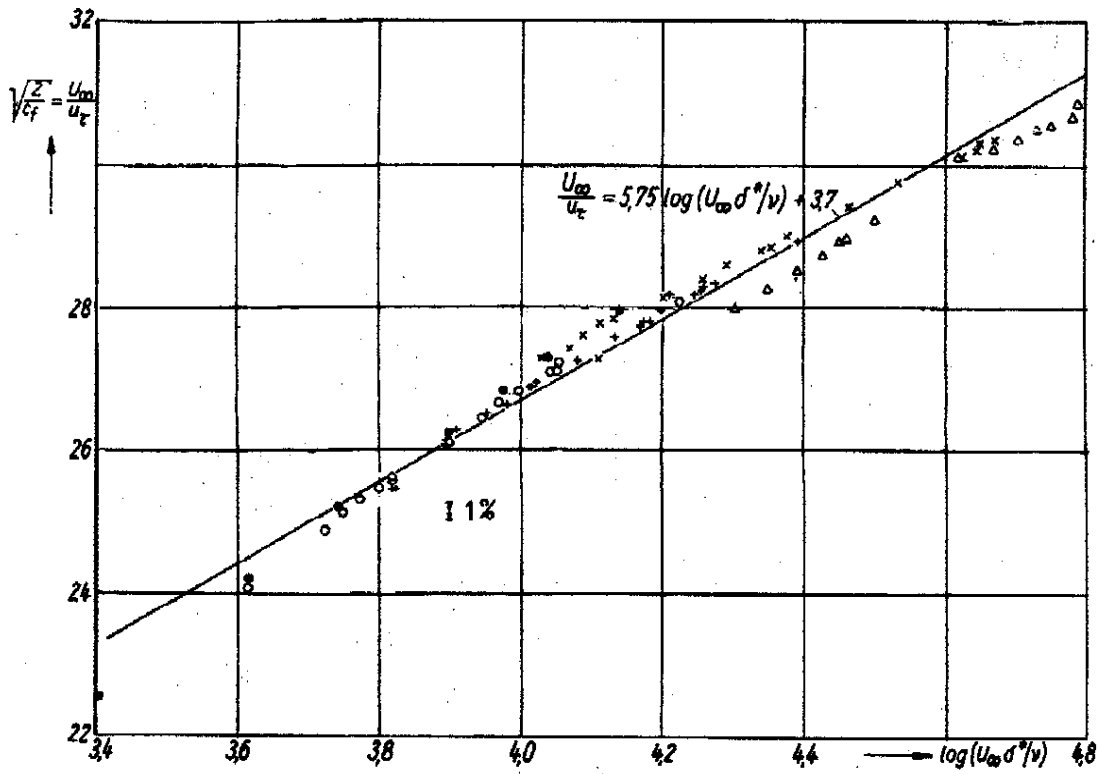

FIGURE 8

Local skin friction coefficient c_f of the turbulent boundary layer on a flat plate with smooth surface as a function of the local Reynolds number $U_\infty \delta^*/\nu$.

Measurements :

- ● SCHULTZ-GRUNOW [15]
- ○ $x = 15.75$ in
- \+ 27.75
- × 39.75
- △ 51.75

} SMITH and WALKER [16]

The similarity of velocity defect is also justified from a theoretical point of view. Introduction of the velocity defect law and corresponding expressions for the Reynolds

stresses into the boundary layer equations shows that exact similarity requires a constant value of the shear stress velocity u_τ. I will not go into the details of the analysis here, but is follows :

Complete similarity of the turbulent boundary layer on a flat plate can be reconciled with the flow equations, if the plate is covered with a roughness distribution continuously varying in such a manner that the representative length scale k_r of the roughnesses is everywhere in constant ratio to the distance x from the leading edge.

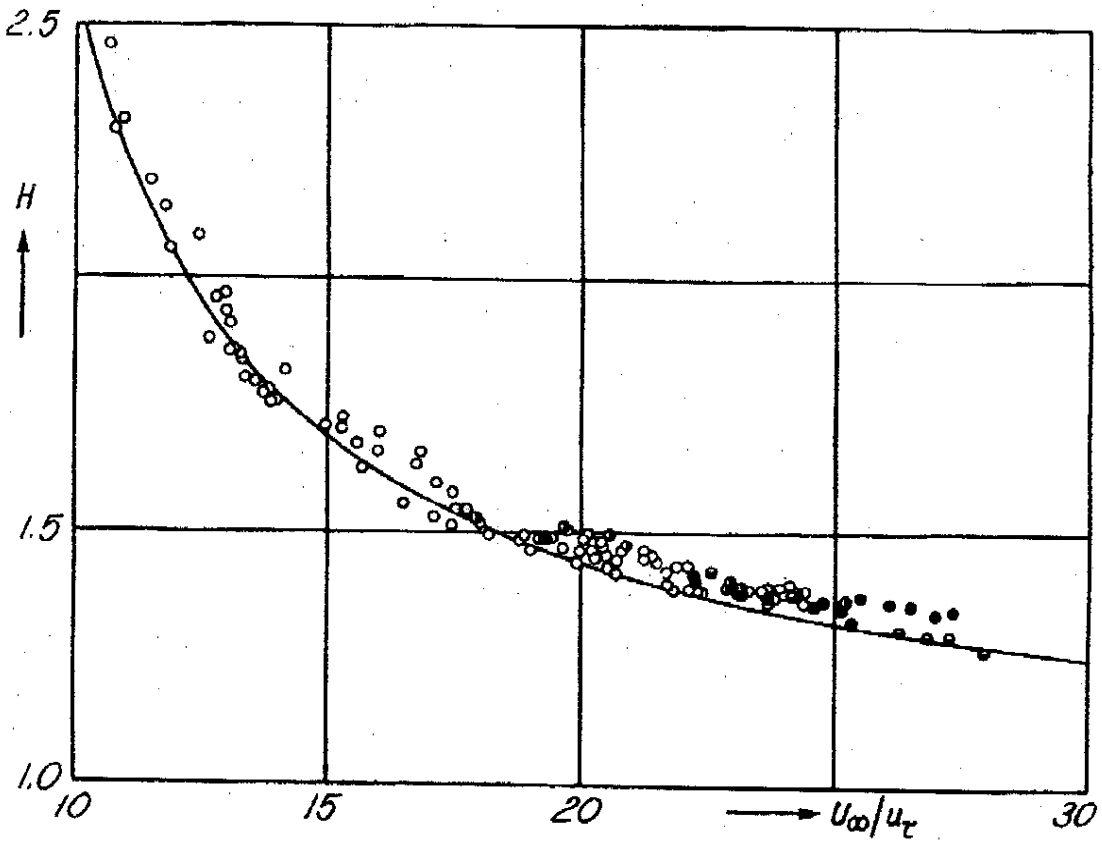

FIGURE 9

Ratio of displacement thickness to momentum thickness $H = \delta^*/\theta$ as a function of local skin friction coefficient after HAMA [17].

——— Eq. (17) with I = 6.1
○ Smooth SCHULTZ-GRUNOW
○ Smooth HAMA
• Smooth } HAMA
○ Rough }

These conditions are not fulfilled with ordinary flat plate boundary layers having smooth or uniformly rough surfaces. However, since the ratio $\frac{u_\tau}{U_\infty}$ has only a weak influence and varies very slowly along the x-axis, there is always sufficient time for the velocity profile to adjust itself to the weakly changing equilibrium conditions.

4. Equilibrium boundary layers

The existence of types of boundary layers for which the velocity profiles $U(x, y)$ at various positions x are similar in shape and differ only by a scale factor in U and y, is not restricted to the case of zero pressure gradient. Corresponding solutions of the laminar boundary layer equations were first treated by FALKNER and SKAN (see for instance SCHLICHTING [28], p. 143). Turbulent boundary layers of this kind have been discussed from a theoretical point of view by myself [13, 14], and an estimate was made on the basis of experimental data obtained from turbulent boundary layers with arbitrary pressure gradients. After CLAUSER [18] had succeeded in verifying experimentally turbulent boundary layers in adverse pressure gradients having velocity profiles of similar shape the problem was again treated theoretically by TOWNSEND [19, 20], CLAUSER [21], and COLES [22]. These layers are termed likewise similar solutions (by analogy with the corresponding laminar solutions), self-preserving layers, and equilibrium layers. The name equilibrium boundory layers prevails in the literature, and will be used here.

The compatibility of equilibrium layers with the flow equations may be examined by postulating similarity distributions of mean velocity and Reynolds stresses and substituting them in the equation of mean motion. These similarity distributions are of the same form as for the const. pressure layer with the difference that the velocity at the outer edge of the layer is now a function of x. The consideration is confined again to the fully turbulent part of the layer, and the flow near the wall is assumed to be in a state of universal equilibrium in accordance with the law of the wall. The case of the constant pressure layer is just a special case of a more general family of solutions. Equilibrium solutions exist if

$$\Pi = \frac{\delta^*}{\tau_w}\frac{dP_\infty}{dx} = \text{const} \tag{19}$$

$$\frac{u_\tau}{U_\infty} = \text{const} \tag{20}$$

$$\frac{d\delta^*}{dx} = \text{const}\,. \tag{21}$$

These conditions are met with the velocity distributions of the types $U_\infty \sim (x - x_0)^m$ in combination with $\delta^* \sim (x - x_0)$, where the exponent m is related to the pressure gradient parameter Π by

$$\Pi = -m\left(\frac{U_\infty}{u_\tau}\right)^2 \frac{d\delta^*}{dx} \tag{22}$$

and with the type $U_\infty \sim e^{\mu(x-x_0)}$ in combination with $\delta^* = \text{constant}$, which yields

$$\Pi = -\mu\left(\frac{U_\infty}{u_\tau}\right)^2 \delta^*\,. \tag{23}$$

The power law velocity distributions with arbitrary exponent require a rough surface, the roughness length scale varying as $(x - x_0)$. Boundary layers in adverse (positive) pressure gradients are obtained with negative values of exponent m. The negative value of m may not exceed a certain limit, otherwise the condition $\left(\frac{u_\tau}{U_\infty}\right)^2 > 0$ is

invalidated. With regard to the problem of pressure recovery and the phenomenon of separation in decelerated flow, the interest is concentrated mostly on boundary layers in adverse (positive) pressure gradients. The only exact results of experimentally established equilibrium boundary layers are those made by CLAUSER [18]. A summary of the values found by CLAUSER for two different pressure distributions together with the data of the constant pressure layer are given in the Table I.

TABLE I

Characteristic data of turbulent equilibrium boundary layers with adverse pressure gradients

	Π Eq. (19)	I Eq. (18)	K Eq. (14)	$\frac{\delta^* U_\infty}{\delta u_\tau}$
Constant Pressure	0	6.1	— 1.4	3.6
Pressure Distribution I .	2	10.1	1.8	6.4
do. II .	7	19.3	12.2	12.0

The layers show the essential features postulated above from theoretical arguments, however, the velocity profiles show a marked difference from those with constant pressure. This difference increases with the pressure gradient parameter Π. The variation of the skin friction coefficient with x is relatively small, however, appreciable differences in c_f exist for the three layers.

A few interesting problems occurred in combination with the equilibrium boundary layers. But I think it is not necessary to discuss these questions in more detail here. I will now change over to turbulent boundary layers in arbitrary pressure gradients.

5. Boundary layers in arbitrary pressure distribution

The pressure distribution on a body or in a duct etc. will probably not have a shape which is required to secure the formation of an equilibrium boundary layer. In the general case, a turbulent layer will develop for which the velocity profiles have different shapes at each position of the surface. In particular, in adverse pressure gradients the velocity profile usually develops in such a way as to increase the shape parameter, defined by the ratio $H = \frac{\delta^*}{\theta}$ or the value of I according to Eq. (18), in the flow direction until the layer eventually separates at some position. The flow at any cross section is affected in an unknown manner by the conditions at all sections upstream.

One of the earliest experimental observations, which has, again and again, found surprisingly good confirmation by various investigators, is the possibility of representing the mean velocity profiles of turbulent boundary layers approximately by a one-parameter family of curves in non-dimensional coordinates. In the investigations on turbulent boundary layers before 1950, the momentum thickness θ and the velocity U_∞ at the outer

edge of the layer was generally adopted as length and velocity scales. As a characterising shape parameter the thickness ratio

$$H = \frac{\delta^*}{\theta} \tag{24}$$

was introduced. If H does actually determine the shape of the velocity profile, then all points of $\frac{U}{U_\infty}$ from measurements of various sources plotted against H at a constant value of $\frac{y}{\theta}$ should fall on a single curve. No theoretical support for this observation can be given. The power-law

$$\frac{U}{U_\infty} = \left(\frac{y}{\delta}\right)^n, \qquad \text{for} \qquad 0 \leqslant y \leqslant \delta, \tag{25}$$

initiated by PRANDTL for presentation of the velocity distribution of turbulent pipe flow and flat plate boundary layer with an exponent $n = \frac{1}{7}$, was generalised by PRETSCH [23] to the profiles of turbulent boundary layers in arbitrary pressure distribution, admitting a varying exponent. The power law is found very useful for the purpose mathematical analysis and is often applied even now.

The essential defect of the power-law is the poor agreement with the actual behaviour in the proximity of the wall. After the experimental verification of the universal law of the wall, it was a logical step to apply the concept of single-parameter velocity profiles to the velocity defect profiles, defined by

$$\frac{U_\infty - U}{u_\tau} = F\left(\frac{y u_\tau}{\delta^* U_\infty}\right). \tag{26}$$

Several velocity profiles from measurements by LUDWIEG and TILLMANN [4] are presented in this manner in *Fig. 10*. The value of I defined by Eq. (18) may be considered as the characterising shape parameter. If these defect profiles form in fact, a one-parameter family, then the constant K of the asymptotic relation (14) is a function of I alone. Furthermore, any higher order moment of velocity distribution is uniquely related to I, for example the third order moment

$$I_2 = \int_0^\infty \left(\frac{U_\infty - U}{u_\tau}\right)^3 d\left(\frac{y u_\tau}{\delta^* U_\infty}\right), \tag{27}$$

which is required for the calculation of the energy thickness. Some experimental results are presented in *Fig. 11* and *12*. From the point of view of boundary layer calculation, it is necessary to know these relations quantitatively.

In order to obtain some numerical support for these purely empirical relations, a simple approximation for the velocity profile has been proposed by ROTTA [13, 14] which was independently also suggested by ROSS and ROBERTSON [24]. The tentative approximation consists of the logarithmic law of the wall, to which a linear term is added,

$$U = u_\tau \frac{1}{\kappa}\left(\ln \frac{u_\tau y}{\nu} + 2\Lambda \frac{y}{\delta}\right) + C\left(\frac{u_\tau k_r}{\nu}\right), \qquad \text{for} \qquad 0 \leqslant y \leqslant \delta \tag{28}$$

where A denotes a free parameter. The thickness of the boundary layer is defined by the condition $U = U_\infty$ for $y = \delta$.

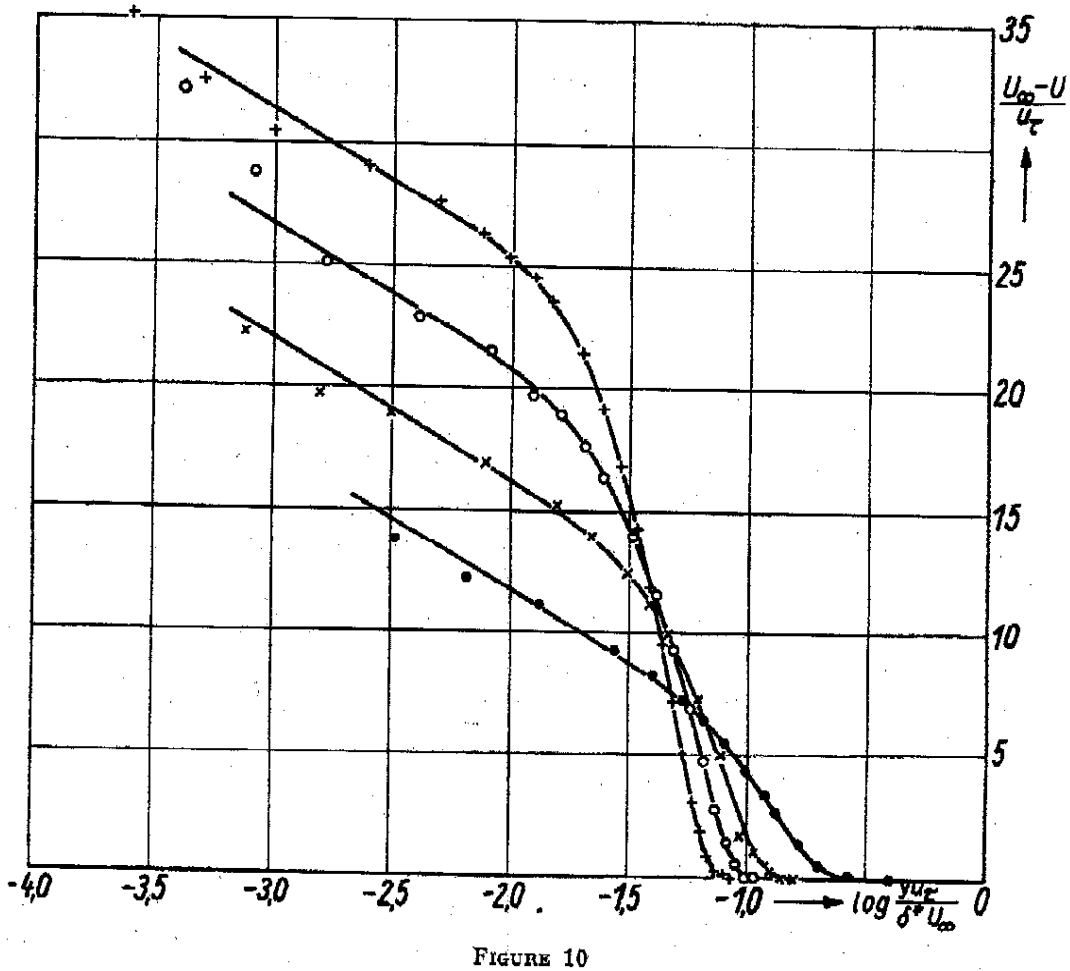

FIGURE 10

Velocity defect profiles for a turbulent boundary layer in adverse pressure gradients according to measurements by LUDWIEG and TILLMANN [4].

•	I = 7.5	H = 1.37	$U_\infty \delta^*/\nu = 1.1 \cdot 10^4$
×	12.0	1.53	$3.1 \cdot 10^4$
○	15.8	1.64	$4.6 \cdot 10^4$
+	20.0	1.79	$6.6 \cdot 10^4$

A similar but more refined approximation to the defect profile has been given by COLES [25]. Instead of by a linear term the departure from the logarithmic law is described by a universal function $w\left(\frac{y}{\delta}\right)$, which is called the law of the wake. The reason for this choice of terminology can be found in the close resemblance of this function to the mean velocity profiles in a plane half-wake or half-jet. The velocity defect profile may then be written as

$$\frac{U_\infty - U}{u_\tau} = -\frac{1}{\kappa} \ln \frac{y}{\delta} + \frac{B}{\kappa}\left[2 - w\left(\frac{y}{\delta}\right)\right], \quad \text{for} \quad 0 \leqslant y \leqslant \delta, \tag{29}$$

The wake function is $w = 0$ for $\frac{y}{\delta} = 0$, $w\left(\frac{y}{\delta}\right) = 2$ for $\frac{y}{\delta} = 1$, and satisfies the normalising condition :

$$\int_0^1 w d\left(\frac{y}{\delta}\right) = 1 .$$

A tentative determination of the wake function is tabulated in the paper by COLES.

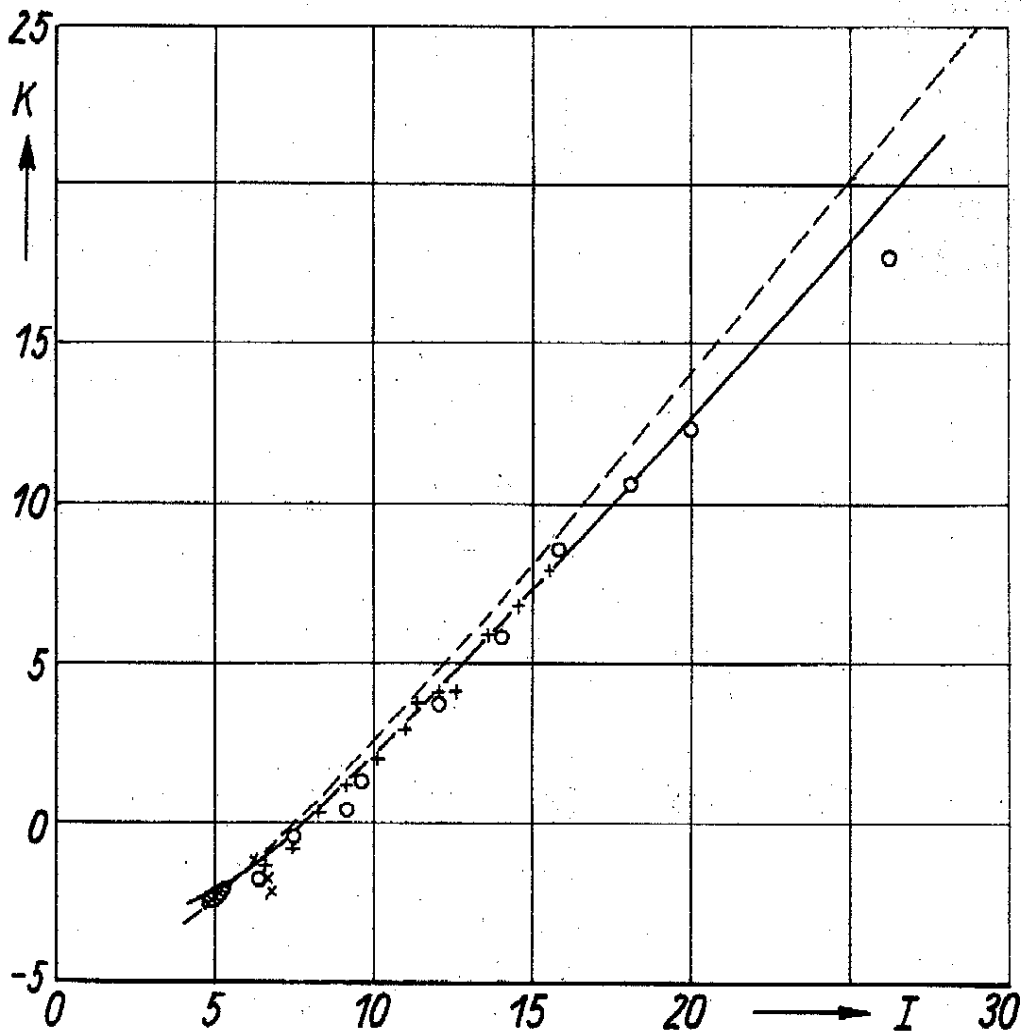

FIGURE 11

Constant K of Eq. (14) as a function of shape parameter I

———— according to velocity profile Eq. (28), $\varkappa = 0.4$

— — — » » » Eq. (29), $\varkappa = 0.4$

Experimental data :

× SCHULTZ-GRUNOW [15] $dP_\infty/dx = 0$

+ ○ } LUDWIEG-TILLMANN [4] $dP_\infty/dx > 0$

□ » » $dP_\infty/dx < 0$

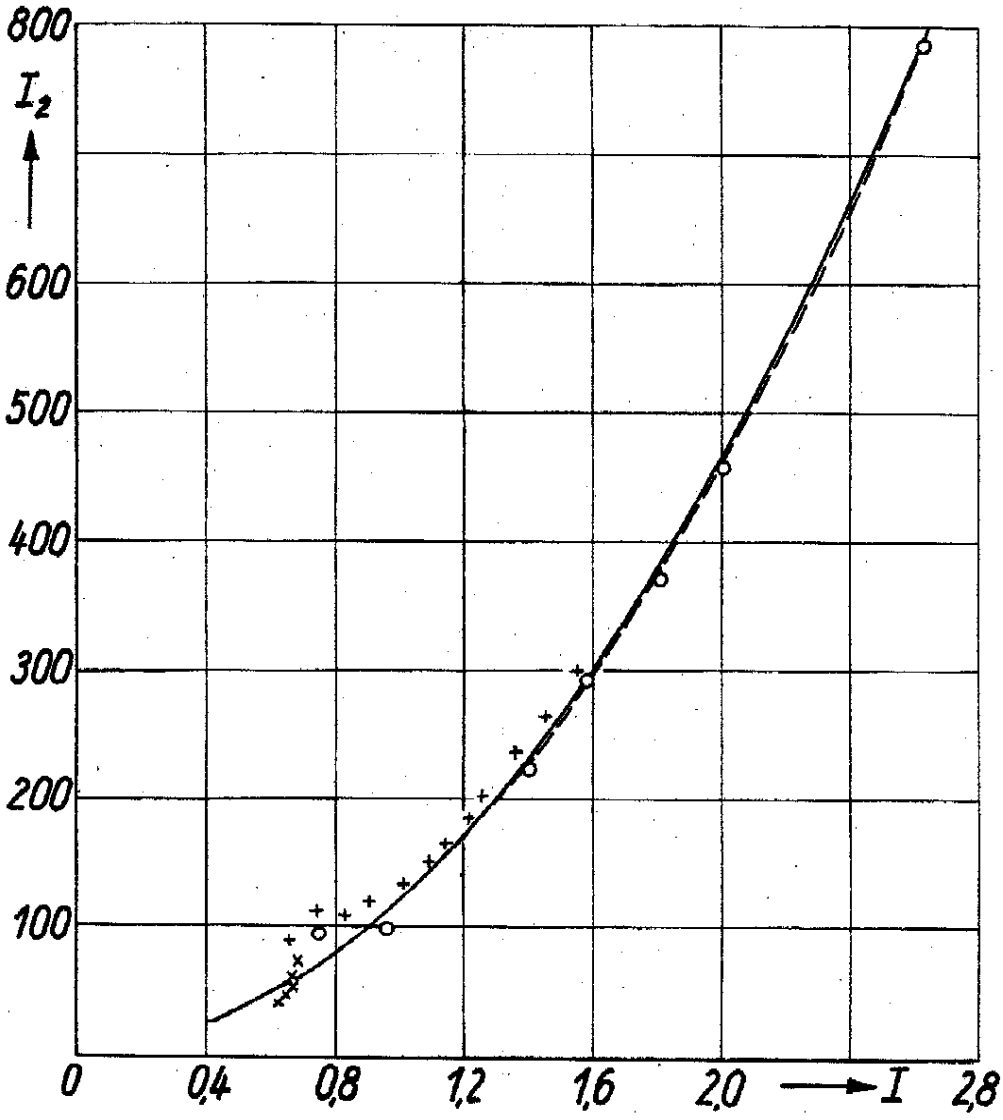

FIGURE 12

Relation between profile parameters $I_2 = \int_0^\infty \left(\frac{U_\infty - U}{u_\tau}\right)^3 d\left(\frac{y u_\tau}{\delta^* U_\infty}\right)$ and I

——— according to Eq. (28) $\varkappa = 0.4$
— — — » » Eq. (29) $\varkappa = 0.4$

Experimental data :
× SCHULTZ-GRUNOW [15] $dP_\infty/dx = 0$
○+ LUDWIEG-TILLMANN [4] $dP_\infty/dx > 0$

A hypothetical velocity profile composed of the law of the wall and the law of the wake is shown in *Fig. 13*. The dashed line represents the law of the wall. The dash-point line denotes the wake-like structure represented in Eq. (29) by the function $w\left(\frac{y}{\delta}\right)$.

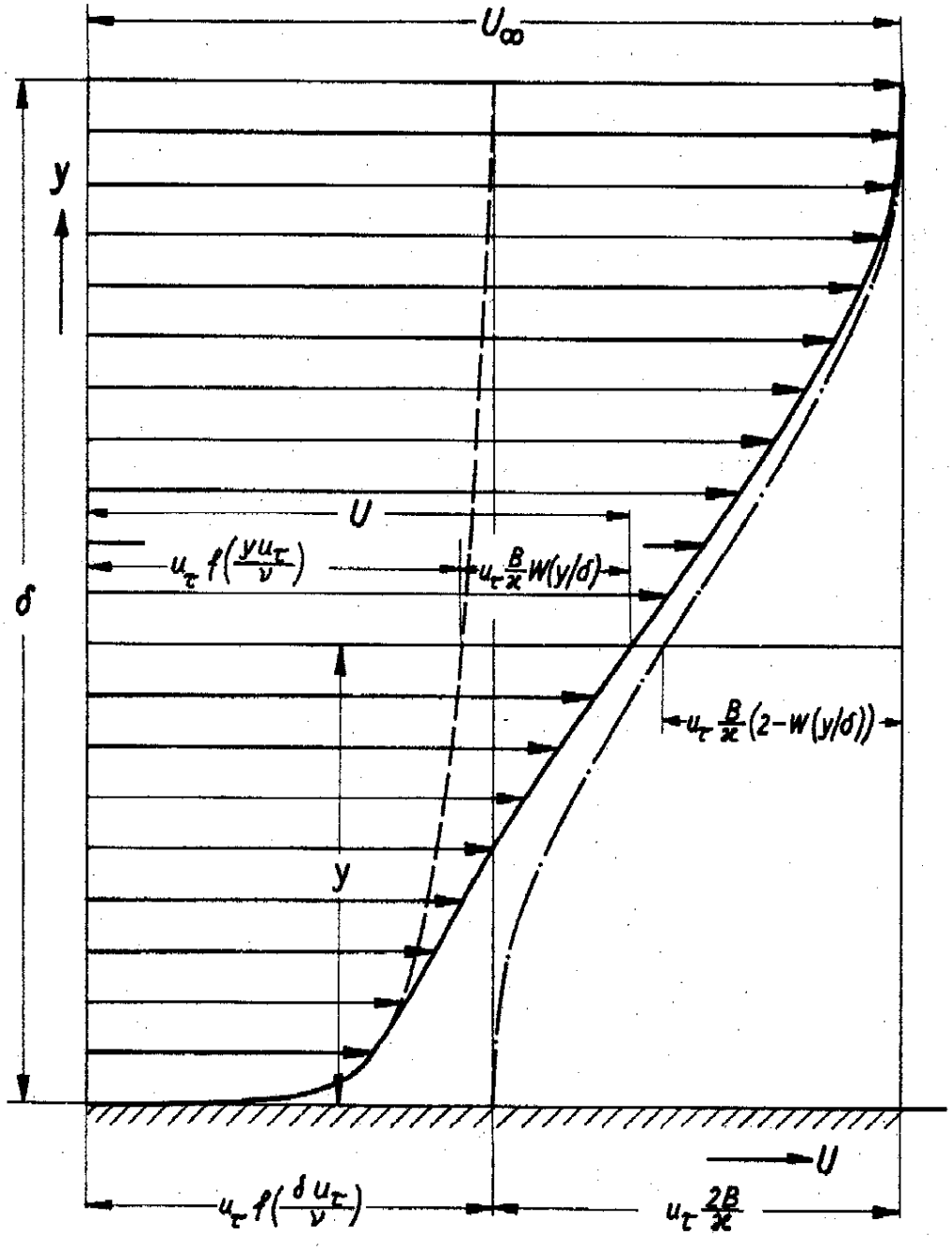

FIGURE 13
Hypothetical velocity profile of turbulent boundary layer
——— total mean velocity profile
— — — velocity distribution according to the law of the wall, Eq. (2)
——·—— velocity distribution of wake flow.

The associated velocity defect $U_\infty - U$ is given by $u_\tau B \frac{(2-w)}{\kappa}$, and the intercept at $y = 0$ of the equivalent wake profile therefore differs from the velocity in the external stream by an amount $\frac{2u_\tau B}{\kappa}$. Since the turbulent motion in the outer part of a boundary layer is effectively unrestricted and the process of entrainment of non-turbulent fluid takes place by processes very similar to those observed in wakes and jets, the boundary layer may be viewed as a wake flow, into which a solid thin plate is placed at the central plane, the velocity defect of the wake being $U_\infty - U = \frac{2u_\tau B}{\kappa}$ at the centre. At the surface of the plate the boundary conditions of vanishing velocity and molecular friction are to be satisfied. These conditions impose an additional constraint on the flow, whose effect is to modify the mean velocity distribution as shown by the solid line in *Fig. 13*. Whereas the similarity laws for the wall flow and also for the velocity defect of the flat plate and equilibrium boundary layers are based on clear physical ideas, the similarity conception involved in Eq. (29) goes far beyond the limits of dimensional analysis. Therefore, these relations can be applied to conditions outside the range of observations only with some reservations. A special caution is in order when the boundary layer is subject to extraordinary conditions as in the neighbourhood of transition from laminar to turbulent flow, near separation, reattachment behind obstacles, and sudden transition from smooth to rough surface or vice versa.

This representation of the velocity profiles enables us to calculate the local skin friction coefficient as a function of local Reynolds number, shape parameter and local surface roughness and is in general of high value to the boundary layer calculation, since it can be used in combination with the momentum integral equation etc. But this possibility can be turned to full advantage not until an additional relation for the variation of the shape parameter along the surface is available. Many attempts have been made to establish an equation for the shape parameter of the velocity profile, but a satisfactory success failed to appear since any rational formalism for the turbulent motion is denied to us.

The following consideration may help to explain the general behaviour of the turbulent layer : If the pressure gradient parameter Π is kept constant in flow direction, the parameter I also settles to a constant value, provided the boundary layer is stable. This case corresponds to the equilibrium layers discussed just before. There will be a unique relation between Π and I in this case. According to the differential equations governing the turbulent boundary layer it is not expected, that such a unique relation will hold, if the pressure gradient varies arbitrarily in the flow direction. *Fig. 14* shows, as an example, the variation of the shape parameter I with the pressure gradient parameter Π for a number of different boundary layers in adverse pressure gradients. There are considerable deviations from the curve for the equilibrium boundary layers, as established from CLAUSER's measurements. In particular it may be noted that sometimes, if the pressure gradient has a maximum value, the shape parameter continues to increase even though Π decreases again. In such cases it can happen that at two different positions of the same boundary layer, at which the pressure gradient parameter Π has the same value, velocity defect profiles of very different shapes are produced. Boundary layers with gradually rising value of Π behave similar to equilibrium layers. These measurements

demonstrate clearly the dynamic character of the turbulent boundary layer flow, according to which the present behaviour of the shape parameter is influenced by the previous history of the flow. This is a corollary of the parabolic character of the equations of motion.

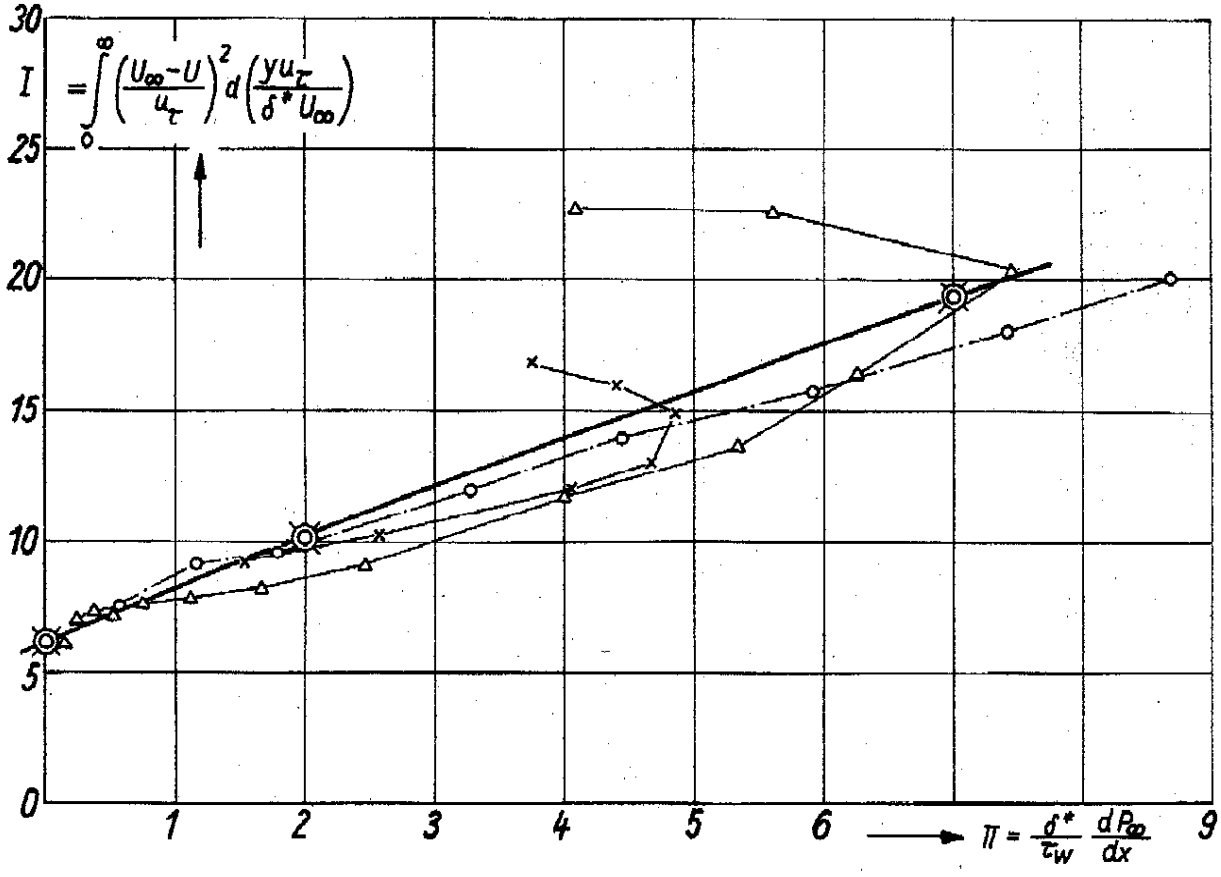

FIGURE 14
Variation of shape parameter I with pressure gradient parameter for different turbulent boundary layers in adverse pressure gradients.
Equilibrium layer, experiments by CLAUSER [18]. The other layers are from measurements by TILLMANN and LUDWIEG (partly unpublished).

It is possible to deduce a differential equation for the variation of the shape parameter from certain integrals of the boundary layer equation like energy integral or moment of momentum integral, in combination with the momentum integral. This requires however an assumption with respect to the shearing stress distribution. If it is assumed that the shearing stress profiles form a one parametric family and if the corresponding parameter is uniquely related to the shape parameter I, then an equation is obtained which gives certainly a better approximation to the actual behaviour than a unique relation between I and pressure gradient parameter II does. In particular, when the energy integral is used to derive the shape parameter equation, the integral of the viscous energy dissipation across the boundary layer occurs, which to a good approxi-

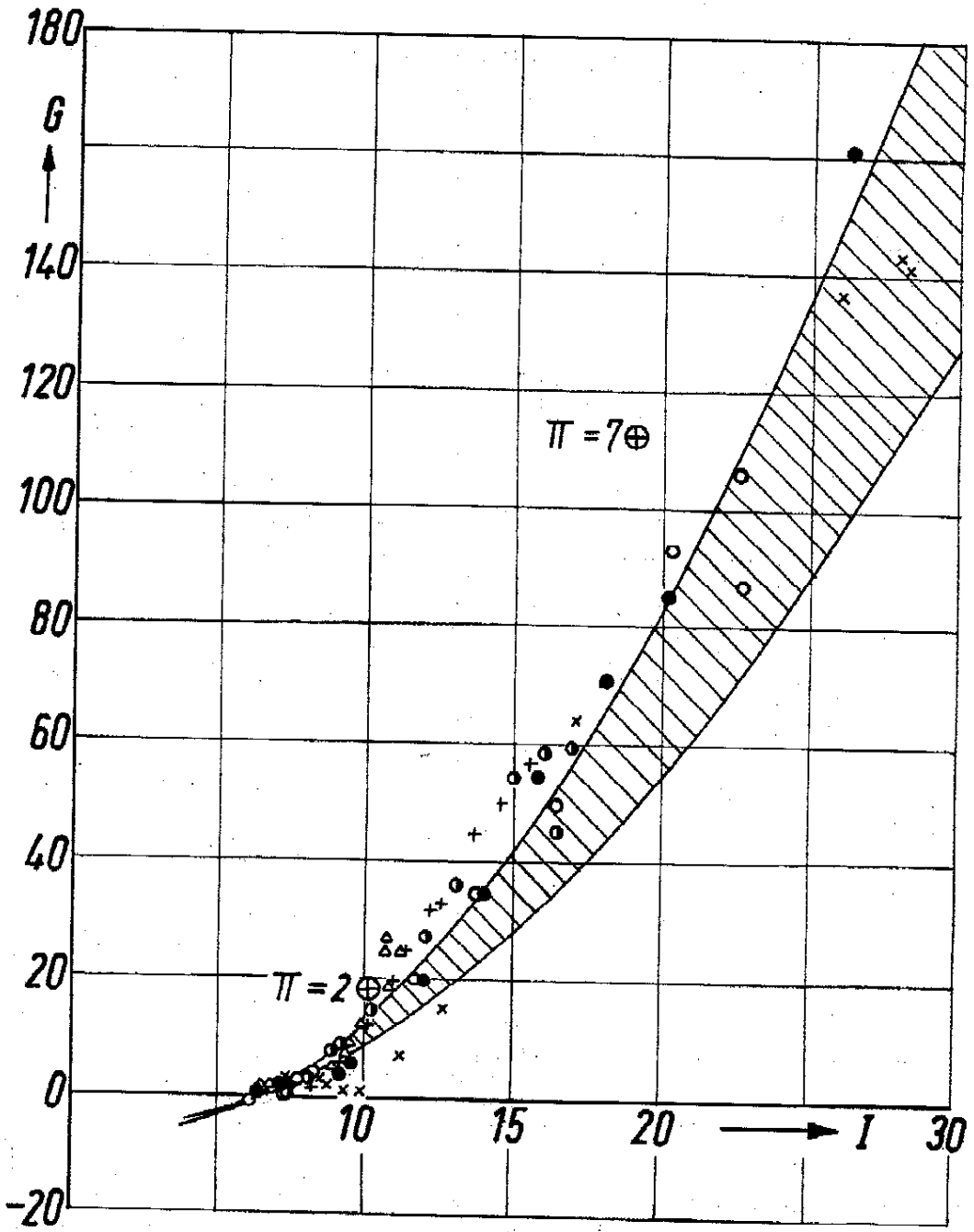

FIGURE 15

The dissipation integral

$$D = u_\tau^3 \left(\frac{1}{\varkappa} ln \frac{U_\alpha \delta^*}{\nu} + G \right).$$

The value of G as a function of shape parameter I for boundary layers in different pressure distributions.
Small spots : Evaluation by a differentiation method [13].
Hatched region : Evaluation by an integration method [27].
⊕ Determined from CLAUSER's equilibrium layers.

mation equals the work done by the mean velocity on the shearing stress. Applying the two-layer concept again, the dissipation integral may be written as

$$D = u_\tau^2 \, [U_\infty + u_\tau \Phi] \tag{30}$$

or

$$D = u_\tau^3 \left(\frac{1}{\kappa} \ln \frac{U_\infty \delta^*}{\nu} + G \right). \tag{30a}$$

When the shearing stress distribution is uniquely related to the mean velocity profile, the value of Φ is a function of shape parameter I only and in the second equation the value of G depends on I and the local surface conditions (roughness). In my papers of 1950 [13] to 1952 [27] I made some attempts, to determine the values of Φ or G respectively from available experimental boundary layers. This, however, turned out to be a difficult job, since the determination of the dissipation integral is sensitive to small errors in the measurements. Two different evaluation methods have been applied, vizz a differentiation method and an integration method. The results with respect to the value of G are shown in *Fig. 15*. The spots are according to the differenciation method, the hatched area according to the integral method. The calculation method which I proposed in 1953 [26] is based on these results. Also indicated are the points as calculated from CLAUSER's equilibrium layers. The values for the boundary layer with $\Pi = 2$ fits quite well in this picture but the layer with $\Pi = 7$ has a remarkably higher value than determined from the layers in arbitrary pressure gradients. It is thus very questionable whether with this assumption sufficiently correct results can be expected in all cases. Actually, also the shear stress distribution is affected by the previous history as became evident from the cited measurements by JACOBS [3]. Any proposals for the shape parameter equation which make proper allowance for these circumstances are not yet known. But at least, one knows now for certain that the insufficiency of the present calculation methods originate here. Any attempts for a positive improvement must start at this point.

6. Non-separating boundary layers in very severe pressure gradients

Let me now mention some theoretical considerations concerning the boundary layer in very severe pressure gradients, which have been made by STRATFORD [7] and TOWNSEND [9] in connection with experiments on a boundary layer with zero wall stress. This case represents, so to speak, a counterpart to the equilibrium layers and may be approached in a manner different from those discussed in the previous section. The generally observed feature of a different and almost independent development of the flow in proximity of the wall and in the outer part of the layer is found under extrem conditions in the present case. Close to the wall there is a balance between pressure and shear forces, and the flow is again expected to depend only on local parameters according to the law of the wall. On the other hand, in the outer part the pressure force is in competition with inertia forces only, while the shearing stress is negligible, if the pressure gradient is sufficiently strong. Then, in accordance with the Bernoulli theorem, the total head is to a good approximation constant along streamlines.

$$P_\infty + \frac{\rho}{2} U^2 = \text{const}, \tag{31}$$

with the condition that the constant has a different value on each streamline. The streamlines are specified by a constant value of the stream function

$$\psi = \int_0^y \mathrm{U}\, dy' \,. \tag{32}$$

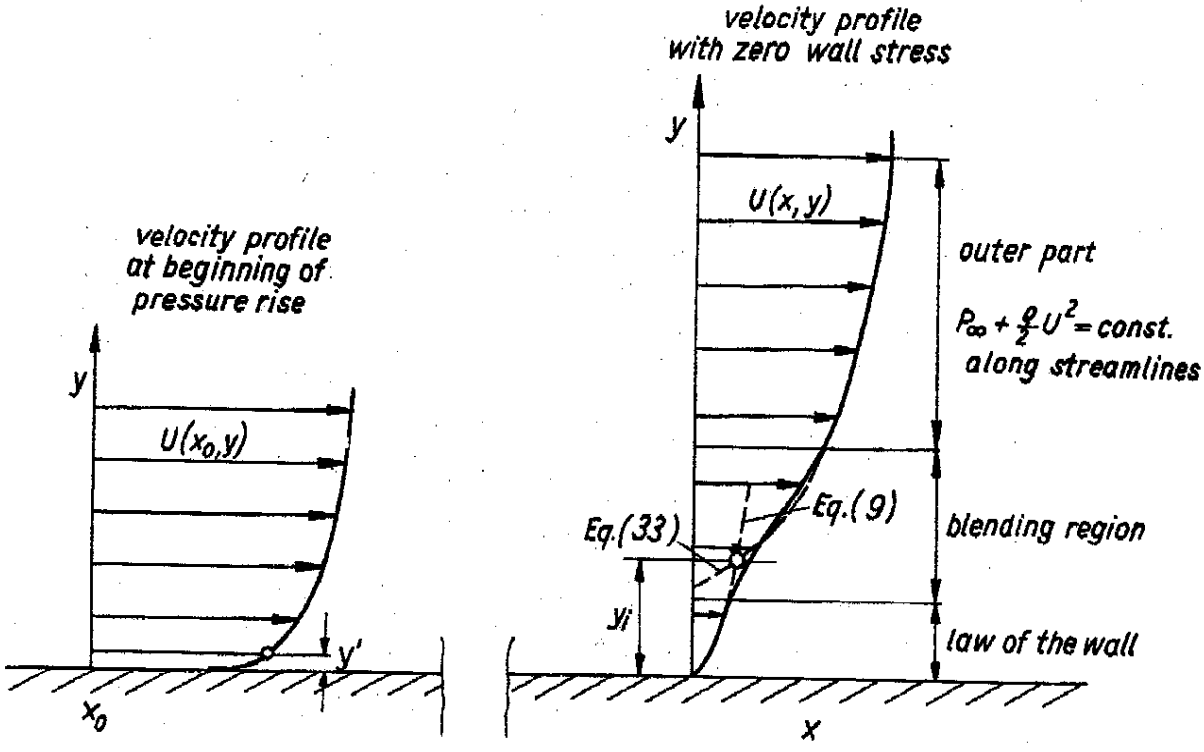

FIGURE 16
Sketch of the turbulent boundary layer with zero wall stress in severe adverse pressure gradient. The solid line represents the actual velocity distribution.

Eq. (32) expresses that the velocity profile in the outer part is determined by the velocity profile at station x_0 and the pressure rise $\mathrm{P}_\infty(x) - \mathrm{P}_\infty(x_0)$. In the blending region between the two layers the pressure forces, inertia forces, and shearing stress are of equal order of magnitude, and the conditions are thus very complicated. In order to arrive at a useful model, it appears admissible to extend the outer law and the wall law formally right into the blending region, where the two curves intersect at position y_i, as sketched in *Fig. 16*. In this way the first condition for joining the two laws is obtained from

$$\mathrm{P}_\infty(x_0) + \frac{\rho}{2}\mathrm{U}^2(x_0, y') = \mathrm{P}_\infty(x) + \frac{\rho}{2}\mathrm{U}^2(x, y_i)\,, \tag{33}$$

where the loci (x_0, y) and (x, y_i) are on the same streamline. The velocity $\mathrm{U}(x_0, y')$ and $\mathrm{U}(x, y_i)$ is introduced according to the law of the wall. The condition that (x_0, y') and (x, y_i) lie on the same streamline, results from the integral of the law of the wall. Now an additional joining condition is required in order to determine the distance of intersection and the shear stress at x. STRATFORD proposed that the wall law and the outer law join tangentially at (x, y_i). TOWNSEND made an alternative suggestion which probably

meets the actual behaviour better. It is based on the idea that (except for the region near the wall) the Reynolds stress is subject to the upstream history as has been discussed earlier. Hence there will be only a slow change in the shearing stress along the streamlines further away from the wall, and it appears plausible to assume the shearing stress to be constant on the streamline through (x, y_i). Moreover, the shearing stress distribuiton must be continuous. The set of equations obtained gives the velocity profile and the wall stress, if the pressure distribution is given. But in general, the set of equations cannot be solved explicitly. The particular case that the wall shearing stress is zero at position x, has been treated by STRATFORD and TOWNSEND. In this case the achieved pressure rise $P_\infty(x) - P_\infty(x_0)$ determines the pressure gradient $\frac{dP_\infty}{dx}$ at position x, which keeps the boundary layer just at the condition of separation. This relation

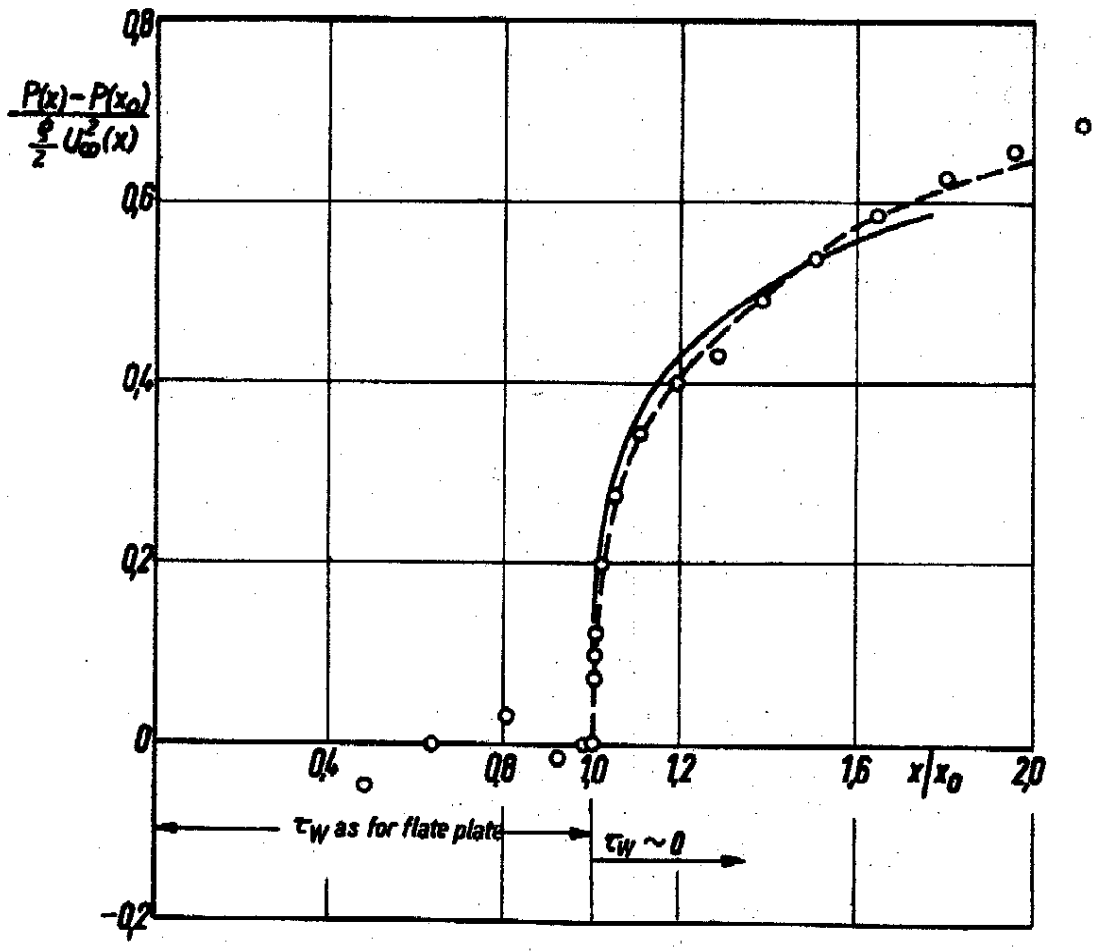

FIGURE 17

Pressure distribution for flow with nearly zero wall stress

$\frac{x_0 U_\infty(x_0)}{\nu} = 10^6 \cdot x =$ distance from virtual origin of turbulent boundary layer.

⊙ Experiment by STRATFORD, measured at the wall

——— Theory after TOWNSEND [9], $\varkappa = 0.4$, $x_0 = 0.5$, $C = 5.2$, $c_f = 3.8 \cdot 10^{-3}$

- - - - - Theory after STRATFORD [7], $x_0 = 0.27$.

provides a useful criterion for separation of the turbulent boundary layer and yields upon integration an approximation to the pressure distribution, in which a turbulent boundary layer develops with continuously zero wall stress. The pressure distribution according to this calculation with two alternative assumptions as suggested by STRATFORD and TOWNSEND, is compared with the experimental pressure distribution for the layer with zero skin friction after STRATFORD in *Fig. 17*. Although both theories exhibit good agreement with the experiment in the initial stage, if a proper value of the constant κ_0 in the law of wall with zero skin friction Eq. (9) is chosen, TOWNSEND's assumption seem to be more reliable on the whole.

I have mentioned this approach here because I believe that the underlying ideas may be applied to other cases, where the boundary layer is subjected to sudden changes as for example the pressure rise in a compression shock or the suction through a single slot.

7. Concluding remarks

In order to summarize in a few words the present knowledge on turbulent boundary layers it may be stated :

1) The behaviour of the flow in the vicinity of the wall is very different from the flow in the outer part of the boundary layer.

2) The flow near the wall is determined by local parameters while, in the outer part, the flow is influenced by the upstream history in a very complex manner.

3) The law of the wall flow has been disclosed by experimental investigations and similarity considerations. It is very desirable that the mechanism of the flow is understood to such an extent that effects caused by variable shearing stress distribution, suction and injection of fluid, compressibility and heat transfer can be predicted with a reliable degree of accuracy.

4) The velocity profile of the outer part can be described to a good approximation in many cases. But many efforts are still required until the outer velocity profile can adequately be related to the pressure distribution.

REFERENCES

[1] FAVRE, A.J., GAVIGLIO, J.J., and DUMAS, R. (1957). Space-time double correlations and spectra in a turbulent boundary layer. *Journ. Fluid Mech.*, **2**, p. 313-342.

[2] FAVRE, A.J., GAVIGLIO, J.J. and DUMAS, R.J. (1958). Further space-time correlations of velocity in a turbulent boundary layer. *Journ. Fluid Mech.*, **3**, p. 344-356.

[3] JACOBS, W. (1939). Umformung eines turbulenten Geschwindigkeitsprofiles. *Z. angew. Math. Mech.*, **19**, S. 87-100.

[4] LUDWIEG, H. and TILLMANN, W. (1949). Untersuchungen über die Wandschubspannung in turbulenten Reibungsschichten. *Ing.-Arch.*, **17**, S. 288-299. Also available as *NACA TM 1285*.

[5] COLES, D. (1955). *The law of the wall in turbulent shear flow*. 50 Jahre Grenzschichtforschung, Braunschweig, S. 153-163.

[6] SZABLEWSKI, W. (1955). Wandnahe Geschwindigkeitsverteilung turbulenter Grenzschichtströmungen mit Druckanstieg. *Ing.-Arch.*, **23**, S. 295-306.

[7] STRATFORD, B.S. (1959). The prediction of separation of the turbulent boundary layer. *Journ. Fluid Mech.*, **5**, p. 1-16.

[8] STRATFORD, B.S. (1959). An experimental flow with zero skin friction throughout its region of pressure rise. *Journ. Fluid Mech.*, **5**, p. 17-35.

[9] TOWNSEND, A.A. (1960). The development of turbulent boundary layers with negligible wall stress. *Journ. Fluid Mech.*, **8**, p. 143-155.

[10] v. KÁRMÁN, Th. (1921). Ueber laminare und turbulente Reibung. *Z. angew. Math. Mech.*, **1**, S. 233-252. Also available as *NACA* TM 1092.

[11] PRANDTL, L. (1927). Ueber den Reibungswiderstand strömender Luft. *Ergebn. Aerodyn. Versuchsanst. Göttingen*, **3**, S. 1-5.

[12] KLEBANOFF, P.S. and DIEHL, Z.W. (1952). Some features of artificially thickened fully developped turbulent boundary layers with zero pressure gradient. *NACA* Rep. 1110.

[13] ROTTA, J. (1950). Ueber die Theorie der turbulenten Grenzschichten. *Mitt. MPI Ström. Forsch.* Nr. 1, S. 1-54. Also available as *NACA* TM 1344.

[14] ROTTA, J. (1951). Beitrag zur Berechnung der turbulenten Grenzschichten. *Ing.-Arch.*, **19**, S. 31-41. Also available as David Taylor Model Basin Translation 242.

[15] SCHULTZ-GRUNOW, F. (1940). Neues Reibungswiderstandsgesetz für glatte Platten. *Luftfahrtforsch.*, **17**, S. 239-246. Also available as *NACA* TM 986.

[16] SMITH, D.W., and WALKER, J.H. (1959). *Skin-friction measurements in incompressible flow.* NASA TR. R-26.

[17] HAMA, F.R. (1954). Boundary-layer characteristics for smooth and rough surfaces. *Trans. Soc. Naval Architects Marine Engrs.*, **62**, p. 333-358.

[18] CLAUSER, F.H. (1954). Turbulent boundary layers in adverse pressure gradients. *Journ. Aero. Sci.*, **21**, p. 91-108.

[19] TOWNSEND, A.A. (1956). The properties of equilibrium boundary layers. *Journ. Fluid Mech.*, **1**, p. 561-573.

[20] TOWNSEND, A.A. (1956). *The structure of turbulent shear flow.* Cambridge University Press.

[21] CLAUSER, F.H. The turbulent boundary layer. *Advances Appl. Mech.*, **4**, p. 1-51, New York, N.Y.

[22] COLES, D. (1957). Remarks on the equilibrium turbulent boundary layer. *Journ. Aero. Sci.*, **24**, p. 495-506.

[23] PRETSCH, J. (1938). Zur theoretischen Berechnung des Profilwiderstandes. *Jb. dtsch. Luftfahrtforsch.* I, S. 60-81.

[24] ROSS, D. and ROBERTSON, J.M. (1951). A superposition analysis of the turbulent boundary layer in an adverse pressure gardient. *Journ. Appl. Mech.*, **18**, p. 95-100.

[25] COLES, D. (1956). The law of the wake in the turbulent boundary layer. *Journ. Fluid Mech.*, **1**, p. 191-226.

[26] ROTTA, J. (1953). *Näherungsverfahren zur Berechnung turbulenter Grenzschichten unter Benutzung des Energiesatzes.* Mitt. MPI Ström. Forsch. Nr. 8, S. 1-51.

[27] ROTTA, J. (1952). Schubspannungsverteilung und Energiedissipation bei turbulenten Grenzschichten. *Ing.-Arch.*, **20**, S. 195-207.

[28] SCHLICHTING, H. (1960). *Boundary Layer Theory.* IV. Edition, New York.

DISCUSSION
de la communication du Dr. ROTTA

Dr. R. MICHEL. — Monsieur ROTTA ayant établi des relations entre certaines caractéristiques de la couche limite, il reste pour traiter un cas donné à déterminer pour ce cas l'évolution suivant x d'au moins l'une des caractéristiques en question.

Dès que le cas est un peu compliqué, notamment dès qu'on fait intervenir un gradient $\frac{dp}{dx}$ on doit se contenter des équations intégrales comme l'équation de KÁRMÁN.:

$$\frac{C_f}{2} = \frac{d\delta_2}{dx} + \delta_2\left(\frac{H+2}{U_e}\frac{dU_e}{dx}\right) \quad \text{(courant plan incompressible)} \tag{1}$$

Il est important de souligner que cette équation provient de l'intégration suivant y d'équations locales incomplètes, dans lesquelles on a négligé notamment les dérivées longitudinales des tensions de Reynolds et des intensités de turbulence, et le gradient de pression normal $\frac{\partial p}{\partial y}$ dû à la courbure de la paroi et des lignes de courant de la couche limite.

Il n'est nullement certain que ces termes soient toujours négligeables, et l'on citera 3 cas ou ils risquent fort de ne pas l'être.

1. Gradients $\frac{\partial p}{\partial x} \gg 0$ (approche du décollement). Presque toutes les expériences effectuées en incompressible montrent qu'un terme supplémentaire S doit être ajouté au C_f pour que l'équation (1) soit vérifiée par l'expérience.

2. Les expériences de POTTER et WHITFIELD sur la transition sur un cylindre montrent que δ et δ_2 croissent très rapidement dans la zone de transition. Le $\frac{d\delta_2}{dx}$ qui devrait y représenter le coefficient de frottement y dépasse largement les valeurs turbulentes.

3. En supersonique, lors de recompression sur paroi concave, la courbure de la paroi conduit à des gradients $\frac{\partial p}{\partial y}$ importants dont il faut tenir compte dans l'équation des quantités de mouvement pour calculer correctement la couche limite.

Professor I. TANI. — In Mr. ROTTA's treatment of incompressible turbulent boundary-layer problems, an empirical formula for the dissipation integral is used to develop an approximate solution. In Dr. WALZ's treatment (1) of compressible turbulent boundary layer problems, the empirical formulae of wall friction and energy dissipation for incompressible flows are used to obtain generalized expressions for compressible flows. The dissipation formula for incompressible flows is that put forward by ROTTA (2) and TRUCKENBRODT (3), but the writer has left some doubt about this formula in that the effect of the form parameter H (ratio of displacement and momentum thicknesses) is unexpectedly small, in marked contrast to the case of laminar boundary layers.

From the analysis of a number of existing experimental data, RUBER and PERSH (4) obtained a dissipation formula showing the dependence on both Reynolds number and H. By assuming the validity of the LUDWIEG-TILLMANN formula for wall friction and similarity of velocity profiles of the form of the velocity defect law, the writer (5) derived from the momentum and energy integrals the energy dissipation in closed form. This describes the dependence on both Reynolds number and H and yielded results agreeing fairly well with those obtained by RUBERT and PERSH. It should be mentioned that the ROTTA-TRUCKENBRODT formula is based primarily on a single experiment of SCHUBAUER and KLEBANOFF (6) and that the wall friction as found in this experiment is known to be too high.

References :

(1) A. WALZ. DVL Berichte 84 (1959) und 136 (1960).
(2) J. ROTTA : Mitt. a.d. Max-Planck Inst. f. Strömungsforschung, 1 (1950).
(3) E. TRUCKENBRODT : *Ing. Arch.*, **20**, 211 (1952).
(4) K.F. RUBERT and J. PERSH : NACA TN 2478 (1951).
(5) I. TANI : *J. Aero. Sci.*, **23**, 606 (1956).
(6) G.B. SCHUBAUER and P.S. KLEBANOFF : NACA TR 1030 (1951).

Author's Reply to Professor TANI's *remark :*

Professor TANI's method of evaluating the dissipation integral implies the supposition that the non-dimensional pressure gradient, expressed by $\frac{\theta}{U_\infty}\frac{dU_\infty}{dx}$, and the shape parameter I of the velocity defect profile are independent from each other. In contrast with this, there exists a functional dependence between the two magnitudes for equilibrium boundary layers. This is suggested by theoretical arguments and has been fully verified by CLAUSER's experiments, as is seen from Table I and Fig. 14. It is not expected that useful results with respect to the dissipation integral can be obtained from the conditions of equilibrium boundary layers, if the relation between the pressure gradient and the shape of the velocity profile is disregarded.

THE STRUCTURE OF THE LAMINAR SUBLAYER

Alan L. KISTLER

Jet Propulsion Laboratory
California Institute of Technology, Pasadena, California (USA)

SOMMAIRE

A la paroi solide d'un écoulement cisaillé turbulent, les tensions de cisaillement sont transmises à la paroi à travers une couche mince appelée sous-couche laminaire. Cette région est décrite comme laminaire car à l'intérieur de cette couche, la tension de cisaillement visqueux, $\mu\,\partial U/\partial y$ est plus importante que la tension de cisaillement turbulent, $\rho\,\overline{u'v'}$ où U représente la vitesse moyenne parallèle à la paroi, et u' et v' les composantes des fluctuations de vitesse selon des axes respectivement parallèle et perpendiculaire à la paroi. Cette région existe puisque la tension de cisaillement reste finie à la limite, mais toutes les composantes de la vitesse y sont nulles. Le fait que la tension de cisaillement moyenne soit approximativement constante près de la paroi est un indice important pour que les régions de cisaillement à prédominance turbulente et laminaire soient intimement couplées. La question fondamentale à laquelle doit répondre une théorie dynamique de la sous-couche est : dans laquelle de ces régions se passent les phénomènes qui exercent une influence prédominante sur la dynamique de la couche limite tout entière ?

Les théories relatives à la structure de la sous-couche ont consisté, dans leur majorité, en des modifications de la théorie de la longueur de mélange, où le but était de développer une relation analytique de la viscosité turbulente qui donnerait la distribution de vitesse moyenne, depuis la paroi jusqu'à la portion logarithmique de la distribution de cette vitesse.

Ces théories ont été fort utiles, particulièrement pour les calculs de transfert de chaleur, mais elles ne jettent pas beaucoup de lumière sur le processus physique de base qui advient dans la sous-couche.

Récemment, deux théories fondées sur des modèles physiques déterminés, ont été présentées comme explication des phénomènes observés dans la sous-couche, l'une par EINSTEIN et LI [1], et l'autre par STERNBERG [2].

Puisque STERNBERG considère la sous-couche comme purement passive, avec des propriétés déterminées par la turbulence dans la région extérieure de la couche limite, et EINSTEIN et LI considèrent la sous-couche comme active, avec des propriétés déterminées par certaines instabilités dans la sous-couche, qui influencent à leur tour la région extérieure, un examen des détails et des conséquences de chaque théorie devrait s'avérer intéressant.

Introduction

At the solid boundary of a turbulent shear flow, the shear stresses are transmitted to the boundary through a thin region called the laminar sublayer. This region is

described as laminar because within this layer the viscous shear stress, $\mu \frac{\partial U}{\partial y}$, is greater than the turbulent shear stress, $\rho \overline{u' v'}$, where U is the mean velocity parallel to the wall and u' and v' are the components of the velocity fluctuations parallel and perpendicular to the wall, respectively. This region exists since the shear stress remains finite at the boundary, but all components of the velocity are zero there. The fact that the average shear stress is approximately constant near the wall is a strong indication that the regions of predominently turbulent shear and predominently laminar shear are closely coupled. The basic question to be answered by a dynamical theory of the sublayer is in which of these regions are phenomena occurring that exert a dominant influence on the dynamics of the entire boundary layer.

Theories relating to the sublayer structure, for the most part, have been modifications of the mixing length theory, where the aim was to develop an analytical relation for the eddy viscosity that would give the mean velocity distribution from the wall to the logarithmic portion of the distribution. These theories have been useful, particularly for heat transfer calculations, but don't shed much light on the basic physical processes occurring in the sublayer.

Recently two different theories based on definite physical models have been presented as an explanation of the observed phenomena in the sublayer, one by Einstein and Li [1] and one by Sternberg [2]. Since Sternberg treats the sublayer as purely passive with properties determined by the turbulence in the outer region of the boundary layer, and Einstein and Li treat the sublayer as active with properties determined by certain instabilities in the sublayer which in turn influence the outer region, an examination of the details and consequences of each theory should prove to be of interest.

The Theory of Einstein and Li

Einstein and Li proposed that the observed properties of the sublayer were the result of an instability of a laminar layer at the wall subjected to the large perturbing forces of the turbulence away from the wall. If we assume that at some instant the turbulence (as well as a finite mean velocity) extends all the wall, then the no slip condition requires a region strongly influenced by viscosity to start growing away from the wall (Rayleigh problem). The laminar region would grow until it was of sufficient thickness that certain unstable disturbances could grow. The layer would break down into turbulence and the process would start again. The theory gives the mean velocity near the wall as well as the fluctuation level of u' if the experimental values for the sublayer thickness are used to estimate the period of the growth-breakdown cycle.

This theory is equivalent to the statement that the sublayer thickness is controlled by the instabilities in a laminar Couette flow, a statement first made by Taylor, I believe. Since there is no known mechanism that will maintain a flow on the stable side of an instability boundary, the flow will cross the boundary, break down, and then, the process will start again.

The specific predictions of the theory that can be checked experimentally are the period of the cycle and the time history of the fluctuations in velocity near the wall. Measurements by Clyde [3] of the pressure fluctuations on the wall and the velocity

fluctuations in the sublayer can be interpreted as being roughly in agreement with the theory although the looked for results did not stand out as sharply as one would like. The time history of the velocity at a point in the sublayer was found to be a slowly varying pattern broken by bursts of high frequency oscillations at random intervals. The bursts and the slowly varying regions were identified as turbulence and laminar flow respectively. The period of occurance of the burst was not regular, but one would really not enpect it to be if it was the result of an instability phenomenon.

The Theory of Sternberg

Sternberg proposed that the calculation of PRANDTL [4] for the fluctuations in velocity near the wall in an oscillating laminar flow could be extended to the calculation of the fluctuations in the sublayer of a turbulent flow. Since the essential element of this calculation is that the fluctuations near the solid boundary are driven by an imposed fluctuating pressure field, it is necessary to know something about the pressure field at the solid boundary of a turbulent flow.

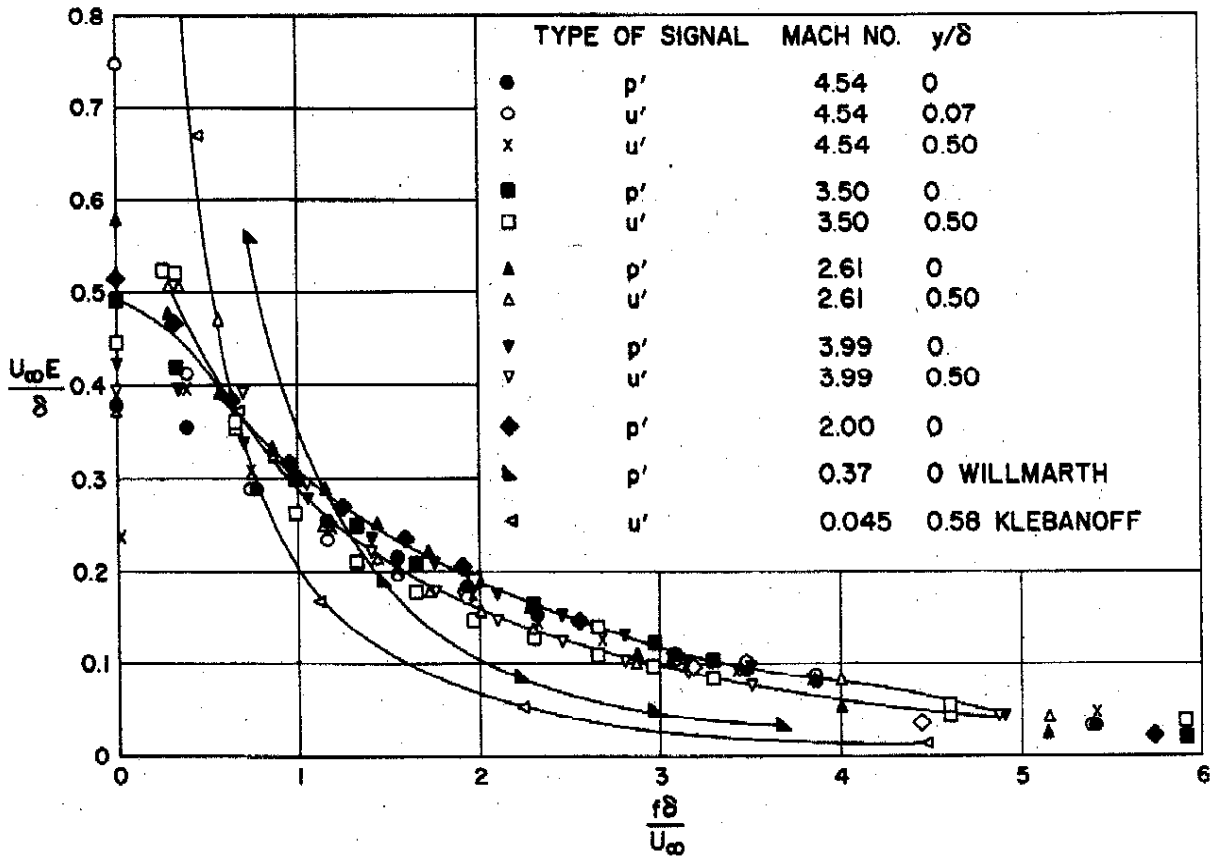

FIGURE 1
Pressure and velocity spectra in turbulent boundary layers.

Measurements of the spectra of the pressure fluctuations at the wall as well as the spectra of the velocity fluctuations near the center of a boundary layer are shown in

figure 1, where some high Mach number data from J.P.L. are used. For subsonic flows no measurements of the two spectra exist for the same flow conditions, so that curves for different Mach numbers have to be compared. It is apparent from the figure that the shapes of the spectra for the two different types of fluctuations are quite similar in the low frequency (small wave number) portion of the curve. Why this should be true can be rationalized from measurements by FAVRE [5] of space correlations and autocorrelations of the fluctuations in a boundary layer, and the comparison of the autocorrelations and space correlations are shown in figure 2. When these functions are plotted using

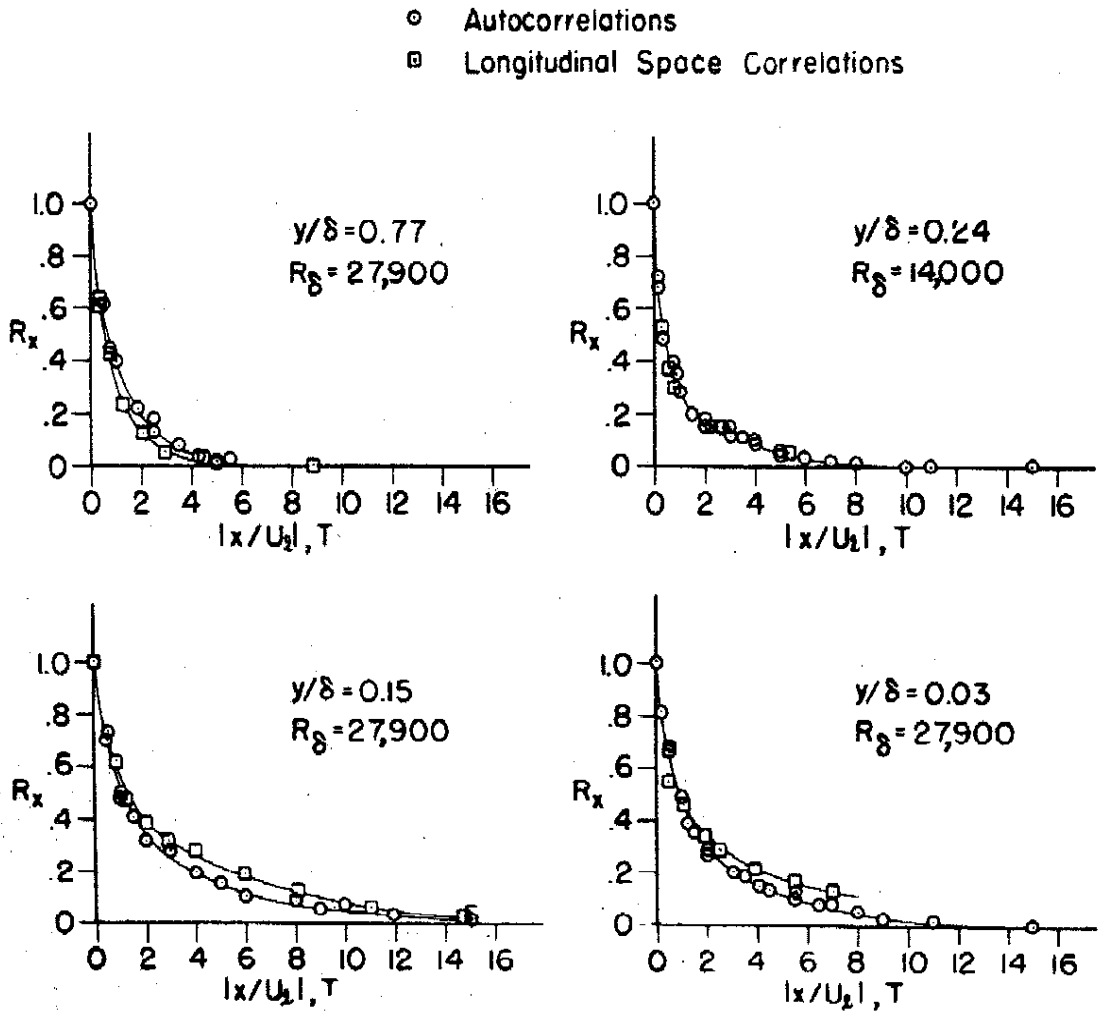

FIGURE 2
Comparison of $u(x, t)\ u(x, t+\mathrm{T})$ and $u(x, t)\ u(x+\mathrm{U}_1\ \mathrm{T}, t)$ in a boundary layer (from Sternberg)

Taylor's hypothesis to relate the time to distance, systematic differences between the curves appear for large time (or spacing). A consistant explanation for these differences is that the large eddy component of the turbulence moves with a velocity independent of the location in the boundary layer. This velocity should be about $0.8\ \mathrm{U}_\infty = \mathrm{U}_c$ for subsonic boundary layers (consistant with Willmarth's pressure measurements). Another

indication of this property of the large eddies is that KLEBANOFF's *spectra* [6] (figure 3) at various positions in the boundary layer are quite similar in the low frequency region when plotted with frequency as the independent variable, even though the local mean velocity changes significantly from one point to another. A consequence of this observation is that near the wall, where the mean velocity must be small because of the no slip condition, the imposed large scale disturbances must be moving at the velocity U_c, and associated with these disturbances there is a pressure fluctuation linear in the velocity fluctuation.

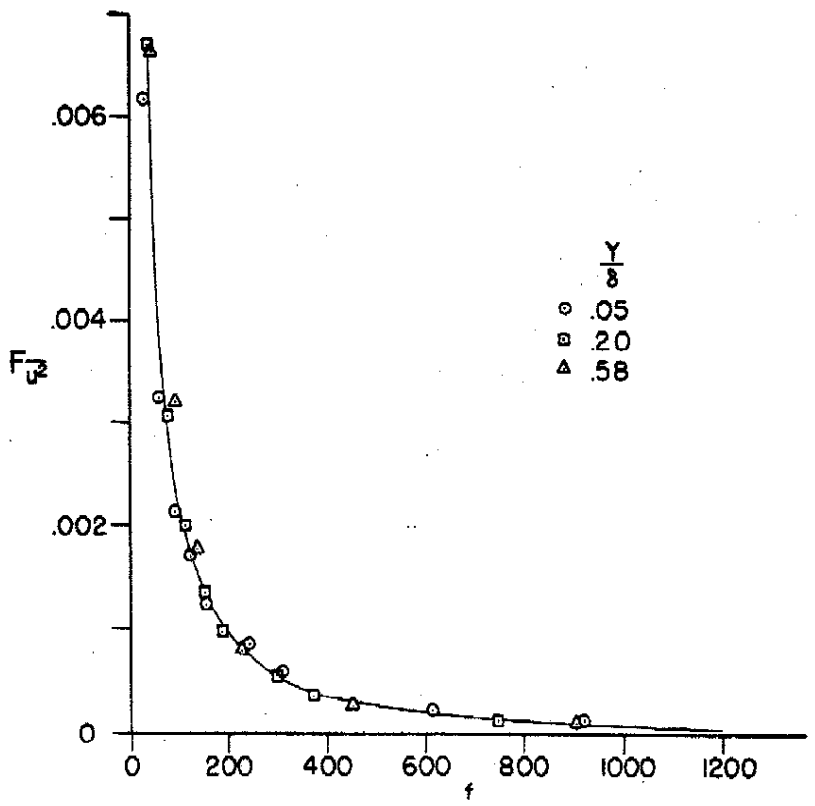

FIGURE 3
Normalized energy spectra in a boundary layer, data from Klebanoff.

Sternberg uses the velocity spectra in the turbulent region directly to obtain the pressure spectra at the wall. As shown previously, the two spectra are quite similar for small wave numbers, but this correspondence cannot be exact. If it is assumed that the local velocity perturbations near the wall but outside the sublayer are small compared to the difference between the convection speed U_c and the local mean velocity then the « X » equation of motion can be linearized to

$$\frac{\partial u'}{\partial t} + U\frac{\partial u'}{\partial x} + v'\frac{\partial U}{\partial y} = -\frac{1}{\rho}\frac{\partial p'}{\partial x}.$$

The assumption of a convection velocity for the disturbance is equivalent to the statement $\frac{\partial}{\partial t} = -U_c\frac{\partial}{\partial x}$ so that the « X » momentum equation becomes

$$(U - U_c)\frac{\partial u'}{\partial x} + v'\frac{\partial U}{\partial y} = -\frac{1}{\rho}\frac{\partial p'}{\partial x}$$

or

$$p' = -\rho(U - U_c)\left[u' + \frac{\partial U}{\partial y}\int^x \frac{U'}{U - U_c}\,dx\right].$$

The second term in the bracket is the local u' fluctuation caused by the displacement of the mean flow. An examination of the terms shows that the pressure is related only to the u' fluctuation following a particle and not to the total measured u' fluctuation. That is, to the first order the displacement of the mean flow causes no pressure disturbance although it does affect the measurement of u'. Therefore the identification of the pressure fluctuation spectra with the u' spectra cannot be correct in general, and will be particularly poor in a region with a large mean velocity gradient.

With this warning in mind, the calculation of the sublayer properties from the properties of the turbulence away from the wall can be carried out as follows. Near the mean velocity is almost zero and the pressure fluctuations associated with the large eddies move along the wall with the velocity U_c. The eddy sizes of interest are of the order of the boundary layer thickness in size, but the sublayer itself is quite thin so that near the wall only the y derivatives need be retained for the viscous shear stress. Under these conditions, the non-linear terms of the equations of motion for the fluctuations velocities near the wall satisfy the equation,

$$\frac{\partial u'_i}{\partial t} + \frac{\partial p'}{\partial x_i} = \nu\frac{\partial^2 u_i}{\partial y^2}. \tag{1}$$

The assumption of a layer of viscous influence near the wall, thin compared with the boundary layer thickness, implies $\dfrac{\partial p}{\partial y} \sim 0$ at the wall.

If the pressure field is decomposed by a two dimensional Fourier transform in the plane of the wall, the equations can be solved for the velocity. The boundary conditions are

$$\left.\begin{aligned} u' &= C_1 \exp t\,(K_x x + K_z z - \beta t) \\ p' &= \rho U_c u', \quad \beta = U_c K_x \end{aligned}\right\} \quad y = \infty$$

$$u' = 0 \qquad p' = p'(\infty) \qquad\qquad y = 0$$

The square of the solution for the u' component of the velocity is shown in figure 4, where $Y = \sqrt{\dfrac{\beta}{2\nu}}\,y$.

The method of using this solution is to find for each frequency the magnitude of C_1 in the fully turbulent part of the layer, $y = \infty$ in the analysis. The variation of the amplitude of the velocity fluctuation for this frequency is then given as a function of distance from the wall by the solution of eq. 1. Knowing the energy spectra of the fluctuations in the turbulent region, the spectra in the neighborhood of the wall can be computed.

From the integral of the computed spectra the energy distribution can also be obtained. The results of this calculation, using the data of Klebanoff are shown in figures 5 and 6.

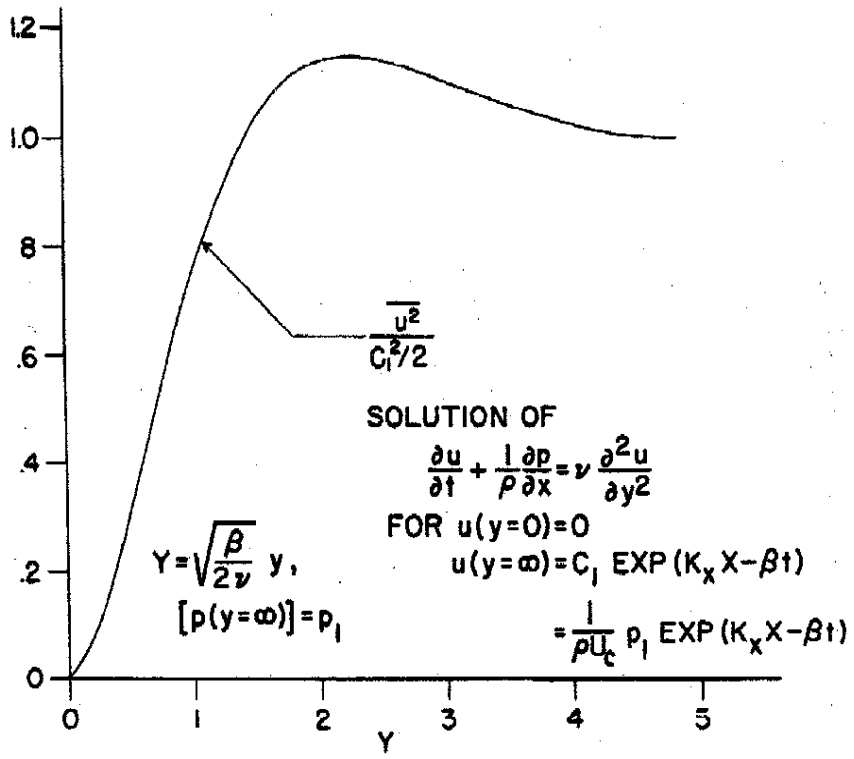

FIGURE 4
Theoretical variation of fluctuation energy in the viscous region.

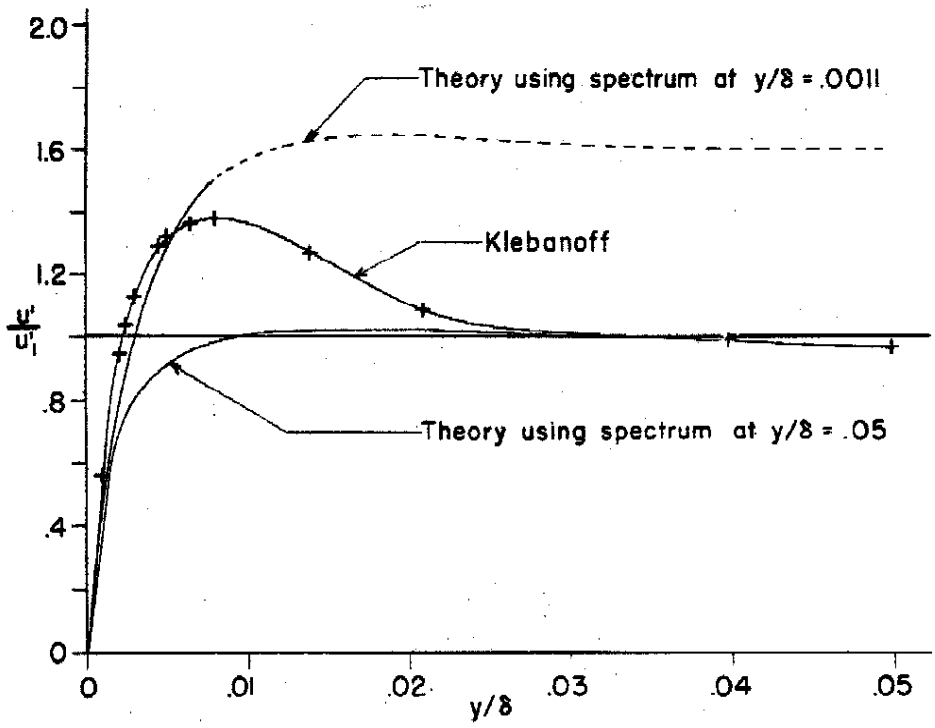

FIGURE 5
Fluctuation levels in sublayer from theory and experiment.

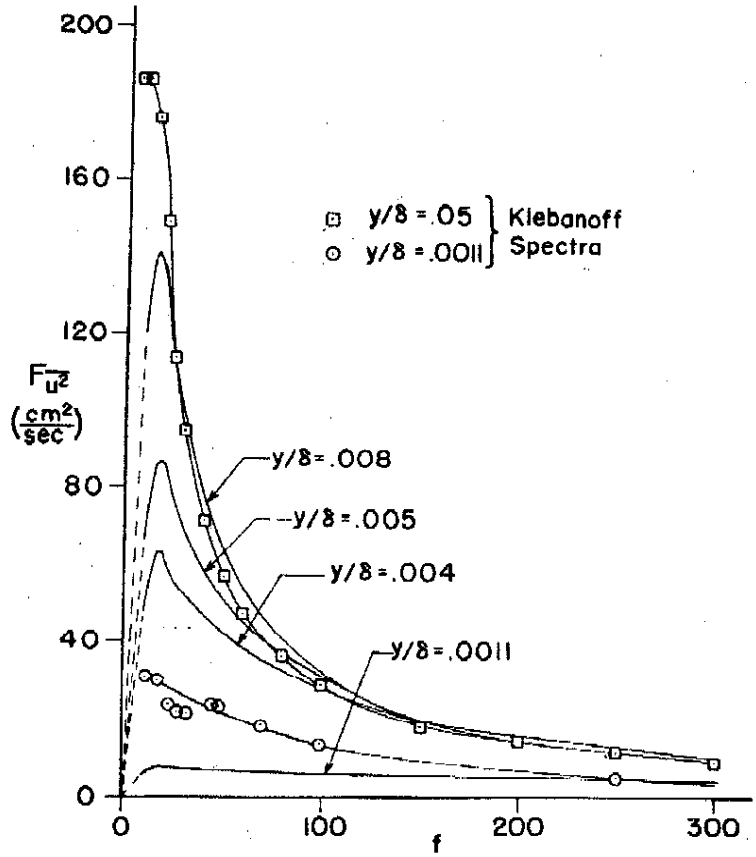

FIGURE 6
Spectra of u' in sublayer where c_1 is obtained from $y/\delta = 0.05$.

It is seen that the calculation accounts for the extent of the sublayer as well as for the variation of fluctuation level near the wall. The measured peak in the turbulence level at the edge of the sublayer is not given by the theory, but most probably in this region u' has a large contribution from the displacement of the large mean velocity gradient. The shape of the spectra in the sublayer $\left(\frac{y}{\delta} = 1.1 \times 10^{-3}\right)$ given by the theory has the same general features as the measured specta, but the low frequency region has insufficient energy.

Discussion

Both the theory proposed by Einstein and Li and that proposed by Sternberg give predictions in qualitative agreement with the measured properties of the laminar sublayer. Also, experimentally obtained information is required in order to compute the sublayer properties with either theory. Therefore, there is no obvious reason to prefer one theory or the other. An examination of the details of each model shows, however, that the pressure model is less questionable than the stability model since the assumptions required in the pressure model are questionable only as to whether they are sufficiently good approximations and not whether they represent a process that is actually occurring. The analysis of the stability model involves assumptions about whole flow patterns

whose existence has never been clearly demonstrated. For instance, the calculation of the growth of the laminar shear layer into the turbulent fluid raises the question of what does turbulence mean when the region of wall influence propagates through it at a rate determined directly by viscosity.

Another basis for comparing the two theories is how the interaction between the sublayer and outer turbulence is treated. The pressure theory uses the properties of one part of the boundary layer to compute the properties of another, so that the interaction is clearly defined. That a strong interaction is required was seen earlier in the discussion of the mean shear distribution. The stability theory gives only a weak interaction between the sublayer and the outer turbulence. The influence of the turbulence on the sublayer is small because its sole function is to contribute the perturbations to the laminar flow and cause its transition. The influence of the turbulence in the sublayer on the outer turbulence is small since, if experimental values of sublayer thickness are used to estimate the wave numbers of the oscillation in the sublayer, the wave numbers correspond to values close to the Kolmogoroff cutoff wave numbers in the outer turbulence. The only interaction most probably occurs in spectral regions where strong dissipation is occurring. Therefore, it seems likely that the pressure theory involves assumptions closer to the facts than the stability theory.

It may be useful to look at the sublayer structure as resulting from pressure forces imposed from the outside. As an example we will estimate the sublayer thickness from « first principles », and also explain the « intermittancy » observed in the sublayer.

When examining figure 6, it was observed that Sternberg's calculations gave insufficient energy for the spectra at low frequencies. This is caused by the fact that, according to the theory, the extent of the viscous wall influence on a fluctuation of frequency β is of the order $y \sim \sqrt{\frac{\nu}{\beta}}$. Therefore, at a fixed distance from the wall fluctuations with frequencies greater than some value $\beta(y)$ will not be influenced by the no slip condition at the wall, whereas frequencies $\beta < \beta(y)$ will have felt some wall influence, the effects increasing as $\beta \to 0$. In the turbulence away from the wall the shear spectra $\overline{u'(\beta)\, v'(\beta)} = S(\beta)$ extend over a wide frequency range. A calculation of the effect of the wall on a velocity fluctuation of frequency β might show that the wall influence extends out to a distance from the wall where high frequency components containing significant shear are not influenced by the wall. Therefore, the calculation should include turbulent shear terms over part of the y region, and this becomes more and more important as the frequency considered becomes smaller. The zero frequency component (the mean flow) cannot be calculated without knowledge of the turbulent shear distribution.

The thickness of the sublayer should be related to the distance from the wall associated with the frequency above which the external turbulence has no significant shear. Measurements of the shear spectra plotted against a Kolmogoroff wave number scale are shown in figure 7 along with measurements of the corresponding u' spectra. The data can be interpreted as showing that for regions of large mean shear, i. e. near the outer edge of the sublayer, the shear spectra departs significantly from the velocity spectra near $K = 0.1\, K_s$, where K_s is the Kolmogoroff wave number. If we assume on this basis that the frequency of the velocity fluctuation above which there is negligible shear is proportional to $K_s \cdot U_\infty$ (or U_c), and also that the dissipation rate in the turbulence outside

the sublayer is approximately $\frac{u'^3}{0.5\,\delta}$ where $u' \sim 0.05\,U_\infty$ and δ is the boundary layer thickness, then the thickness of the layer associated with the frequency $0.1\,K_s \cdot U_\infty$ is

$$\delta_c = \sqrt{\frac{2\,\pi\nu}{0.1\,K_s\,U_\infty}} = 22\,\delta\,R\,e_\delta^{-1/8}$$

This result is in good agreement with measurements of the sublayer, both in magnitude and in the exponent of the Reynolds number.

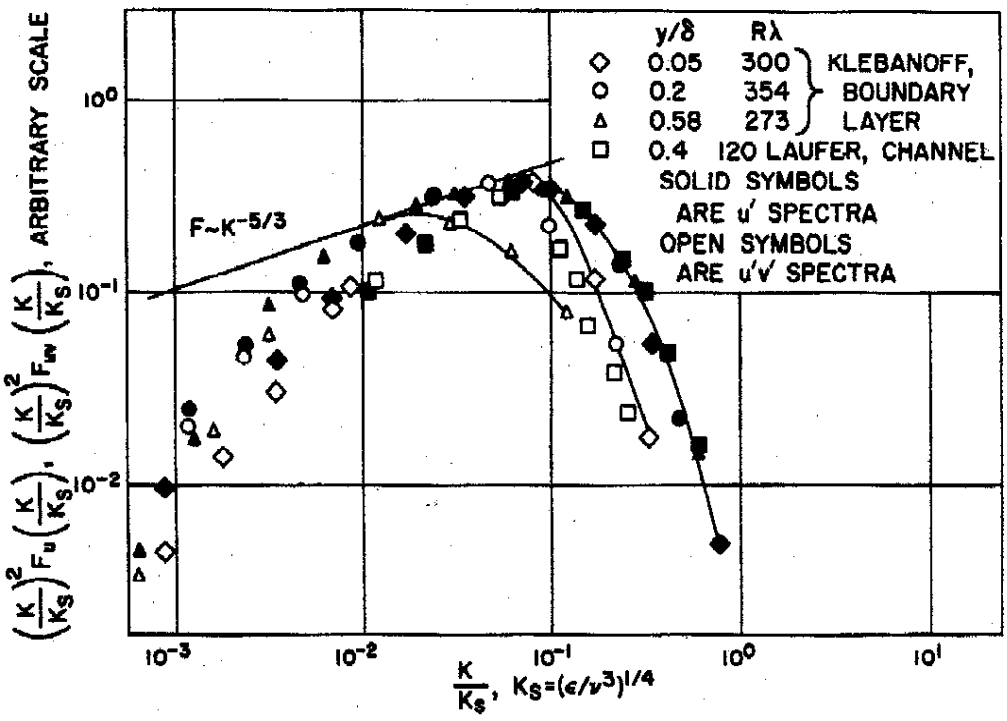

FIGURE 7
Comparison of u' and $u'v'$ spectra.

The property of the pressure driven sublayer to attenuate low frequency energy with respect to high frequency energy at a given distance from the wall can be an explanation of the " intermittancy " observed by Clyde in the sublayer. If the spacial derivative of the turbulence outside the sublayer has an intermittant spacial structure, the sublayer would tend to emphasize this intermittancy by its filtering action. It is an observed fact that the derivatives of a turbulent flow are spacially intermittant, but not enough data are available to relate this to the sublayer properties.

Conclusions

The idea of a sublayer with properties controlled by pressure fluctuations imposed from outside the sublayer appears to be a promising start toward a complete theory of the turbulent flow near a solid boundary. Extensions of this idea or any similar ideas involving the turbulent stresses would depend on a much better understanding of the

detailed relations between the velocity and pressure fluctuations in a turbulent flow, an understanding that will come only through closely coupled theoretical and experimental work.

REFERENCES

[1] Einstein, H.A. and Li, H. (1956). The Viscous Sublayer Along a Smooth Boundary, *Proc. Am. Soc. Civ. Eng.*, Paper 945.

[2] Sternberg, J. (1961). *A Theory for the Laminar Sublayer of a Turbulent Flow*, BRL Report 1127.

[3] Clyde, C.G. (1961). *Fluctuations of Total Head Near a Smooth Wall in a Turbulent Open Channel Flow*, Ph.D. Thesis, Univ. of California, Berkeley.

[4] Prandtl, L. (1921). Bemerkungen über die Entstehung der Turbulenz, *ZAMM*, **1**, p. 431.

[5] Favre, A.J., Gaviglio, J.J. and Dumas, R. (1958). Further space-time correlations of velocity in a turbulent boundary layer. *Journ. Fluid. Mech.*, **3**, p. 344-356.

[6] Klebanoff, P.S. (1954). Characteristics of Turbulence in a Boundary Layer with Zero Pressure Gradient, *NACA* Tech. Note 3178.

COMPRESSIBLE TURBULENT BOUNDARY LAYERS

par A. WALZ

Deutsche Versuchsanstalt für Luftfahrt Freiburg i. Br.
and Technische Hochschule, Karlsruhe

SOMMAIRE

On considère la situation actuelle des connaissances théoriques et expérimentales sur les couches limites turbulentes compressibles, avec transfert de chaleur, et gradient de pression au long de l'écoulement. Les tentatives méritoires pour généraliser les lois de similitude admises pour la distribution de vitesse moyenne établies en domaine incompressible n'ont pas encore réussi, à cause de la pénurie de données expérimentales valables relatives à des expériences en soufflerie hypersonique. De sérieux désaccords entre les résultats expérimentaux et les prévisions théoriques n'ont encore pu être évités.

A défaut d'une connaissance plus approfondie, on a exposé au point de vue de l'ingénieur sur les distributions de vitesse et de température moyennes en couches limites turbulentes compressibles, avec transport de chaleur et gradient de pression.

Cette conception semble caractérisée par le fait que le nombre d'hypothèses plus ou moins arbitraires, existant dans beaucoup de tentatives sur ce problème, est réduit au minimum.

Ce but paraît réalisable grâce à l'introduction d'une loi généralisée concernant la dissipation turbulente. Avec cette loi, liée à une loi généralisée du frottement aux parois, les conditions intégrales pour que les quantités de mouvement et l'énergie donnent un système d'équations d'où deux grandeurs caractéristiques de la couche limite telles qu'un paramètre de forme du profil de vitesse moyenne, et un paramètre d'épaisseur, peuvent être obtenues. (Dans la plupart des approximations-connues, ce paramètre de forme est supposé constant). Les coefficients locaux et moyens de frottement aux parois, calculés pour l'écoulement sur une plaque plane, coïncident remarquablement bien avec les données expérimentales sûres, obtenues par la mesure de forces.

Finalement, les expériences en soufflerie hypersonique de LOBB, WINKLER et PERSH [11], et de WINKLER et CHA [41] sont discutées de façon critique.

On a trouvé qu'au moins la loi d'énergie présidant aux relations entre les champs de vitesse et de température, est fortement transgressée. De plus, on a montré que l'évaluation de la pente à la paroi en vue de déterminer le coefficient de frottement local à la paroi entraîne de grandes incertitudes.

Une nouvelle loi empirique pour le coefficient de frottement à la paroi C_f suggérée par WINKLER et CHA [41] est discutée à la lumière des considérations théoriques précitées.

SOMMAIRE

The present status of theoretical and experimental information on compressible turbulent boundary layers with heat transfer and streamwise pressure gradient is reported. Meritorious attempts of generalizing the approved similarity laws for the mean velocity distribution established on the incompressible field had not yet been successful because of a lack of reliable experimental data from hypersonic tunnel tests. Serious discrepancies between experimental results and theoretical predictions could not yet be removed.

In default of better knowledge, an engineering concept of mean velocity and temperature distribution across compressible turbulent boundary layers with heat transfer and pressure gradient is developed. This concept seems to be distinguished by the fact, that the number of more or less arbitrary assumptions, present in many approaches about this problem, is reduced to a minimum. This aim appeared realizable by the introduction of a generalized law for turbulent dissipation. With this law in connection with a generalized wall friction law, the integral conditions for momentum and energy form a system of equations, from which two characteristical boundary layer quantities, as a shape parameter of the mean velocity profile and a thickness parameter, may be determined. (In most known approaches, this shape parameter is considered constant). Calculated local and averaged wall friction coefficients for the flat plate flow agree fairly well with reliable experimental data obtained by force measurement.

Finally the hypersonic wind tunnel tests of LOBB, WINKLER and PERSH [11] and of WINKLER and CHA [41] are critically discussed. It is found that at least the energy law governing the relation between the velocity and temperature field is strongly violated. In addition it is shown that the wall slope evaluation for determining the local wall friction coefficient involves large uncertainties.

A new empirical law for the wall friction coefficient c_f suggested by WINKLER and CHA [41] is discussed in the light of the foregoing theoretical considerations.

Introduction

When changing over from incompressible to compressible flow, the theoretical and experimental treatment of turbulent boundary layer flow involves some specific problems additional to those pointed out in the contribution of Prof. KESTIN and Mr. ROTTA.

Among these additional problems ,the following ones appear to be of principal interest :

1. The influence of compressibility and heat transfer on the turbulent motion across boundary layers.
2. The influence of compressibility and heat transfer on the mean velocity and temperature distribution across boundary layers.
3. Generalization of empirical laws for wall friction and dissipation.
4. Integral conditions for momentum and energy.
5. Calculation of heat transfer.
6. Critical notes on hypersonic boundary layer surveys.

Items 1. and 2. have been thoroughly treated within the section of Prof. KOVASZNAY, especially by the contribution of Prof. MORKOVIN. Hence, in the present contribution main interest may be focussed on the items 3. to 6. which are central problems of aero-space engineering. It may, however, be useful to review briefly in chapter 1. and 2. of the present contribution some outstanding physical facts and relations needed as a basis for the subsequent considerations.

1. The influence of compressibility and heat transfer on the turbulent motion across boundary layers

Recent information from refined theoretical and experimental research about this problem essentially due to KOVASZNAY, MORKOVIN et al. [1], [2], [3] (for detailed references see the contributions of the mentioned authors) suggests the conclusion that the turbulent motion in a compressible boundary layer in presence of heat transfer and dissipation is very similar to the turbulent motion in the incompressible case. The limit for this similarity appears to be reached when the velocity fluctuations themselves have sonic or supersonic speed. (Former conjectures in this direction see for instance [4]). This limiting case is generally present when the free stream MACH-number exceeds the value 4 or 5 as may easily be estimated by PRANDTL's mixing length theory [4]. Probably this limit will be identical with the beginning of energy sound radiation with an order of magnitude comparable with the energy of the turbulent motion or the dissipation as may be conjectured with regard to the contribution of J. LAUFER.

2. The influence of compressibility and heat transfer on the mean velocity and mean temperature distribution across boundary layer

2.1. *Classical similarity concepts.*

It is undoubtlessly due to the above stated features of similarity between the compressible and incompressible turbulent motion that measurered shear stress and mean velocity distributions in supersonic turbulent boundary layers are very similar to those observed in incompressible turbulent boundary layers. Surprisingly, even up to hypersonic free stream MACH numbers between 5 and 9 there are, roughly checked, no outstanding differences between compressible and incompressible types of mean velocity distributions, even in presence of heat transfer as is evident by the comparison demonstrated in fig. 1. The only noticeable deviation is a thickening of the laminar sublayer with increasing MACH number, while the main outer portion of the velocity distribution follows in both the incompressible and compressible cases very closely a power-law with wall distance.

This gross similarity concept between compressible and incompressible mean velocity profiles has proved to be a rather good basis for engineering theories, aiming at wall friction and heat transfer estimations in connections with other more or less accurate assumptions and empirical relations. Some important facts related to this gross similarity concept will be summarized in chapter 2.2 with regard to the considerations about engineering theories in chapter 3 to 5. We must, however, appreciate here the intense efforts of many authors to clarify the physical background of this similarity — as the ideal aim — to set up similarity theories analogous to those proved successfully in the incompressible field, for instance basing upon the two layer concept of the turbulent boundary layer.

As already outlined by Prof. MORKOVIN, some authors (i. e. COLES [5], HILL [6], FENTER and STALMACH [7]) proposed a simple generalisation of the " law of the wall ", such that the similarity function remains the same as in the incompressible case,

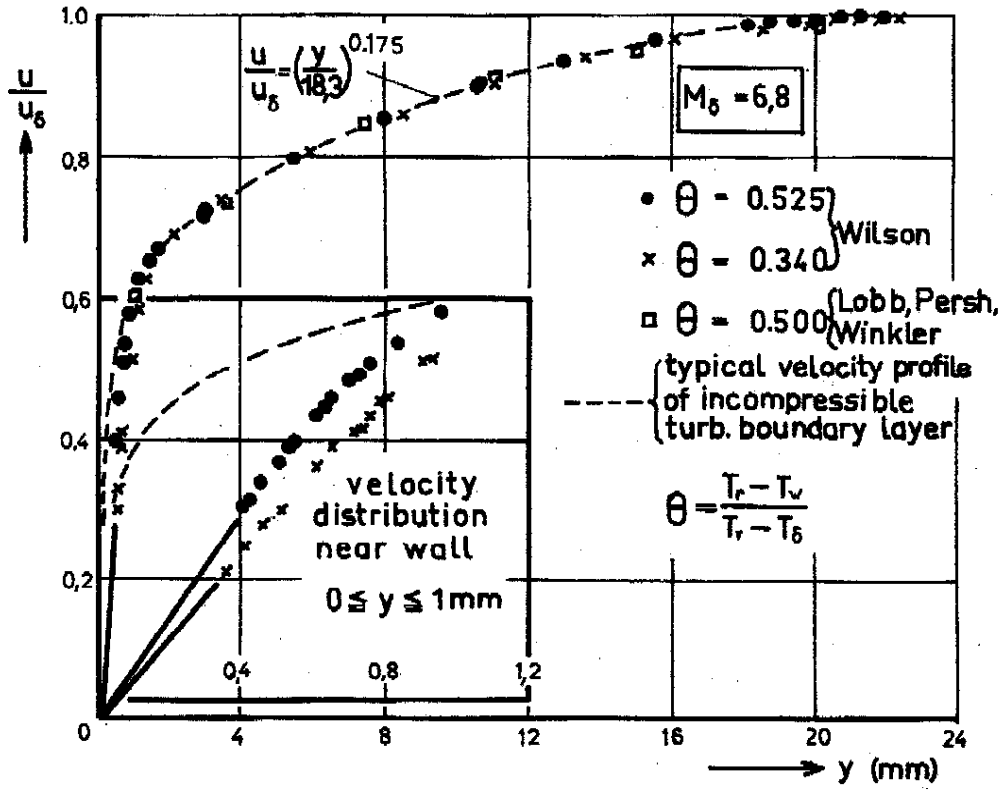

FIGURE 1
Comparison of typical velocity profiles of turbulent boundary layers at hypersonic and low speeds.

Comparison with experiments seems to confirm such approaches as turns out from fig. 2, which gives a reproduction of the results of HILL [6]. In fig. 2 the dimensionless velocity $\frac{u}{u_\tau}$ is plotted versus the dimensionless wall distance

$$\eta = \frac{y u_\tau}{\nu_w}, \tag{1}$$

where

$$u_\tau = \sqrt{\frac{\tau_w}{\rho_w}} \tag{2}$$

is the shear velocity and

$$\nu_w = \frac{\mu_w}{\rho_w} \tag{3}$$

is the kinematic viscosity formed with the viscosity μ_w and the density ρ_w at the wall. The relations

$$\frac{u}{u_\tau} = \eta \tag{4}$$

for the laminar sublayer as well as for the " law-of-the-wall " region

$$\frac{u}{u_\tau} = f(\eta) = 5{,}5 + 5{,}75 \log_{10}(\eta) \tag{5}$$

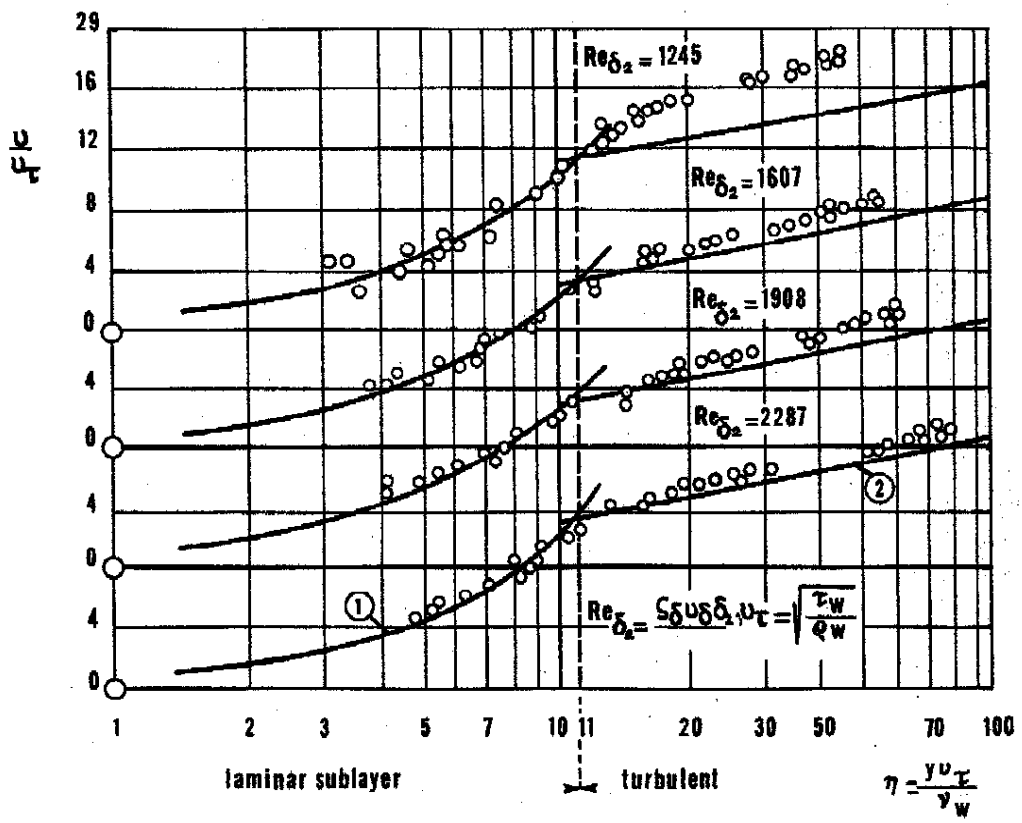

FIGURE 2

The law of the wall and the laminar sublayer in a hypersonic flow, $M_\delta = M_\infty = 9$, with small favorable pressure gradient. Comparison of theory and experiment according to HILL [6]. 1 from equ. (4), 2 from equ. (5).

are identical with the corresponding relations for incompressible turbulent boundary layers when u_τ and ν_w are defined with (2) and (3).

Recently, ROTTA [9] [10] promoted the research on this field by generalizing the two-layer similarity concept, assuming that the similarity function of the law of the wall is influenced by compressiblity and by the rate of heat transfer. This generalization was also extended to the velocity-defect law of the outer portion of the velocity profile and to the relations for the mean temperature profile.

ROTTA's generalization of the *law of the wall* writes :

$$\frac{u}{u_\tau} = f_1 \left[\eta, M_\tau, \beta_q, (Pr_t, \kappa, \omega)\right] ; \tag{6}$$

Pr_t = turbulent PRANDTL number, $\kappa = \frac{C_p}{C_v}$ = ratio of specific heats.

ω = power of the viscosity law.

The two new parameters M_τ and β_q permit to account for explicit influences of MACH number and heat transfert on $\frac{u}{u_\tau}$. The definitions are :

$$M_\tau = \frac{u_\tau}{a_w} ; \qquad a_w = \text{speed of sound at wall conditions} \tag{7}$$

$$\beta_q = \frac{q_w}{\rho_W u_\tau c_p T_w} \; ; \; q_W = -\left(\lambda \frac{\partial T}{\partial y}\right)_W = \text{heat flux at the wall} \tag{8}$$

For $M_\tau \to 0$, $\beta_q \to 0$, the similarity function f_1 becomes identical with the function f, equ. (5), of the incompressible case.

Equ. (6) involves two constants of integration, which must be determined as functions of the parameter M_τ and β_q by comparison of the new theory with experiments.

To establish generalized relations for the velocity defect law and the mean temperature distribution, tangential joining conditions for the inner and outer parts of both the velocity and temperature distribution must be fulfilled. This leads to rather complicate relations with some additional constants, which again must be determined from experiments.

Another, physically very transparent approach solving this problem was published recently by DEISSLER and LOEFFLER [42]. This approach includes a variation of the similarity functions with frictional-heating. MACH number, REYNOLDS number and heat transfer respectively.

The only experiments recently available to ROTTA and DEISSLER-LÖFFLER for checking the above-mentioned theories or for determining empirical constants have been those of LOBB, WINKLER, PERSH [11], and of HILL [6].

As already noticed by Prof. MORKOVIN, these very difficult experiments display discrepancies and probable errors (we will refer to this question in chapter 6.). Hence, some reasonings and conclusions implied in the approaches of the above-mentioned authors, related to these and similar experiments, must be regarded with caution.

Thus, we are led to the somewhat unsatisfactory conclusion that actually it is rather difficult to decide which generalized form of the similarity laws, governing the mean velocity and temperature distribution of compressible turbulent boundary layers with heat transfer is the most reliable one.

2.2. *Engineering similarity concept.*

2.2.1. *General remarks.*

The lack of better knowledge, on the one hand, and actual technological interest in approximate solutions or even rough estimations, on the other hand, have stimulated many studies in the field of compressible turbulent boundary layers, which are based on a simplified concept of mean velocity and temperature distribution. There are indeed some theoretical justifications for such attempts :

a) Calculations of wall friction, heat transfer and separation behaviour of turbulent boundary layers along surfaces with arbitrary pressure distributions must be based upon integral conditions for momentum and energy. The integral terms occurring in these equations, as the displacement thickness δ_1, the momentum-loss thickness δ_2, and the energy-loss thickness δ_3 as well as the ratios $\frac{\delta_1}{\delta_2}$ and $\frac{\delta_3}{\delta_2}$ (in the special definitions (75) (76) mostly used as shape parameters of the velocity profile) prove to be not sensible to uncertainties in the course of the velocity profile, especially to those near the wall. Hence the wall slope $\left(\frac{\partial u}{\partial y}\right)_w$ as a property of the velocity profile near the wall may be

varied in a wide range without practically influencing the shape parameter of the velocity profile. Consequently, the gain of accuracy in the final results, to be expected by considering last refinements in the two-layer concept theory, is in general not noticeable.

b) The local wall friction coefficient $c_f = 2\frac{\tau_w}{\rho_\delta u_\delta^2}$ may be measured directly without exact knowledge of the velocity distribution near the wall (i.e. of the wall stope $\left(\frac{\partial u}{\partial y}\right)_w$), for instance by a thermal wall element as used by LUDWIEG-TILLMANN [12] in the incompressible case or by a mechanical skin-friction element (local wall force measurement), as it was employed recently by MATTING, CHAPMAN, NYHOLM and THOMAS [8]. Hence, c_f may be determined and represented as a function of gross boundary layer properties like the shape parameter of the main outer part of the velocity profile and a local REYNOLDS number, for instance formed with the momentum-loss thickness δ_2.

c) For PRANDTL numbers near unity, as existing in turbulent boundary layers of gases, the temperature T and velocity u are uniquely related (see VAN DRIEST (C. C. LINJ [13], SPENCE [17]). Therefore, with given velocity profiles the temperature profiles are known with adequate accuracy (see 2.2.3.).

2.2.2. *Two-parameter concept of turbulent velocity boundary layers.*

With regard to the above statements, a " two-parameter concept " as a suitable base for representing and calculating turbulent boundary layers including the compressible case with heat transfer and streamwise pressure gradient is suggested as follows :

a) The full turbulent portion of all velocity profiles observed in incompressible and compressible turbulent boundary layers (hence the portion related to the region of the law of the wall and the defect law) may be represented by a one-parametric family of curves

$$\frac{u(x,y)}{u_\delta(x)} = f\left[\frac{y}{\delta(x)}, \mathrm{H}(x)\right]. \tag{9}$$

$\delta_L < y < \delta$; $\delta_L \ll \delta$

δ_L = thickness of the laminar sublayer

u_δ is the velocity at the outer edge $y = \delta$ of the boundary layer, and H is a shape parameter of the velocity profile, which may be defined arbitrarily. For flows with zero or moderate streamwise pressure gradient the power law

$$\frac{u(x,y)}{u_\delta(x)} = \left(\frac{y}{\delta(x)}\right)^{k(\mathrm{H})}; \quad \delta_L < y < \delta \tag{10}$$

is found by many authers to fit the outer part of measured velocity profiles very closely (see Fig. 1). A theoretical interpretation of this somewhat surprising fact was given by LUDWIEG and TILLMANN [12] (pages 295-296 of this reference).

As was shown by PRETSCH [15], relation (10) is also applicable to turbulent boundary layers in flows with favorable and adverse pressure gradients, the range of the power k then being about

$$0{,}1 < k < 0{,}7 \tag{11}$$

wehre $k \approx 0{,}6$ characterizes the velocity profile near turbulent separation. The power k is uniquely related to any other properly defined shape parameter H.

b) The relative thickness $\frac{\delta_L}{\delta}$ of the laminar sublayer is assumed to be a function of the local friction coefficient c_f only. When smooth surfaces are considered (we will confine all following derivations to this practically most interesting case), c_f may be replaced by a suitably defined local REYNOLDS number R, according to empirical relations formed with a characteristical boundary layer thickness term.

Since $\frac{\delta_L}{\delta}$ decreases with increasing REYNOLDS number R, we may assume the phenomenological relation

$$\frac{\delta_L}{\delta} = f\left(\frac{1}{R}\right) \tag{11a}$$

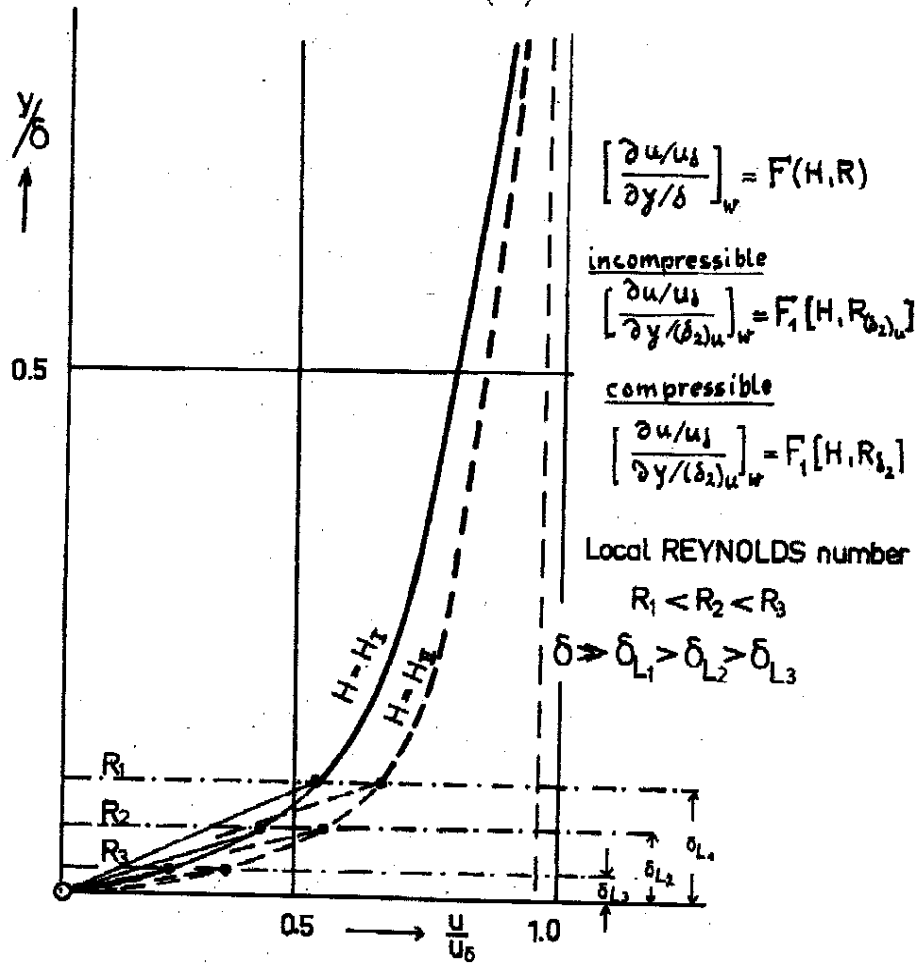

FIGURE 3

Schematic illustration of the two-parameter concept for turbulent boundary layers.
R = local REYNOLDS number, formed with the momentum-loss thickness or the flow length.
δ_L = thickness of the laminar sublayer (schematicly increased).
H = form parameter of the velocity profile.

c) With the statements of *a*) and *b*), the total boundary layer profile may be composed of the laminar sublayer $0 < y < \delta_L$ and the outer fully turbulent part $\delta_L < y < \delta$, with or without tangential joining conditions at $y = \delta_L$,as schematically illustrated in fig. 3.

With this concept the slope

$$\left[\frac{\partial\left(\frac{u}{u_\delta}\right)}{\partial\left(\frac{y}{\delta}\right)_w}\right]$$

is a function of the shape parameter H and the REYNOLDS number R,

$$\left(\frac{\partial u/u_\delta}{\partial y/\delta}\right)_w = F(H, R)\,, \tag{11b}$$

whether the velocity u within the laminar sublayer is varying linearly with the wall distance y [1] (as drawn in fig. 3) or not. *According to this concept, the turbulent velocity profile is, strictly regarded, characterized by two parameters, H and R which may principally vary independently from each other. R indeed has in a first approximation — because of* $\delta_L \ll \delta$ *— no influence on the integral terms* δ_1, δ_2, δ_3, $\frac{\delta_1}{\delta_2}$, $\frac{\delta_3}{\delta_2}$, *i. e. on H.*

d) The parameters H and R or appropriate functions of them may be introduced as unknowns of an approximate boundary layer theory and determined by solving the simultaneous system of the integral conditions for momentum and energy, when the initial and external flow conditions are known (see 4.). With this solution the parameters H (x) and R (x) are uniquely related. Hence the composition of the velocity profile (and accordingly that of the temperature profile due to T (u)) can not accomplished before having solued the mentioned two-equation-system. *With this two-parameter concept the physically correct coupling of the quantites H and R or H and* $c_f = 2\frac{\tau_w}{\rho_\delta u_\delta^2}$ is automatically warranted by simultaneously satisfying both the integral conditions of momentum and energy [2].

A presupposition for applying these two integral conditions is the knowledge of the empirical laws for the wall friction and dissipation in compressible turbulent boundary layers with heat transfer and arbitrary streamwise pressure gradient (or other assumptions must be introduced). We deal with this question in chap. 3. Let us first precisely formulate the concept of the boundary layer according to the reasoning under 2.2.1*c*.

1. This is exactly true only for zero pressure gradient and constant temperature T within the sublayer. We will deal with this question under 6.3.

2. The quantities used in the classical theories of the two-layer concept (see for instance ROTTA [9] [10]) are functions of H and R, defined such that a certain coupling of H and R is anticipated. This anticipatory coupling is correct and physically comprehensible for equilibrium boundary layers and fairly correct for the flat plate boundary layers, but doubtful for all other flow types. Both mentioned special cases, however, are correctly included in the above two-parameter concept, as will turn out later on.

2.2.3. *Concept of the thermal boundary layer.*

Analogous to the case of compressible laminar boundary layers at a flat plate, an exact solution of the fundamental boundary layer equations for continuity, momentum and energy may be obtained also for compressible turbulent boundary layers with heat transfer [13] [14], when reasonable assumptions about the shear stress distribution $\frac{\tau}{\tau_w}\left(\frac{n}{u_\delta}\right)$ are introduced.

The essential details about this solution will be summarized in chapter 4.2. For Pr_t near unity, for instance $Pr_t \approx 0{,}9$ (as a value consistent with observed values of the recovery factor $r \approx 0{,}9$) and isothermal wall, $\frac{dT_w}{dx} = 0$, the solution $T(u)$ writes :

$$\frac{T}{T_\delta} = a + b\frac{u}{u_\delta} + c\left(\frac{u}{u_\delta}\right)^2 \tag{12}$$

with the abbreviations

$$a = 1 + r\frac{\kappa - 1}{2} M_\delta^2 (1 - \Theta) \; ;$$

$$b = \Theta r \frac{\kappa - 1}{2} M_\delta^2 \; ;$$

$$c = -r\frac{\kappa - 1}{2} M_\delta^2 \; ;$$

$$\left(\kappa = \frac{c_p}{c_v}\right)$$

where

$$\Theta = \frac{T_r - T_w}{T_r - T_\delta} \tag{17}$$

is the heat transfer parameter, T_r the recovery temperature and

$$r = \frac{T_r - T_\delta}{T_0 - T_\delta} \; ; \qquad \left(\frac{T_r}{T_\delta} = 1 + r\frac{\kappa - 1}{2} M_\delta^2\right) \tag{18) (19}$$

the recovery factor.

At adiabatic walls ($\Theta = 0$, $b = 0$) equ. (12) holds also for arbitrary streamwise gradients $\frac{dp}{dx}$. On the other hand, for zero pressure gradient equ. (12) is generally valid for any heat transfer rate. Hence, equ. (12) is a good approximation even in cases with moderate pressure gradient and arbitrary heat transfer. For determining the density profile

$$\frac{\rho}{\rho_\delta} = \frac{T_\delta}{T}\left(\frac{\partial p}{\partial y} = 0\right) \tag{19}$$

occurring in the integral terms δ_1, δ_2, δ_3, this approximation warrants sufficients accuracy. For calculating heat transfer rates, however, higher accuracy is desired. We will deal with an improvement of this approximation in chapter 5, including the case $\frac{dT_w}{dx} \neq 0$.

3. Generalization of empirical laws for wall friction and dissipation based upon incompressible flow conditions

3.1. *General remarks.*

The number of ideas and theories for computing turbulent wall friction and heat transfer rates in hypersonic flows are about as numerous as the investigators having dealt with this important problem. It is therefore impossible to give here a comprehensive survey (a statement of references up to date is given in [8]).

When we try to criticize the reasoning of the different authors, we find that the theories which give the best fitting with experimental data are not those with the best physically cleared background. Indeed, during the last years the experimental research on this field provided much new material for establishing empirical relations which predict wall friction coefficients over a wide range of Mach number, heat transfer rate and Reynolds number with surprising accuracy. One of these successful calculation methods is the so-called T' (reference temperature)-method originally developed by RUBESIN and JOHNSON [17] for laminar boundary layers and applied by FISHER and NORRIS [18] to turbulent boundary layers, later on improved by SOMMER and SHORT [19]. For comparison with experiments see for instance [8] and [19].

The author prefers to describe here in detail a method for solving the present problem, which involves (as he believes) a minimum of assumputions and no empirical constants determined from difficult and sometimes not reliable hypersonic boundary layer tests (see the remarks of Prof. MORKOVON and the discussions under 6.).

The method which will be described, is based upon well-founded and generally accepted half-empirical relations in the field of incompressible turbulent boundary layers. This analysis appears to be supported by recent informations about the turbulent motion in compressible flow, briefly reviewed in chapter 1 of this contribution. In addition, the two-parameter concept as displayed in chapter 2.2.2 and illustrated in fig. 3, is involved in the physical idea of generalization.

3.2. *The generalized wall friction law.*

3.2.1. *Basic relation for incompressible flow.*

There exist some empirical relations for the wall friction coefficient in a flow without pressure gradient, practically equivalent with regard to accuracy, namely (in chro. sequence and perhaps not complete) : The formulae of PRANDTL [20], v. KARMAN-SCHOENHERR [21], PRANDTL-SCHLICHTING [22], SCHULTZ-GRUNOW [23], LUDWIEG-TILLMANN [12], ROTTA [24].

Different modes of representation of these laws are used. The *local* friction coefficient

$$c_{f_i} = 2\frac{\tau_w}{\varrho_\delta u_\delta^2} \quad (u_\delta = u_\infty;\ \varrho_\delta = \varrho_\infty,\ \text{when}\ \frac{dp}{dx} = 0) \tag{20}$$

or the *average* friction coefficient

$$C_{F_i} = \int_0^1 c_{f_i}\, d\left(\frac{x}{L}\right) \qquad (L = \text{flat-plate length}) \tag{21}$$

are expressed as functions of the Reynolds numbers

for c_{f_i} : $R_x = \frac{\rho_\delta u_\delta x}{\mu_\delta}$ ($u_\delta = u_\infty$, $\rho_\delta = \rho$, $\mu_\delta = \mu_\infty$) (x = turbulent flow-length) (22)

for C_{F_i} : $R_L = \frac{\rho_\infty u_\infty L}{\mu_\infty}$ (23)

For representing the local friction coefficient c_{f_i} some authors [12] [23] prefer to use a Reynolds number defined with the local momentum-loss thickness $(\delta_2)_u$ [equ. (28)] instead of the flow length x, last but not least because of the difficulties and uncertainties of experimental data reduction needed in connection with the R_x-representation (see for instance [8] and [19]).

Undoubtlessly the most general and — from the mathematical point of view — most convenient representation of the wall friction law is that developed by Ludwieg and Tillmann [12]. This law is characterized by the following advantageous features :

a) It is valid in flows with arbitrary pressure gradient $\frac{dp}{dx}$.

b) Its dependence on $\frac{dp}{dx}$ was deduced theoretically only basing upon the similarity law of the wall for the flat plate $\left(\frac{dp}{dx} = 0\right)$ and was completely confirmed by direct wall friction measurements with the « thermal wall element ».

c) It appears well adapted to the planned generalization on the field of compressible turbulent boundary layers with heat transfer and streamwise pressure gradient.

In its original form for incompressible flow this law writes as follows :

$$c_{f_i} = 2\frac{\tau_w}{\rho_\delta u_\delta^2} = \frac{\alpha(H_{12})}{R^n_{(\delta_2)_u}}\ ; \quad n = 0{,}268 \tag{24}$$

with

$$R_{(\delta_2)_u} = \frac{\rho_\delta u_\delta (\delta_2)_u}{\mu_w} \quad (\mu_w = \mu_\delta) \tag{25}$$

$$\alpha(H_{12}) = 0{,}246 \cdot 10^{-0{,}678\, H_{12}} \tag{26}$$

$$(\delta_1)_u = \int_0^\delta \left(1 - \frac{u}{u_\delta}\right) dy\ ;\ (\delta_2)_u = \int_0^\delta \frac{u}{u_\delta}\left(1 - \frac{u}{u_\delta}\right) dy \tag{27) (28}$$

$$H_{12} = \left(\frac{\delta_1}{\delta_2}\right)_u \tag{28a}$$

The function $\alpha(H_{12})$, equ. (26), was determined for smooth walls. For rough walls a somewhat modified relation would be found. As already indicated, we confine our considerations to the case of smooth surfaces.

A physical interpretation of equ. (24) in connection with the two-parameter concept of chapter 2.2.2 with fig. 3, useful for the planned generalizations, is readily established. Eq. (24) may be rewritten as follows :

$$c_{f_i} = 2\frac{\tau_w}{\rho_\delta u_\delta^2} = 2\frac{\left(\mu \frac{\partial u}{\partial y}\right)_w}{\rho_\delta u_\delta^2}\frac{(\delta_2)_u}{(\delta_2)_u} = 2\frac{\left[\frac{\partial u/u_\delta}{\partial y/(\delta_2)_u}\right]_w}{\frac{\rho_\delta u_\delta (\delta_2)_u}{\mu_w}} = 2\frac{\left[\frac{\partial u/u_\delta}{\partial y/(\delta_2)_u}\right]_w}{R_{(\delta_2)_u}} \tag{29}$$

Equating (24) and (29) yields :

$$\left[\frac{\partial u/u_\delta}{\partial y/(\delta_2)_u}\right]_w = \frac{1}{2}\,\alpha\,(H_{12})\,[R_{(\delta_2)}]_u^{1-n} = F\,[H_{12}, R_{(\delta_2)_u}] \tag{30}$$

Equation (30) is in its physical sense identical with equ. (11*b*). The reasoning under 2.2.2, however, is now refined in so far as suitable definitions for the shape parameter $H \equiv H_{12}$ and $R \equiv R_{(\delta_2)_u}$ are introduced. Indeed, from equ. (30) we learn that the dimensionless slope of the velocity at the wall increases with the Reynolds number $R_{(\delta_2)_u}$ such that, together with the denominator $[R_{(\delta_2)_u}]^1$ in equ. (29) c_{f_i} decreases with the n^{th} power of $R_{(\delta_2)_u}$. The function $\alpha\,(H_{12})$ decreases with increasing shape parameter H_{12}. This happens in flows with adverse pressure gradient. Approaching turbulent separation $\alpha\,(H_{12})$ takes values near zero and c_{f_i} tends to zero for any value $R_{(\delta_2)_u}$. The thickness δ_L of the laminar sublayer which is important in the two-parameter concept of fig. 3, does not explicitely occur in equ. (30).

In the defining equ. (25) for $R_{(\delta_2)_u}$, we have quite formally written the density ρ with subscript δ and the viscosity μ with the subscript w with regard to the definition of c_{f_i} in equ. (24) and (29). The chosen distinguishing designation of μ and ρ, however, proves to be instructive and decisive for the considerations in the following chapter.

3.2.2. *Generalizing idea.*

The local friction coefficient c_f in a compressible turbulent boundary layer with heat transfer is formally identical with the first term of (29), defined as

$$c_f = 2\,\frac{\tau_w}{\rho_\delta\, u_\delta^2} \tag{31}$$

For the further reasoning, however, we must keep in mind the following differences between incompressible and compressible boundary layer flow :

a) The local Reynolds number R_{δ_2} as the ratio of the *averaged* momentum loss to the wall-shear stress τ_w or as a ratio of functions of these two physical quantities, i. e.

$$\frac{\rho_\delta\, u_\delta^2 \dfrac{\delta_2}{\delta}}{\mu_w \dfrac{u_\delta}{\delta}} = \frac{\rho_\delta\, u_\delta\, \delta_2}{\mu_w} = R_{\delta_2} \tag{32}$$

must be defined with the real momentum-loss thickness

$$\delta_2 = \int_0^\delta \frac{\rho\, u}{\rho_\delta\, u_\delta}\left(1 - \frac{u}{u_\delta}\right) dy\,, \tag{33}$$

such that the product $\rho_\delta\, u_\delta^2\, \delta_2$ gives the real averaged momentum loss. (The real wall shear-stress is in any case proportional to the molecular viscosity μ_w at the wall).

It is, therefore, obvious that the definition (32) for R_{δ_2} must contain in the nominator the quantity ρ_δ and in the denominator quantity μ_w.

b) The dimensionless wall slope of the velocity profile is not explicitly dependent upon Mach number and heat transfer. The justification for this assumption is as follows :

The turbulent motion is sensitive to the flow-medium-properties ρ and μ, which are influenced, indeed, by the temperature distribution through the boundary layer, regardless to the source of the temperature field. The only decisive parameter for the turbulent motion is the Reynolds number in which the influence of varying values ρ and μ with Mach number and heat transfer is conglomerated. This assumption (the only assumption of this theory) appears valid until the turbulent motion itself exceeds the sound speed limit (see chapter 1).

Hence, as characteristical length in the compressible version of equ. (30) for the wall slope, we cannot use the real momentum-loss thickness δ_2, as defined with (33), because this quantity depends upon M_δ and Θ, due to the factor $\frac{\rho}{\rho_\delta}$. We must choose a quantity (a length), which is uniquely related to geometrical proportions of the velocity profile, for instance the length $(\delta_2)_w$, defined with equ. (28). The thickness δ_L of the laminar sublayer, however, is controlled by the Reynolds number R_{δ_2}, defined with (32), as a dynamic quantity. Consequently, for compressible turbulent boundary layers with heat transfer, the dimensionless wall slope must be introduced as

$$\left[\frac{\partial u/u_\delta}{\partial y/(\delta_2)_w}\right] = F(H_{12}, R_{\delta_2}) = \frac{1}{2}\alpha(H_{12})\, R_{\delta_2}^{1-n}, \tag{34}$$

where F and $\alpha(H_{12})$ are the same functions as in the incompressible case, equ. (30). The only difference between equ. (34) and equ. (30) consists in the definition of the Reynolds number R_{δ_2}. It is important to note here that with this definition of R_{δ_2} (with μ_w in the denominator), the slope decreases with increasing wall temperature, hence with Mach number at adiabatic walls, which is consistent with experimental results [6] [11] [14]. Accordingly with decreasing R_{δ_2} the thickness of the laminar sublayer increases. Therefore, equ. (11*a*) writes

$$\frac{\delta_L}{\delta} = \Psi\left(\frac{1}{R_{\delta_2}}\right) \tag{34a}$$

The properties of the function Ψ may be studied in two limiting cases, $R_{\delta_2} \to \infty$ and $R_{\delta_2} \to 1$. For $R_{\delta_2} \to \infty$ we must expect that the turbulent diffusion towards the wall increases in such an amount that holds

$$R_{\delta_2} \to \infty\ ; \qquad \frac{\delta_L}{\delta} \to 0 \tag{34b}$$

For $R_{\delta_2} \to 1$ the zone of the influence of the molecular viscosity will have spread in y-direction and have damped the turbulent motion so strongly that (in accordance with known results of the stability theory) the turbulent part of the boundary layer is vanishing. Hence we may expect that yields

$$R_{\delta_2} \to 1\ ; \qquad \frac{\delta_L}{\delta} \to 1 \tag{34c}$$

From (34*c*) and (34*a*) the order of magnitude of $\frac{\delta_L}{\delta}$ may be estimated as

$$\frac{\delta_L}{\delta} \sim \frac{\delta_L}{\delta_2} \sim \frac{1}{R_{\delta_2}} = \frac{\frac{\mu_w}{\rho_\delta u_\delta}}{\delta_2} \tag{34d}$$

with

$$\delta_L \sim \frac{\mu_w}{\rho_\delta u_\delta} \tag{34e}$$

We now come back to equ. (31) which, analogous to equ. (29), may be formally written with consideration of (34) as follows :

$$c_f = 2\frac{\tau_w}{\rho_\delta u_\delta^2}\frac{\delta_2}{\delta_2} = 2\frac{\left[\dfrac{\dfrac{\partial u}{u_\delta}}{\partial y}\right]_w}{\dfrac{\rho_\delta u_\delta \delta_2}{\mu_w}}\frac{\delta_2}{(\delta_2)_u} = \frac{\alpha(H_{12})\,R_{\delta_2}^{1-n}}{R_{\delta_2}}\frac{\delta_2}{(\delta_2)_u} \tag{35}$$

$$= \left\{\frac{\alpha(H_{12})}{R_{\delta_2}^n}\right\}\frac{\delta_2}{(\delta_2)_u}\,; \quad n = 0.268$$

Equ. (35) permits the following important conclusion :

a) The term in parenthesis is formally identical with the original law of LUDWIEG-TILLMANN for incompressible flow with zero heat transfer, equ. (24), when the general definition (32) for R_{δ_2} is also accepted for incompressible flow. Indeed, $R_{(\delta)_u}$ defined by (25), is a special form of (32), viz.

$$R_{(\delta_2)_u} = (R_{\delta_2})_{M_\delta = 0,\,\Theta = 0} \tag{36}$$

The function $\alpha(H_{12})$ is given with equ. (26), while equ. (28*a*) holds for H_{12}, as a pure shape-parameter. We avoid to replace in (35) the expression $\dfrac{\alpha(H_{12})}{R_{\delta_2}^n}$ by c_{f_i}, equ. (24), because in a related incompressible case H_{12} may have another value than in the compressible case.

b) The explicit influence of MACH number and heat transfer is concentrated in the ratio $\dfrac{\delta_2}{(\delta_2)_u}$, which, for a oneparametric family of velocity profiles, for instance according to equ. (9), and with a correlated temperature profile described by equ. (12), is a known universal function of the parameters H_{12}, M_δ and Θ. This function tends to zero with $M_\delta \to \infty$ (see 4.4, equ. (90)) and to unity for $M_\delta \to 0$.

We should like to emphasize that with the introduction of the quantities $(\delta_1)_u$ *and* $(\delta_2)_u$, *equ. (27) and (28), no reference or transformation to a corresponding incompressible case is made. All quantities* $(\delta_1)_u$, $(\delta_2)_u$, δ_1 *and* δ_2 *are related to the same velocity profile and to the same total boundary layer thickness* δ *occurring in the compressible case.*

For computing the local wall friction coefficient for a given problem as a function of x, the local values of $R_{\delta_2}(x)$ and $H_{12}(x)$ must be known by solving the system of interal conditions derived in chapter 4. The average wall friction coefficient C_F then follows by integration from (21).

Before dealing with this problem, we will derive a generalized expression for the dissipation integral for turbulent boundary layers. This generalization or — instead of this — physically more difficult assumptions are needed, when it is intended to use

the integral condition for energy for compressible boundary layers. For comparison of theoretical and experimental wall friction data we refer to chapter 4. and 6.

3.3. *The generalized law for the dissipation integral.*

For the dissipation integral d within turbulent (and laminar) boundary layers yields :

$$d = \int_0^{u_\delta} \tau \, du \tag{37}$$

or in dimensionless terms :

$$c_D = \frac{d}{\rho_\delta u_\delta^3} = \frac{\tau_W}{\rho_\delta u_\delta^2} \int_0^1 \frac{\tau}{\tau_W} d\left(\frac{u}{u_\delta}\right) = \frac{1}{2} c_f \int_0^1 \frac{\tau}{\tau_W} d\left(\frac{u}{u_\delta}\right) \tag{38}$$

Equ. (38) expresses the proportionality of c_D and c_f. Since c_f is known with equ. (35), it remains to study the behaviour of the dimensionless dissipation integral-term in (38). For this let us first consider the incompressible case. Evaluations of numerous experimental data performed by ROTTA [24] and rearranged in terms of H_{12} and $R_{(\delta_2)_u}$ by TRUCKENBRODT [25] have led to the following semi-empirical relation :

$$c_{D_i} = \frac{\beta\,(H_{12})}{R_{(\delta_2)_u}{}^N} \approx \frac{\beta}{(R_{(\delta_2)_u})^N} = \frac{1}{2}(c_f)_i \left[\int_0^1 \frac{\tau}{\tau_W} d\left(\frac{u}{u_\delta}\right)\right]^i$$

with

$$N = 0{,}168 \text{ and } \qquad \beta = 0{,}0056 \tag{40) (41}$$

where $R_{(\delta_2)_u}$ is defined with (25). Equ. (39) expresses that c_{D_i} is practically independent of the shape parameter of the velocity profile. This is a very noticeable feature [1].

With equ. (24), the dissipation integral term in equ. (39) may be written as :

$$\left\{\int_0^1 \frac{\tau}{\tau_W} d\left(\frac{u}{u_\delta}\right)\right\} = 2\frac{c_{D_i}}{c_{f_i}} = \frac{2\beta}{\alpha(H_{12})} R_{\delta_2}^{n-N} = \Phi\,[H_{12}, R_{(\delta_2)_u}]\,; \tag{42) (43}$$

$$n - N = 0{,}1$$

There is a certain similarity between equ. (42) and (30) insofar as in the compressible case both the wall slope term (30) and the dissipation integral term (42) may be assumed to be not explicitly dependent upon MACH number and heat transfer by the arguments displayed under 3.2.2*b*.

Hence, we may write for the compressible case

$$\int_0^1 \frac{\tau}{\tau_w} d\left(\frac{u}{u_\delta}\right) = \Phi(H_{12}, R_{\delta_2}) = 2\frac{\beta}{\alpha(H_{12})} R_{\delta_2}^{n-N}, \tag{44}$$

where R_{δ_2} again is defined with equ. (32) and $2\frac{\beta}{\alpha(H_{12})}$ is the same function as in the incompressible case. The use of R_{δ_2} in the definition (32) (with μ_w in the denominator) may be physically motivated by the fact that the maximum of dissipation indeed occurs within or near the laminar sublayer, where $\mu \approx \mu_w$.

1. It may be noticied here, that equ. (39) is, indeed, one of the most important relations of turbulent boundary layer theory and a key to the use of the integral conditions for the energy. Thus, the empirical equations of GRUSCHWITZ [26] and v. DOENHOFF-TETERVIN [27] with limited validity may be replaced by an integral condition of general validity.

Now, we introduce (44) and (35) into (38), and find the generalized form of the dissipation law as

$$c_D = \frac{\beta\,(H_{12})}{(R_{\delta_2})^N}\cdot\frac{\delta_2}{(\delta_2)_u} \approx \frac{\beta}{(R_{\delta_2})^N}\cdot\frac{\delta_2}{(\delta_2)_u}\,; \qquad \begin{matrix}\beta = 0{,}0056\\ N = 0{,}168\end{matrix} \tag{45}$$

Again, the influence of MACH number and heat transfer is contained in the universal function $\frac{\delta_2}{(\delta_2)_u} = \frac{\delta_2}{(\delta_2)_u}(H_{12}, M_\delta, \Theta)$. An analytic expression see 4.4, equ. (90).

With the generalized relations (35) and (45) for wall friction and dissipation, combined with the expressions (10) and (12) for the velocity and temperature profile, we are enabled to make use of the integral conditions for momentum and energy. We need, indeed, only these two equations, since all above mentioned expressions only contain the two unknows H_{12} and R_{δ_2} as variables, while the parameters $M_\delta(x)$ and $\Theta(x)$ may be supposed to be given with any special problem.

In the following chapter 4, we will derive a form of these equations, which appears suitable for both theoretical inlook and engineering calculations.

4. Integral conditions for momentum and energy

4.1. *Basic equation system.*

We base upon PRANDTL's simplifying boundary layer assumptions and introduce, with reference to the reasoning of VAN DRIEST [13], temporal mean values for all physical quantities participating in the turbulent motion. Thus, the fundamental equations for the conservation of mass, momentum and energy in a two-dimensional mean steady-state flow write in usual terms as follows :[1]

$$\frac{\partial(\rho u)}{\partial x} + \frac{\partial(\rho v)}{\partial y} = 0 \qquad \text{continuity} \tag{46}$$

$$\rho u\frac{\partial u}{\partial x} + \rho v\frac{\partial u}{\partial y} = -\frac{dp}{dx} + \frac{\partial \tau}{\partial y} \qquad \text{momentum} \tag{47}$$

$$\rho u\frac{\partial i}{\partial x} + \rho v\frac{\partial i}{\partial y} = u\frac{dp}{dx} + \tau\frac{\partial u}{\partial y} + \frac{\partial}{\partial y}\left(\frac{\lambda}{c_p}\frac{\partial i}{\partial y}\right) \qquad \text{energy} \tag{48}$$

Boundary conditions : $y = 0 : u = 0,\ v = 0;$
$i = i_w$
$y = \delta_u : u = u_\delta;$
$y = \delta_t : i = i_\delta$

i = enthalpy;
δ_u = thickness of the velocity boundary layer;
δ_t = thickness of the thermal boundary layer.

In addition holds

$$\tau = (\mu + \varepsilon_\tau)\frac{\partial u}{\partial y} \tag{49}$$

1. For simplicity we resign to indicate the temporal averaging process by bars, since other than temporal mean values do not occur in this analysis.

$\mu =$ molecular viscosity
$\varepsilon_\tau =$ eddy viscosity
$c_p =$ specific heat at constant pressure
$\lambda =$ effective heat conductivity (including eddy heat diffusity)

For perfect gases additional equations are available as the equation of state

$$i = c_p T \qquad g = \text{earth acceleration} \tag{50}$$

$$p = \rho g \mathcal{R} T \qquad \mathcal{R} = \text{gas constant} \tag{51}$$

$$\mu(T) = 1{,}486 \cdot 10^{-7} \frac{T^{3/2}}{T + 110{,}4};$$

(T in [°KELVIN], μ in [kg.sec./m^2])

Further more, the mean value of the turbulent PRANDTL number across the boundary layer

$$Pr_t = \frac{\varepsilon_\tau}{\frac{\varepsilon_q}{c_p}}; \qquad \varepsilon_q \equiv \lambda = \text{eddy heat diffusity} \tag{53}$$

is known [1]

4.22. *Exact solution for the temperature profile* $\frac{T}{T_\delta}$.

Following VAN DRIEST's analysis for flat plate flow $\left(\frac{dp}{dx} = 0\right)$ and isothermal wall $\left(\frac{dT_w}{dx} = 0\right)$, an exact solution for the temperature profile $\frac{T}{T_\delta}$ may be obtained from the simultaneous system of equations (46) (47) (48) :

$$\frac{T}{T_\delta} = 1 + \frac{T_r - T_w}{T_\delta}(f_1 - 1) + r\frac{\kappa - 1}{2} M_\delta^2 (1 - f_2) \tag{54}$$

where the abbreviations f_1 and f_2 are defined as

$$f_1 = \frac{\Sigma}{s}; \qquad f_2 = 2\frac{P}{r} \tag{55) (56}$$

with

$$\Sigma = Pr_t \int_0^{u/u_\delta} \left(\frac{\tau}{\tau_w}\right)^{Pr_t - 1} d\left(\frac{u}{u_\delta}\right);$$

$$P = Pr_t \int_0^{u/u_\delta} \left(\frac{\tau}{\tau_w}\right)^{Pr_t - 1} \left[\int_0^{u/u_\delta} \left(\frac{\tau}{\tau_w}\right)^{1 - Pr_t} d\left(\frac{u}{u_\delta}\right)\right] d\left(\frac{u}{u_\delta}\right)$$

and

$$(\Sigma)_0^1 = s = \text{REYNOLDS analogy factor} \tag{59}$$

$$2(P)_0^1 = r = \text{recovery factor} \tag{60}$$

1. An interesting, but not well-known theoretical investigation about the value of Pr_t by use of the theory of probability was published in 1949 by K. ELSER [28]. The result is

$$Pr_t = \sqrt{\frac{8}{3\pi}} = 0{,}921$$

which reasonably agrees with the experimental findings.

For PRANDTL numbers near unity, especially for $Pr_t \approx 0{,}9$, the functions f_1 and f_2 are very closely described by

$$f_1 \approx \frac{u}{u_\delta}; \qquad f_2 \approx f_1^2 \approx \left(\frac{u}{u_\delta}\right)^2 \tag{61) (62}$$

and equ. (54) reduces to the quadratic polynomial in $\frac{u}{u_\delta}$ as already noticed under 2.2.3,

$$\frac{T}{T_\delta} = a + b\frac{u}{u} + c\left(\frac{u}{u_\delta}\right)^2 \tag{63}$$

where a, b, c are functions of the MACH number M_δ and the heat transfer parameter Θ defined with (13) through (16). Mean values of the REYNOLDS analogy factor s and the recovery factor r from equ. (59) and (60) (with special assumptions about the shear-stress distribution $\frac{\tau}{\tau_w}$) valid over a wide range of values M_δ and Θ, with a few per cent uncertainty, are

$$s = 0{,}85; \qquad r = 0{,}89 \tag{64) (65}$$

These values are also consistent with experimental data (see for instance [8]).

We refer to the reasoning displayed in chapter 2.2.3, from which follows that equ. (63) may be regarded as a good approximation even in cases with streamwise pressure gradients $\frac{dp}{dx}$ and gradients $\frac{dT_w}{dx} \neq 0$, when use is intended only for the evaluation of integral term occurring in the integral condition for momentum and energy. Because of $\frac{dp}{dx} = 0$, we have for the " density profile "

$$\frac{\rho}{\rho_\delta} = \frac{T_\delta}{T} \tag{66}$$

4.33. *Concept of approximate solution.*

The quasi-exact solution (63) for the temperature profile was possible for Pr_t near unity since the power $Pr_t - 1$ of $\frac{\tau}{\tau_w}$ is near zero, hence $\left(\frac{\tau}{\tau_w}\right)^{Pr_t - 1} \approx 1$. This means that the temperature profile is not sensible to the shear-stress distribution.

Therefore, the empirical character of the shear-stress distribution $\frac{\tau}{\tau_w}$ did not hamper the above solution for $\frac{T}{T_\delta}$, except the small influence of $\frac{\tau}{\tau_w}$ on the values s and r. (See also the findings of DEISSLER [42] about this question.)

For determining the velocity profile $\frac{u}{u_\delta}$ in the general case of compressible turbulent boundary layers with heat transfer and streamwise pressure gradient, it is difficult to aim at exact solutions with regard to the uncertainty involved in the shear-stress distribution $\frac{\tau}{\tau_w}$. (Many attempts in this direction have been started, among which

those of the ref. [10] [42] may be considered as typical and advanced ones). Hence, efforts for obtaining approximate solutions are of great importance. The classical way to promote this simplified problem, first proposed by Th. v. KARMAN [29], was indicated and prepared in chapter 2 and 3. It essentially consists in assuming the velocity profile $\frac{u}{u_\delta}$ to be a one-parametric family of curves according to equ. (9) or (10), correlated to the temperature profiles by (63), and introducing the half-empirical laws for wall friction and dissipation, equ. (35) and (45). The shape parameter $H(x)$ and the boundary layer thickness, as the two unknowns of the simplified problem, may then be determined by solving a simultaneous system of two 1. order differential equations : The integral conditions for momentum and energy. With these equations some important features of the system (46) (47) (48) are at least fulfilled in the average across the velocity — and thermal boundary layer.

4.4. *The system of two integral conditions.*

We introduce the following definitions (recalling some definitions already used formerly) :

$$\delta_1 = \int_0^\delta \left(1 - \frac{\rho u}{\rho_\delta u_\delta}\right) dy; \qquad (\delta_1)_u = \int_0^\delta \left(1 - \frac{u}{u_\delta}\right) dy \qquad \text{displacement thickness} \qquad (67)\ (68)$$

$$\delta_2 = \int_0^\delta \frac{\rho u}{\rho_\delta u_\delta}\left(1 - \frac{u}{u_\delta}\right) dy; \qquad (\delta_2)_u = \int_0^\delta \frac{u}{u_\delta}\left(1 - \frac{u}{u_\delta}\right) dy \qquad \text{momentum-loss thickness} \qquad (69)\ (70)$$

$$\delta_3 = \int_0^\delta \frac{\rho u}{\rho_\delta u_\delta}\left[1 - \left(\frac{u}{u_\delta}\right)^2\right] dy; \quad (\delta_3)_u = \int_0^\delta \frac{u}{u_\delta}\left[1 - \left(\frac{u}{u_\delta}\right)^2\right] dy \qquad \text{energy-loss thickness} \qquad (71)\ (72)$$

$$\delta_4 = \int_0^\delta \frac{\rho u}{\rho_\delta u_\delta}\left[\frac{\rho_d}{\rho} - 1\right] dy; \qquad (\delta_4)_u = 0 \qquad \text{density-loss thickness} \qquad (73)\ (74)$$

(quantities with subscript u are only dependent on velocity-profile features, but are not related to an incompressible reference case)

$$\boxed{\frac{(\delta_3)_u}{(\delta_2)_u} \equiv H = \text{shape parameter}} \quad ; \quad \frac{(\delta_1)_u}{(\delta_2)_u} \equiv H_{12}(H) \qquad (75)\ (76)$$

$$\frac{\frac{\delta_4}{\delta_2}}{r\frac{\kappa-1}{2}M_\delta^2} = \frac{\delta_3}{\delta_2} - \Theta = H^*(H, M_\delta, \Theta) \; ; \quad H^*_{M_\delta = 0,\, \Theta = 0} = H \qquad (77)\ (78)$$

((77) follows from (63) (69), (71) and (73)).

$$\boxed{\delta_2 R_{\delta_2}^n = Z \; ; \quad R_{\delta_2} = \frac{\rho_\delta u_\delta \delta_2}{\mu_w}} \qquad \begin{matrix}(n = 1 \text{ for laminar boundary layers}) \\ n = 0{,}268\end{matrix} \qquad (79)\ (80)$$

The integral condition of momentum obtained by partial integration of equ. (47)

with respect to y and the integral condition of energy, derived analogously from equ. (48) then write (for details of derivation see [30]) :

$$\frac{dZ}{dx} + Z\frac{\dfrac{du_\delta}{dx}}{u_\delta}\left[F_1(H, M_\delta, \Theta) + n\frac{\dfrac{\dfrac{d\mu_w}{dx}}{\mu_w}}{\dfrac{\dfrac{du_\delta}{dx}}{u_j}}\right] - F_2(H, M_\delta, \Theta) = 0 \qquad \textit{momentum} \quad (81)$$

$$\frac{dH^*}{dx} + H^*\frac{\dfrac{du_\delta}{dx}}{u_\delta}\cdot F_3(H, M_\delta, \Theta) - \frac{1}{Z}F_4(H, M_\delta, \Theta, R_{\delta_2}^{n-N}) = 0 \qquad \textit{energy} \quad (82)$$

For the universal functions F_1 through F_4 holds

$$F_1 = 2 + n + (1+n)\frac{\delta_1}{\delta_2}; \quad F_2 = (1+n)\frac{\delta_2}{(\delta_2)_u}\alpha_t(H) \qquad (83)\ (84)$$

with

$$\alpha_t(H) = \frac{0{,}246}{10^{0{,}678\,H_{12}}}; \quad \beta_t \approx 0{,}0056$$

$$N = 0{,}168; \quad n - N = 0{,}1 \qquad (87)\ (88)$$

($N = 1$ for laminar boundary layer)

For the ratio $\dfrac{\delta_1}{\delta_2}(H, M_\delta, \Theta)$ we find from the defining equ. (67) through (74) the representation

$$\frac{\delta_1}{\delta_2} = \frac{\dfrac{(\delta_1)_u}{(\delta_2)_u}}{\dfrac{\delta_2}{(\delta_2)_u}} + \frac{\delta_4}{\delta_2} = \frac{H_{12}}{\dfrac{\delta_2}{(\delta_2)_u}} + r\frac{\kappa-1}{2}M_\delta^2\,H^* \qquad (89)$$

In addition, for the universal function $\dfrac{\delta_2}{(\delta_2)_u}(H, M_\delta, \Theta)$, playing a decisive role in the generalized expressions for the wall friction (35) and dissipation (45) (and in the related functions F_2 and F_4), we may derive the analytic expression

$$\frac{\delta_2}{(\delta_2)_u} = \frac{1}{1 + r\dfrac{\kappa-1}{2}M_\delta^2\,H^*\,\varphi} \qquad (90)$$

where φ is an auxiliary function, known from exact evaluation of $\dfrac{\delta_2}{(\delta_2)_u}$ [see (97)].

Up to here, all relations, except those for α_t, β_t and φ are generally valid for laminar and turbulent, compressible and incompressible boundary layers and not related to a certain statement for the velocity profile.

When the power law (10) for $\frac{u}{u_\delta}$ is accepted, the following special relations result from the definitions (67) through (76)

$$H_{12} = 1 + 2k \; ; \quad H = 2\frac{1+2k}{1+3k} \; ; \quad k = \frac{2-H}{3H-4} \qquad (91)\ (92)\ (93)$$

$$\alpha_i(H) \approx 0{,}0555\,H - 0{,}0832 \qquad (94)$$

$$\frac{\delta_3}{\delta_2} = H \cdot g(H, M_\delta, \Theta), \qquad (95)$$

auxiliary functions :

$$g = 1 + (2-H)\,[0{,}004\,M_\delta + 0{,}0075\,M_\delta^2 - 0{,}00018\,M_\delta^4]\left[1 - \frac{\Theta}{0{,}9\,(H^2-1{,}1)}\right]^1 \qquad (96)$$

$$\varphi = (2-H)\,[1 - 0{,}0719\,M_\delta + 0{,}00419\,M_\delta^2]\,[1 - 0{,}02\,\Theta\,(1{,}87 - \sqrt{M_\delta})]$$

These functions g and φ have been determined from an evaluation of the integral terms (67) through (76), with use of (10) and (12).

The shape parameter H takes values between about 1,85 (accelerated flow) and 1,57 (retarded flow), where $H < 1{,}57$ designs turbulent separation.

It may be interesting to note that the term $Z\frac{\frac{du_\delta}{dx}}{u_\delta}$ in equ. (81) is related to CLAUSER'S π-function (see ROTTA'S paper equ. (19) by

$$\pi = \frac{(\delta_1)_u}{\tau_w}\cdot\frac{dP_\infty}{dx} = \frac{H_{12}}{\alpha(H_{12})}\,Z\frac{\frac{du_\delta}{dx}}{u_\delta} \qquad (98)$$

4.5. *Solution of the system* (81) (82).

4.5.1. *General remarks.*

The system of equations (81) (82) must in general be solved numerically by known methods of applied mathematics. Since all universal functions are given analytically, the solution may also be obtained by use of electronic computers.

Transformations to an incompressible reference case as proposed by several authors (as STEWARTSON-ILLINGWORTH [31], CULICK-HILL [32], SPENCE [14] [33]) appear not worthwhile with regard to the inherent simplicity of the system (81) (82).

A simple quadrature method of solution is described in [34]. We confine here to deal with the solution of (81) (82) for a few special cases of outstanding interest. Such cases are the " similar solutions " (also called "equilibrium flow solutions ") and the flow along a flat plate. For laminar flow the flat plate case is included in the general family of similar solution. For turbulent flow, however, this is, as is well-known, true only in a rough approximation.

4.5.2. *Similar solutions.*

We define the case of similarity by $\frac{dH}{dx} = 0$, $H = \text{const.}$, i. e. constant value of the shape parameter. In the case of turbulent boundary layers, this condition $H = \text{const.}$

1. From ref. [35].

is not equivalent to CLAUSER's condition for equilibrium boundary layer $\pi = \text{const.}$, $\frac{u_\tau}{u_\infty} = \text{const.}$, $\frac{d(\delta_1)_u}{dx} = \text{const.}$ (see equ. (98), but comparable with it.

More details on this question will be published separately.

To show how the system (81) (82) principally works out, we first consider the very transparent case of incompressible laminar boundary layers, for which yields $H^*_{M_\delta = 0,\ \Theta = 0} = H$, $n - N = 0$ (no influence of R_{δ_2} on F_4). F_1, F_2, F_3, F_4 then are functions of H only.

For $\frac{dH^*}{dx} = \frac{dH}{dx} = 0$, equ. (82) reduces to :

$$\frac{\frac{du_\delta}{dx}}{u_\delta} = \frac{F_4}{HF_3} = \text{const.} \tag{99}$$

By substitution of (99) in (81) follows :

$$\frac{dZ}{dx} = \text{const.} \tag{100}$$

and

$$Z = \text{const.}\ x. \tag{101}$$

From (101) and (99) then results after integration

$$u_\delta(x) \sim x^m; \qquad m = \frac{F_4}{HF_2F_3 - F_1F_4} = \text{const.} \tag{102) (103}$$

as the general condition for similar solutions, $m = 0$ being related to the flat plate flow. This is consistent with the well-known result of the exact theory of incompressible laminar boundary layers. We note that equ. (102) was obtained without introducting a special expression for the one-parametric family of velocity profiles.

We now deal with the case of incompressible turbulent boundary layer. The derivation differs from the above by that the function F_4 depends also upon the REYNOLDS number R_{δ_2}.

Hence, for $\frac{dH}{dx} = 0$, we obtain from (82) :

$$Z\frac{\frac{du_\delta}{dx}}{u_\delta} = \frac{F_4(H, R_{\delta_2}^{n-N})}{HF_3}; \qquad n - N = 0{,}1 \tag{104}$$

Substitution of (104) in (81) now leads to an ordinary differential equation, which permits no closed solution. Nevertheless, the system (81) (82) may be solved by numerical methods, thus delivering the distributions (accelerated or retarded flows), for which the shape parameter H remains constant. Special results of such calculations will be published soon (Thesis of H. FERNHOLZ, *Techn. Univ. Karlsruhe* [35]).

4.5.3. *Flat-plate flow, incompressible.*

We now will focuse our interest on the special case of turbulent flat-plate flow, which proves to be not a similar solution of (81) (82), contrary to the laminar case.

For the flat plate flow the system (81) (82) reduces to

$$\frac{dZ}{dx} = F_2 \tag{105}$$

$$\frac{dH^*}{dx} = \frac{F_4}{Z} \tag{106}$$

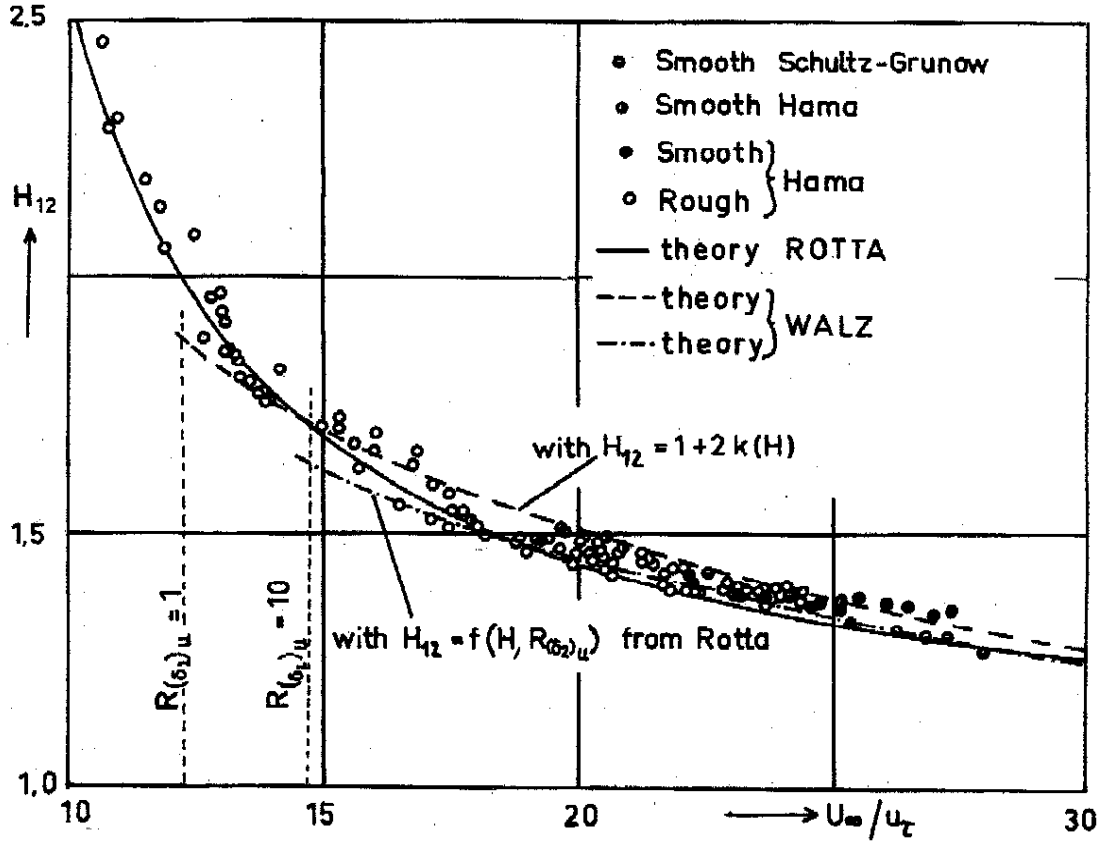

FIGURE 4
Incompressible turbulent boundary layer at a flat plate.
Variation of the shape parameter $H_{12} = \left(\frac{\delta_1}{\delta_2}\right)_u$ of the velocity profile with $\frac{u_\infty}{u_\tau} = \sqrt{\frac{2}{c_{f_1}}}$.
Comparison of experiments with the theories of ROTTA and WALZ
(figure reproduced from ROTTA's paper [44], refcrences see there).

Considering first the incompressible case with

$$\frac{dH^*}{dx} = \frac{dH}{dx}; \qquad F_2 = F_2(H); \qquad F_4 = F_4(H, R_{\delta_2}^{z-N}),$$

we easily find that there exists no solution for $\frac{dH}{dx} = 0$, since F_4 has, mathematically spoken, no finite zero point. The zero points of F_4 are varying with R_{δ_2}, which itself

varies with x. Indeed, from the solution of the simultaneous system (105) (106), the shape parameter H_{Pl} results as a function of the REYNOLDS number $R_{\delta_2}(x)$:

$$H_{Pl}(x) = f[R_{\delta_2}(x)] \tag{107}$$

(For details of calculation see [34]).

To establish the relation to usual representations of this result in terms of H_{12} and c_f or $\frac{u_\tau}{u_\infty}$ we have calculated $H_{12}(H)$ and $\frac{u_\infty}{u_\tau} = \sqrt{\frac{2}{c_{f_i}}}$ from equ. (24), basing upon (76) and plotted in fig. 4 H_{12} against $\frac{u_\infty}{u_\tau}$, as has done ROTTA [44] in fig. 9 of his paper. Without roughness, the boundary layer would be laminar when $R_{(\delta_2)_u}$ is smaller then about 100. Nevertheless, the theoretical curves are drawn down to $R_{(\delta_2)_u} = 10$ and 1 respectively.

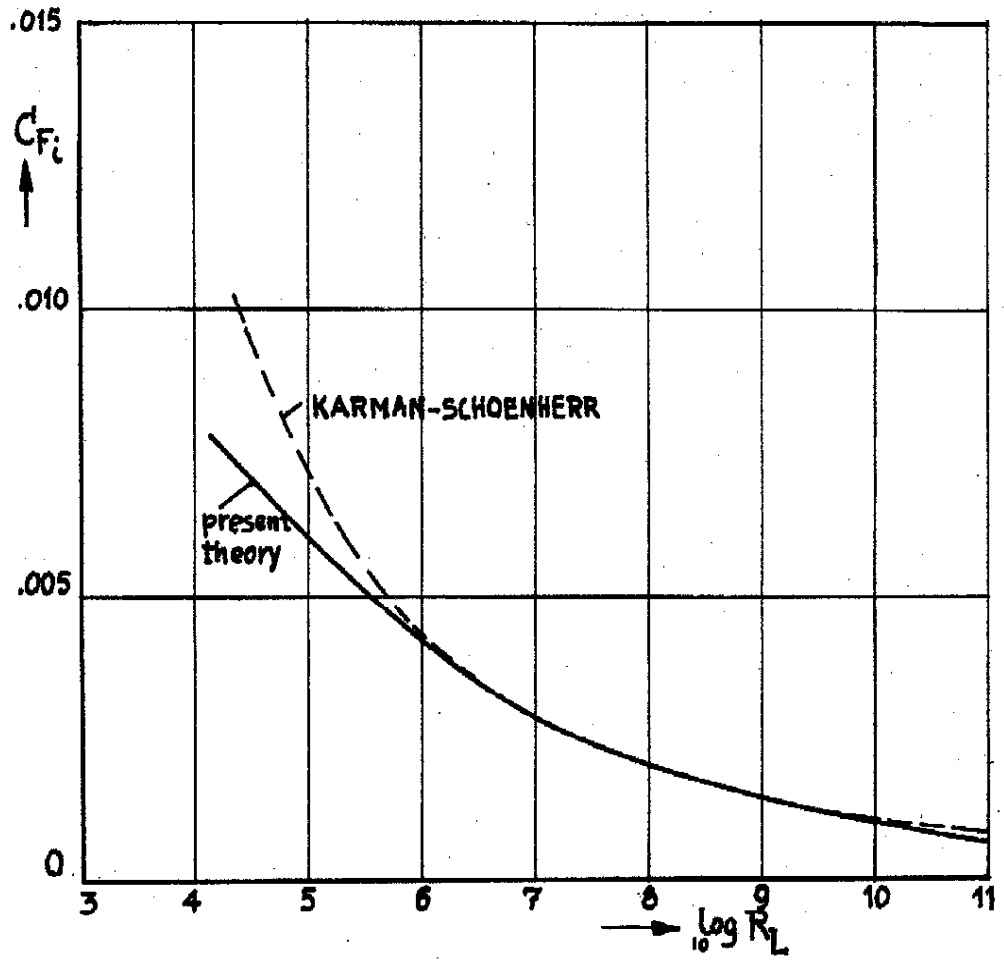

FIGURE 5

Incompressible turbulent boundary layer at a flat plate.

Average wall friction coefficient $C_{F_i} = \int_0^{*1} c_{f_i}\, d\left(\frac{x}{L}\right)$ as a function of $R_L = \frac{\rho_\infty u_\infty L}{\mu_\infty}$.

Comparison of the present theory with the law of KÁRMÁN-SCHOENHERR.

It is seen that the results of our theory based upon the two-parameter concept and applied to the flat plate case are equivalent to the two-layer concept theory described in the paper of ROTTA [44], except the case of roughness (which could be included by a modification of the function $\alpha\,(H_{12})$, equ. (26)). By integration according to (21), we may derive the relation between the average friction coefficient C_F and R_L, equ. (23). The result $C_F\,(R_L)$ is plotted in fig. 5 and compared with the corresponding KARMAN-SCHOENHERR-relation [21]. Complete agreement is obtained in the range $10^6 < R_L < 10^9$.

4.5.4. *Flat plate flow, compressible.*

The system (105) (106) may be solve without principal difficulty also when compressible flow with heat transfer is present. In this case the shape parameter H of the turbulent boundary layer turns out to be a function of R_{δ_2}, M_δ and Θ (see [34]). We confine to give here the results of this calculation for the friction coefficients c_f and C_F, equ. (35) and (21), related as usual to the incompressible values c_{f_i} and C_{F_i}. With regard to the difficulties that are present when c_f and c_{f_i} are expressed in terms of the REYNOLDS number R_x, equ. (22), formed with the flow length x, we prefer to take c_f and c_{f_i} at the same local value R_{δ_2}, where for incompressible flow R_{δ_2} is identical with $R_{(\delta_2)_x}$, (see equ. (25) and (32)).

Since the shape parameter H is found to be a function of R_{δ_2}, M_δ, Θ, this is true also for the functions α and $\frac{\delta_2}{2_{(\delta_2)_x}}$, occurring in the expression (35) for the local friction coefficient. Thus $\frac{c_f}{c_{f_i}}$ may be expressed as a function of R_{δ_2}, M_δ and Θ. Correspondingly, the ratio $\frac{C_F}{C_{F_i}}$ for the averaged friction coefficient is obtained as a function of R_L (equ. 23)), M_δ and Θ.

In fig. 6 $\frac{c_f}{c_{f_i}}$ is plotted against M_δ with R_{δ_2} as parameter for adiabatic walls ($\Theta = 0$).

Fig. 7 shows $\frac{c_f}{c_{f_i}}$ versus M_δ for the fixed value of $R_{\delta_2} = 10^3$ for various heat transfer rates expressed by the parameter Θ (equ. (17)).

Finally, in fig. 8, $\frac{C_F}{C_{F_i}}$ versus M_δ is represented, with R_L and Θ as paramater.

In these three figures also comparison is made with experimental data.

By reasons displayed in chapter 6, at MACH numbers $M_\delta > 5$, only those experimental data for c_f or $\frac{c_f}{c_{f_i}}$ appear reliable, which are determined by local force measurements [8]. But also for some of these experiments the comparison with the theory is somewhat hampered by the fact that the REYNOLDS number R_L is given instead of R_{δ_2}. Since the relation between R_{δ_2} and R_L may be estimated (see [34]), and the influence of R_{δ_2} on $\frac{c_f}{c_{f_i}}$ in the usual range of R_{δ_2} ($10^3 < R_{\delta_2} < 10^4$) is small, the resulting possible errors are not exceeding a few per cent.

From the figures 6 to 8, we may conclude that the developed theory agress fairly well with reliable experimental data.

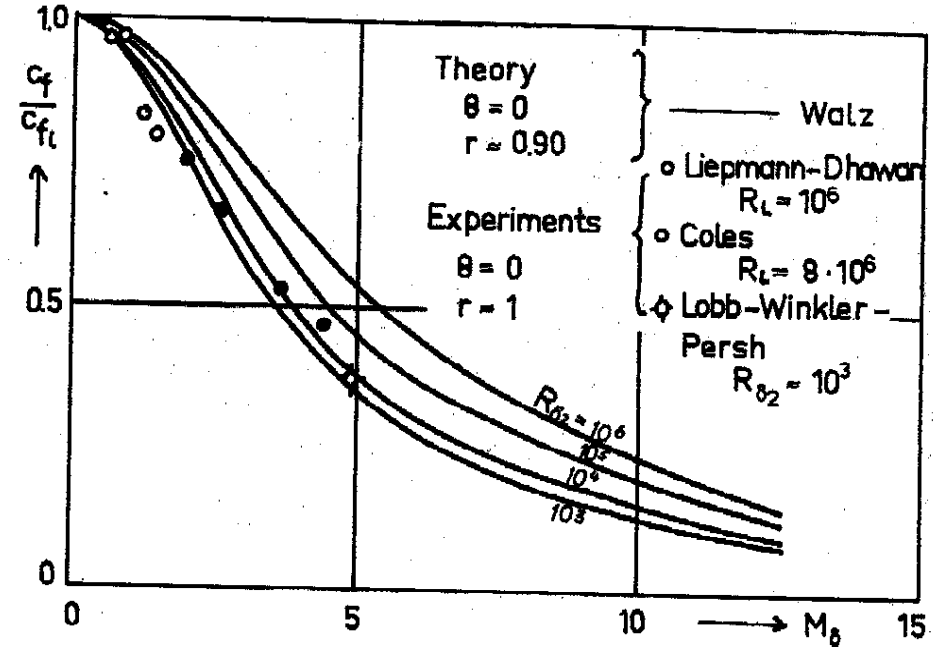

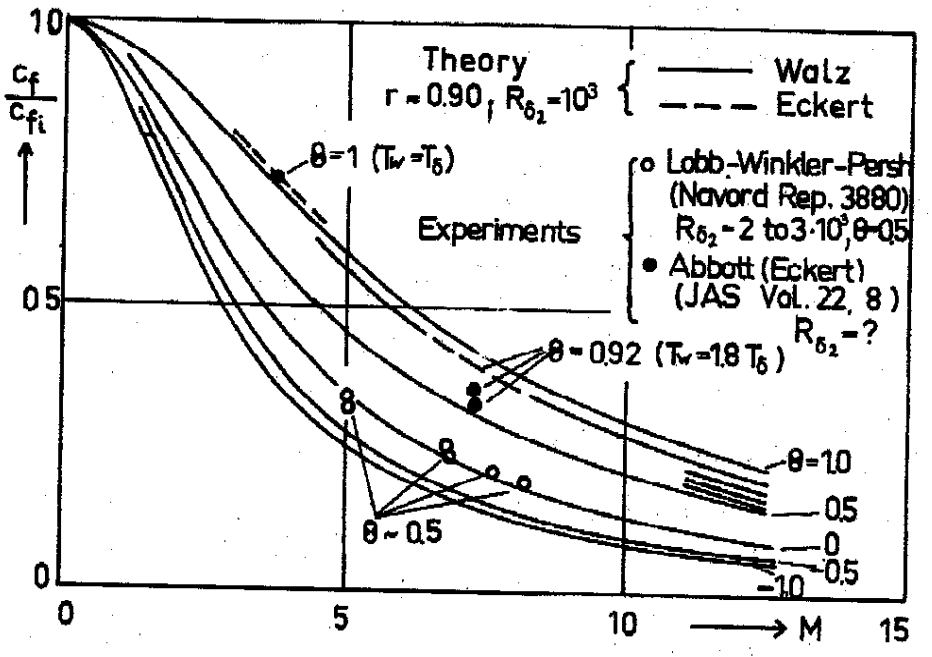

FIGURE 6 and 7

Compressible turbulent boundary layer a ta flat plate. Ratio $\frac{c_f}{c_{fi}}$ of local wall-friction coefficients (taken at same values, $R_{\delta 2} = R_{(\delta 2)_u}$) as a function of the free stream Mach number $M_\delta = M_\infty$. *Fig. 6* with $R_{\delta 2} = \frac{\rho_\delta u_\delta \delta_2}{\mu_w}$ as parameter; *Fig. 7* with $\Theta = \frac{T_r - T_w}{T_r - T_\delta}$ as heat transfer parameter, for a fixed value $R_{\delta 2} = 10^3$. Comparison with experiments.

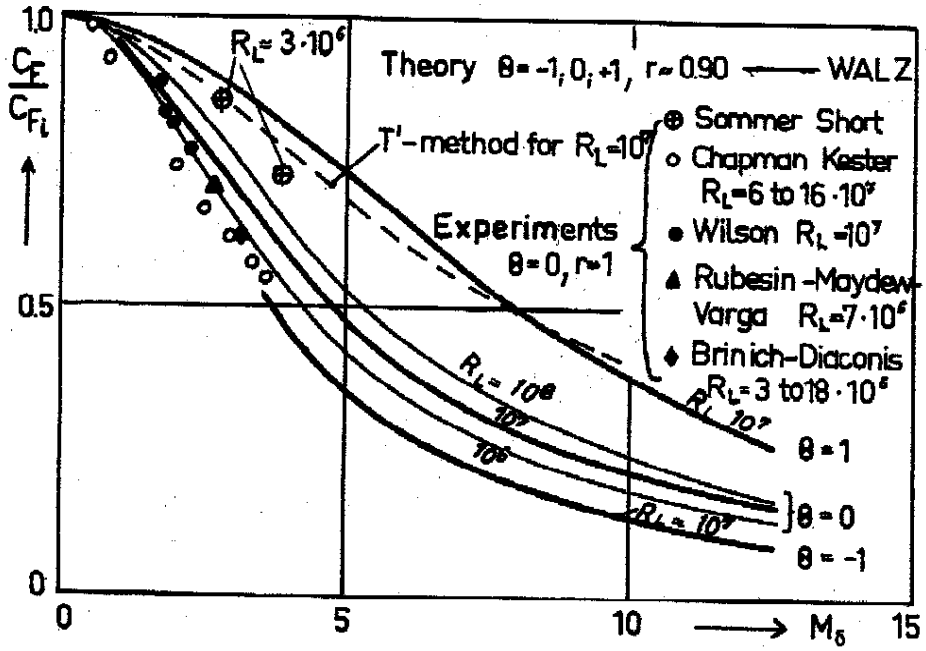

FIGURE 8

Compressible turbulent boundary layer at a flat plate. Ratio $\frac{C_F}{C_{F_i}}$ of averaged wall-friction coefficients heat transfer parameter. Comparison with the T'-method [19] and experiments (force measurements). (taken at same values R_L) as function of the free stream MACH number $M_\delta = M_\infty$ with $\Theta = \frac{T_r - T_\infty}{T_r - T_\delta}$ as

In fig. 9, in addition, we have reproduced the results of a comparison between recent experimental data and several theories for predicting the wall friction coefficients at adiabatic walls as a function of MACH number and REYNOLDS number, published by MATTING, CHAPMAN, NYHOLM and THOMAS [8] (fig. 22 of this publication).

This figure also contains the theoretical results for $\frac{c_f}{c_{f_i}}$ from the above coutlined analysis (drawn from an earlier publication [36] of the present writer, and transformed for comparison at equal values R_x). There is a discrepancy between this theory and the experimental data, in so far as the experiments show no variation of $\frac{c_f}{c_{f_i}}$ with R_x, while the present theory predicts a small increase of $\frac{c_f}{c_{f_i}}$ with increasing R_x. Detailed investigations for clearing the discrepancy are in operation, but could not be completed before this paper was written [1].)

1. In the expression for c_f/c_{f_i}, the REYNOLDS number R_x occurs with a small power, which is obtained as the difference between two about equal numbers. Therefore, small errors may have a relatively large effect. It is conjectured that the simplification $\beta(H) \approx \beta \approx 0{,}0056$, equ. (45), introduced by TRUCKENBRODT [25], as well as the simplification $\alpha \frac{\delta_2}{(\delta_2)_i} \approx A(M_\delta, \Theta) R_{\delta_2}^{B(M_\delta, \Theta)}$ in [30] and [34] are the source of the observed discrepancies. Both simplifications are omitted in a repeated calculation which is in operation.

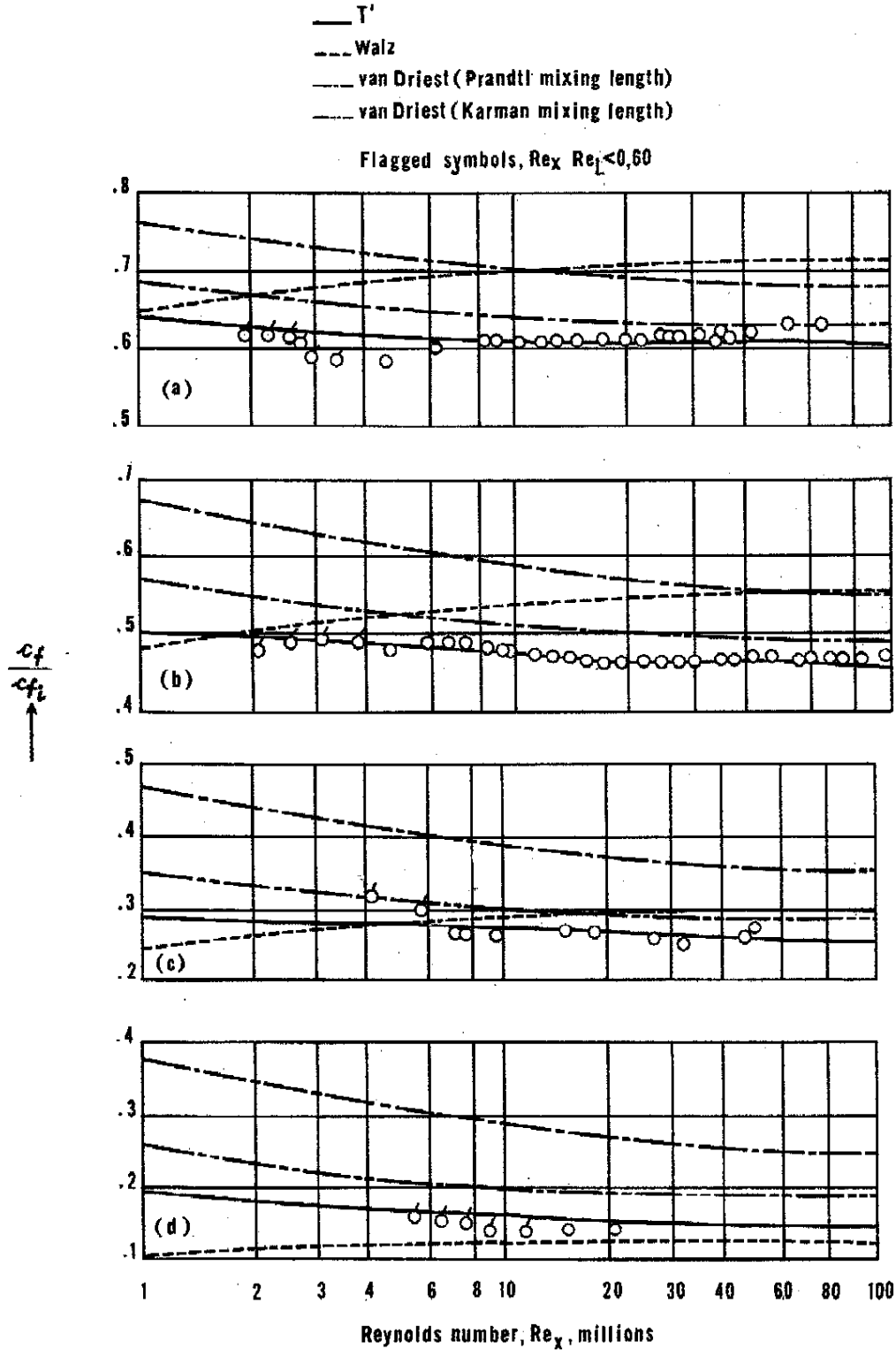

(a) $M_a = 2,95$
(b) $M_a = 4,2$
(c) $M_a = 6,7$
(d) $M_a = 9,9$

$$M_a \equiv M_\infty ; \; Re_x \equiv R_x = \frac{S_\infty \, \mu_\infty \, x}{\mu_\infty}$$

FIGURE 9

Compressible turbulent boundary layer at a flat plate. Ratio $\frac{c_f}{c_{f_i}}$ of local wall-friction coefficients (taken at same values $R_x = \frac{\rho_\infty u_\infty x}{\mu_\infty}$) as a function of the REYNOLDS number R_x for different free-stream MACH numbers $M_\delta = M_\infty = 2,95$; 4,2; 6,7 and 9,9. Comparison of different theories with experimental data of ref. [8], measured with the "wall-force element".

5. Calculation of heat transfer

5.1. *Reynolds analogy.*

The local heat transfer, with regard to equ. (12), writes :

$$q(x) = -\left(\lambda \frac{\partial T}{\partial y}\right)_w = -c_p \left(\frac{\lambda}{\mu c_p}\right)_w \left(\frac{dT}{du}\right)_w \left(\mu \frac{\partial u}{\partial y}\right)_w$$

$$= -\frac{c_p}{(Pr)_w} \frac{T_\delta}{u_\delta} \left[\frac{d\left(\frac{T}{T_\delta}\right)}{d\left(\frac{u}{u_\delta}\right)}\right]_w \cdot \tau_w \qquad (108)$$

or in dimensionless terms with $b\,(M_\delta, \Theta)$ from (14) :

$$\frac{q(x)}{\rho_\delta u_\delta^3} = -\frac{1}{(Pr)_w} \frac{c_p T_\delta}{2 u_\delta^2} \frac{\tau_w}{\rho_\delta u_\delta^2} b\,(M_\delta, \Theta) =$$

$$= -\frac{\frac{c_f}{2}}{(Pr)_w (\kappa - 1) M_\delta^2} b = -\frac{r}{(Pr)_w} \frac{c_f}{4} \Theta \qquad (109)$$

When $\left(\frac{dT}{du}\right)_w$ is determined directly from VAN DRIEST's solution (54) with (55), (57), and (17), we find

$$\left(\frac{dT}{du}\right)_w = \frac{T_\delta}{u_\delta} \frac{T_r - T_w}{T_\delta} \frac{(Pr)_w}{s} \left[\left(\frac{\tau}{\tau_w}\right)^{Pr_t - 1}\right]_{\tau = \tau_w} = \frac{T_\delta}{u_\delta} \frac{(Pr)_w}{s} r \frac{\kappa - 1}{2} M_\delta^2 \Theta \qquad (110)$$

Hence, a somewhat refined expression for the dimensionless local heat transfer follows from combining (108) and (110) :

$$\frac{q(x)}{\rho_\delta u_\delta^3} = -\frac{r}{2} \frac{c_f}{2s} \Theta = -\frac{r}{2} St\, \Theta ; \qquad \Theta = \frac{T_r - T_w}{T_r - T_\delta} \qquad (111)$$

where

$$\frac{c_f}{2s} = St \qquad (112)$$

in the STANTON number.

Expression (111) holds, because of the unique relation (63) between the velocity and temperature field, according to the REYNOLDS analogy between heat transfer and wall friction.

We must, however, keep in mind that this relation is exactly valid only for zero streamwise pressure gradient $\frac{dp}{dx} = 0$, and isothermal walls $\frac{dT_w}{dx} = 0$, and that general use of this relation is justified only for evaluating the integral terms (67), through (76).

Since the mentioned conditions are not fulfilled in many cases, an improvement of the above heat transfer calculation is desirable, which leads to the so-called " modified " REYNOLDS analogy.

5.2. *Modified Reynolds analogy.*

5.2.1. *Present state of development (method of Cohen).*

Since the exact solution of the system (46) (47) (48) with consideration of streamwise pressure and temperature gradients is a difficult attempt, this problem was attacked by several authors by means of integral conditions.

The publications known to the author, however, account only for the influence of a pressure gradient $\frac{dp}{dx}$, but include not a streamwise temperature gradient, which in the laminar case proved to be very important. See for instance the approaches of CHAPMAN and RUBESIN [36], SCHLICHTING [37], DIENEMANN [38].

An analysis typical for many others, which aims at a modified REYNOLDS analogy considering the influence $\frac{dp}{dx}$ only, is that of COHEN [39]. (List of references about this topic see for instance [39].)

First WIEGHARDT's [40] form of the energy equation is derived by multiplying PRANDTL's equation (47) with u :

$$\rho u \frac{\partial\left(\frac{u^2}{2}\right)}{\partial x} + \rho v \frac{\partial\left(\frac{u^2}{2}\right)}{\partial y} = -u\frac{dp}{dx} + u\frac{\partial \tau}{\partial y} \tag{113}$$

By addition of (113) and (48) with consideration of (46), a new form of the energy equation is obtained, in which the pressure term cancels and the term of the shear-work in (113) and the dissipation term of (48) are combined, viz. :

$$\frac{\partial(\rho\, uh)}{\partial x} + \frac{\partial(\rho\, vh)}{\partial y} = \frac{\partial(u\tau)}{\partial y} + \frac{\partial}{\partial y}\left(\frac{\lambda}{c_p}\frac{\partial i}{\partial y}\right); \qquad i = c_p\, \mathrm{T} \tag{114}$$

with the abbreviation for the total energy

$$h = i + \frac{u^2}{2} \tag{115}$$

Now, by partial integration of (114), with respect to y from $y = 0$ to $y = \mathrm{Y}$; $\mathrm{Y} = \text{const.} >$ any $\delta(x)$ yields :

$$\frac{d}{dx}\left[\int_0^{\mathrm{Y}} \rho u h dy\right] + [\rho v h]_0^{\mathrm{Y}} = -\left(\frac{\lambda}{c_p}\frac{\partial i}{\partial y}\right)_0 = -q(x); \qquad [u\tau]_0^{\mathrm{Y}} = 0 \tag{116) (117}$$

$$(\rho v)_0^{\mathrm{Y}} = -\frac{d}{dx}\left[\int_0^{\mathrm{Y}} \rho u\, dy\right] \qquad \text{(from equ. (46))}; \tag{118}$$

Thus the term related to the shear-work and dissipation cancels, too.

Equ. (116) is now combined with the integral condition for the momentum, which contains the local wall friction c_f and the pressure gradient $\frac{dp}{dx}$. In this way, a generalized relation between $c_f(x)$ and $q(x)$ is established, which accounts for $\frac{dp}{dx}$.

This analysis, however, involves an assumption about the relation between the total energy and the velocity, similar to (12). In addition, the relation between c_f and the shape parameter of the velocity profile is estimated only.

5.2.2. *Proposal of general treatment.*

For general treatment of the problem of modified REYNOLDS analogy, a generalized relation of the type (12)

$$\frac{T}{T_\delta} = f\left(\frac{u}{u_\delta}, M_\delta, \Theta, K(x)\right) \tag{119}$$

should be attempted, where the correcting function $K(x)$ implies the direct influence of $\frac{dp}{dx}$ (or $\frac{du_\delta}{dx}$) and $\frac{dTw}{dx}$. The (mostly prevailing) indirect influence of these two parameters is automatically considered with the sensibility of $\frac{u}{u_\delta}$ to these parameters, where the sensibility to $\frac{dp}{dx}$ is dominant. Hence, for moderate values of $\frac{dTw}{dx}$, it is indeed justified to introduce $K(x)$ as a correcting function, which may be determined by a process of iteration beginning with $K^{(0)}(x) = 0$.

Therefore, we establish a form of (119), which becomes identical with (12), when $K(x)$ tends to zero :

$$\frac{T}{T_\delta} = a + b\,(1 + K(x))\,\frac{u}{u_\delta} + c\left(1 - \frac{b\,K(x)}{c}\right)\left(\frac{u}{u_\delta}\right)^2 \tag{120}$$

The coefficients a, b, c are functions of M_δ and θ only, as given with (13) (14) (15). For $\frac{u}{u_\delta} = 1$, we have $\frac{T}{T_\delta} = 1$, as must be for a PRANDTL number near unity.

For determining $K(x)$, we need an equation additional to the two integral conditions (81) (82).

This additional equation is given by the integral condition (116). Though this integral condition is physically identical with (82), the mathematical identity would be achieved only when the exact solutions of $T(x, y)$ or $\rho(x, y)$ respectively, and $u(x, y)$ are introduced. Now, since (120) is an approximation with the free function $K(x)$, this function may be determined from the condition that both the equations (82) and (116) are valid simultaneously. This leads to an equation for $K^{(1)}(x)$ of the type

$$\frac{dK^{(1)}}{dx} + K^{(1)}\,\frac{\frac{du_\delta}{dx}}{u_\delta}\,\varphi_1^{(0)} + \varphi_2^{(0)} = 0 \tag{121}$$

where $\varphi_1^{(0)}$, $\varphi_2^{(0)}$, are known functions including the given functions $\frac{du_\delta}{dx}\frac{1}{u_\delta}$ and $\frac{dTw}{dx}\frac{1}{Tw}$ (from $\frac{d\Theta}{dx}\frac{1}{\Theta}$), when the boundary problem (81) (82) was solved with the assumption $K^{(0)}(x) = 0$. With $K^{(1)}(x)$, an improved relation for $\frac{T}{T_\delta}$ and for the local

heat transfer is obtained which writes

$$\frac{q(x)}{\rho u_\delta^3} = -\frac{r}{2} \mathrm{ST}\,\Theta\,(1 + \mathrm{K}^{(1)}) \tag{122}$$

If necessary, a second approximation $\mathrm{K}^{(2)}(x)$ may be procured by repeating the boundary layer calculation basing upon (120). In general, the first iteration step will be sufficient, since the integral terms (67) (69) (71) (73) are not very sensitive to variations of $\frac{T}{T_\delta} = \frac{\varrho_\delta}{\varrho}$ near the wall. Indeed, the correcting function K essentially affects the wall slope $\left(\frac{\partial T}{\partial y}\right)_w$, thus giving the required improvement of heat transfer calculation.

Numerial calculations according to the above idea of a modified Reynolds analogy are prepared. The results will be reported separately.

6. Critical notes on hypersonic boundary layer surveys

6.1. *Introducing remarks.*

During the last ten years the hypersonic tunnel technique was developed to a high completion in manipulating boundary layer surveys up to free stream Mach numbers of about 10.

Thus, experimental information about the behaviour of turbulent boundary layers at high Mach numbers and various heat transfer conditions at the wall was now available from an increasing number of more and more refined measuring techniques. There are some publications of this kind, namely those of Lobb, Winkler and Persh [11], Hill [6], Winkler and Cha [41], which have found special attention by authors who attempted to improve theoretical approaches about compressible boundary layers with heat transfer. These very difficult measurements provided extensive experimental data about the velocity and temperature distribution, also very close to the wall, such that parts of the laminar sublayer or at least of the buffer-layer were included. From this original test material, values of local wall friction and heat transfer rate have been derived, essentially basing upon the assumption that the configuration of test points permits to construct the wall slope $\left(\frac{\partial u}{\partial y}\right)_w$ or $\left(\frac{\partial T}{\partial y}\right)_w$ respectively. In the case case of the velocity distribution, a straight line course of $u(y)$ between the point $u = 0$ and the more or less averaged location of the last test points was accepted as an adequate fitting.

As already indicated by Prof. Morkovin, serious discrepancies between these results for the local wall friction coefficient c_f and results from available free flight experiments (Sommer and Short [19]) on the one hand, and between credible theoretical derivations on the other hand, gave reason to regard the experimental results of [11], [6] and [41] with some caution. Under the following items 6.2 and 6.3, we concern with some features which may be helpful in criticizing the mentioned discrepancies.

6.2. *Comparison of measured and calculated temperature profiles.*

The references [11] and [41] contain detailed numerical results for the velocity profile $\frac{u}{u_\infty}\left(\frac{y}{\delta}\right)$ and the temperature profile $\frac{T}{T_\infty}\left(\frac{y}{\delta}\right)$, hence, the relation $\frac{T}{T_\infty}\left(\frac{u}{u_\infty}\right), M_\infty, \Theta$ for different free stream Mach numbers $M_\delta = M_\infty$, and heat transfer rate, characterized by the ratio $\frac{(T_r - T_w)}{T_r}$. This ratio is related to the heat transfer parameter Θ used in our analysis by

$$\Theta = \frac{T_r - T_w}{T_r - T_\delta} = \frac{T_r - T_w}{T_r} \frac{1 + r\frac{\kappa - 1}{2} M_\infty^2}{r\frac{\kappa - 1}{2} M_\infty^2}, \tag{123}$$

$$(T_\delta \equiv T_\infty\,,\ u_\delta \equiv u_\infty\ T_r \equiv Te \text{ in [11] and [41]})$$

where the recovery factor is $r = 0{,}89$.

Since, according to test descriptions, the pressure gradient $\frac{dp}{dx}$ and the temperature gradient $\frac{dTw}{dx}$ may be neglected (in [11] a small favorable pressure gradient is conceded), the relation (12) with (13) (14) (15) may be considered as a very acurate solution of the energy equation. This relation was evaluated for the different Mach numbers $M_\delta\,(= M_\infty)$ and heat transfer parameter Θ given in [11] and [41], and compared with the corresponding experimental results. From the 29 measured and calculated curves $\frac{T}{T_\infty}\left(\frac{u}{u_\infty}\ M_\infty, \Theta\right)$, six typical curves from the two references respectively are represented in the figures 10 through 21. For about zero heat transfer, the experimental and theoretical curves agree very well, while with increasing heat transfer (cooling), the curves deviate more and more, except the wall and outer-edge points. In the case of ref. [11] (Lobb, Winkler, Persh), the experimental points are lying below the theoretical result, in the case of ref. [41] (Winkler, Cha), the experiments give in the average higher temperature than predicted by the (quasi-exact) theory. The maximum discrepancies are in both cases of the order of 20 %. The experimental curves $\frac{T}{T_\infty}\left(\frac{u}{u_\infty}\right)$ of [41] appear when $\Theta > 0$, to be related to a higher Mach number, while the curves of [11] make believe that smaller Mach numbers are present. To give an example: the experimental curve $\frac{T}{T_\infty}\left(\frac{u}{u_\infty}\right)$ for $M_\infty = 8{,}18$, $\Theta = 0{,}536$, fig. 15 resembles very closely a theoretical curve calculated from (12) for $M_\infty = 5{,}55$ and $\Theta = 0$.

Figure 10 to 21

Comparison of measured and calculated temperature distributions $\frac{T}{T_\infty}\left(\frac{u}{u_\infty}\right)$. Theory: thick ful lines.

Fig. 10 to 15 experimental data from Lobb, Winkler, Persh ref. [11]; *Fig. 16 to 21* experimental data from Winkler, Cha ref. [41].

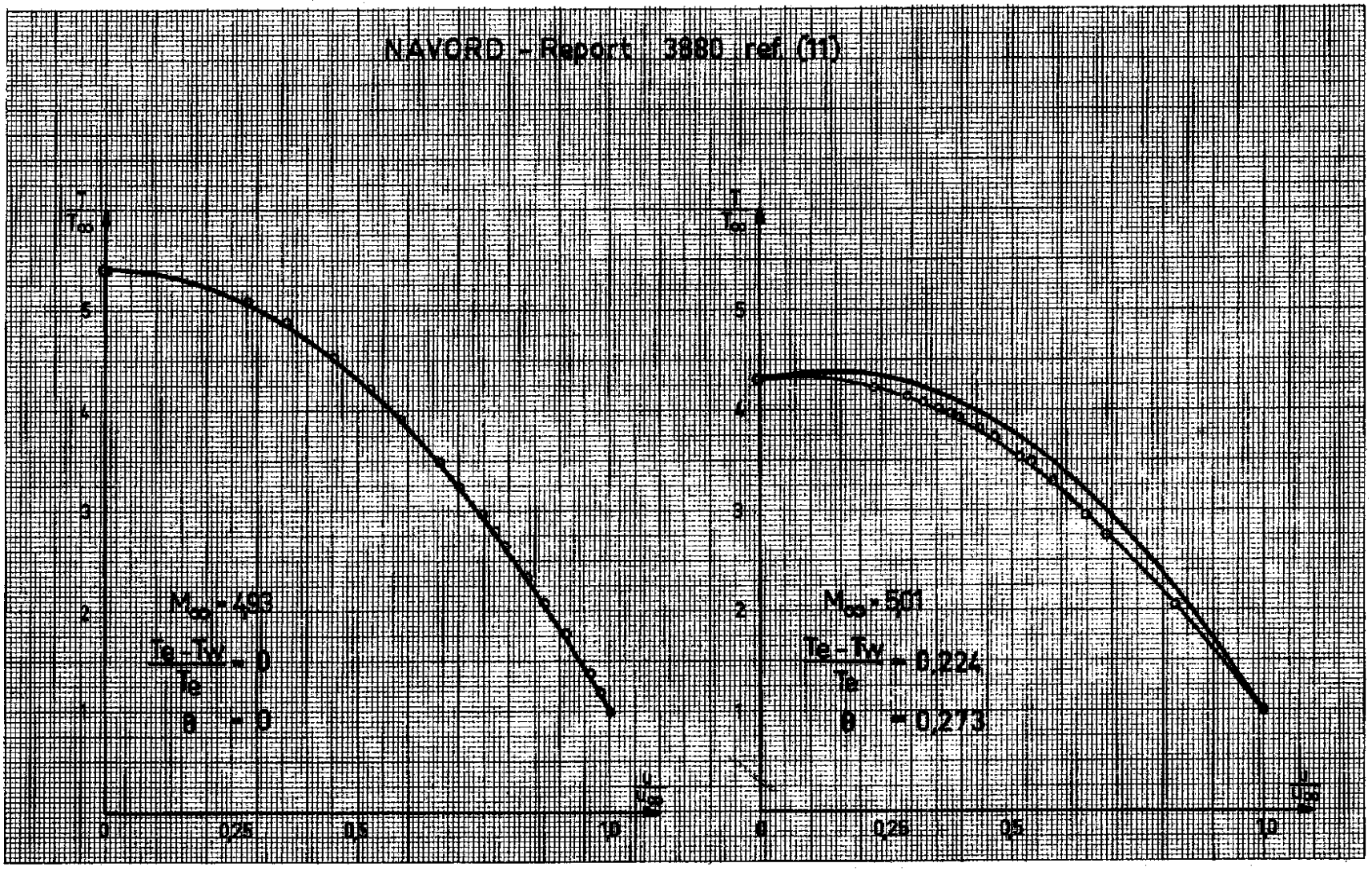

FIGURE 10

FIGURE 11

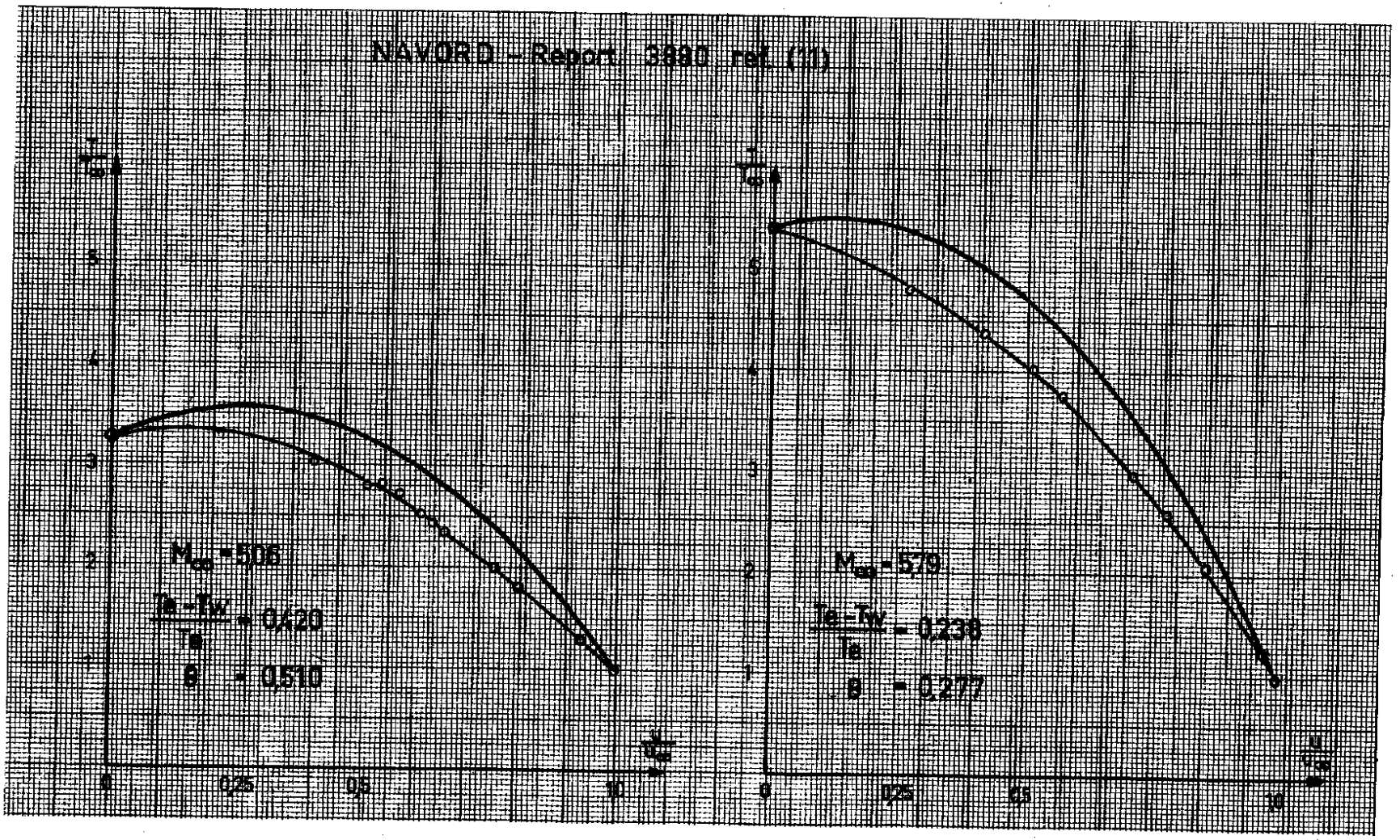

FIGURE 12

FIGURE 13

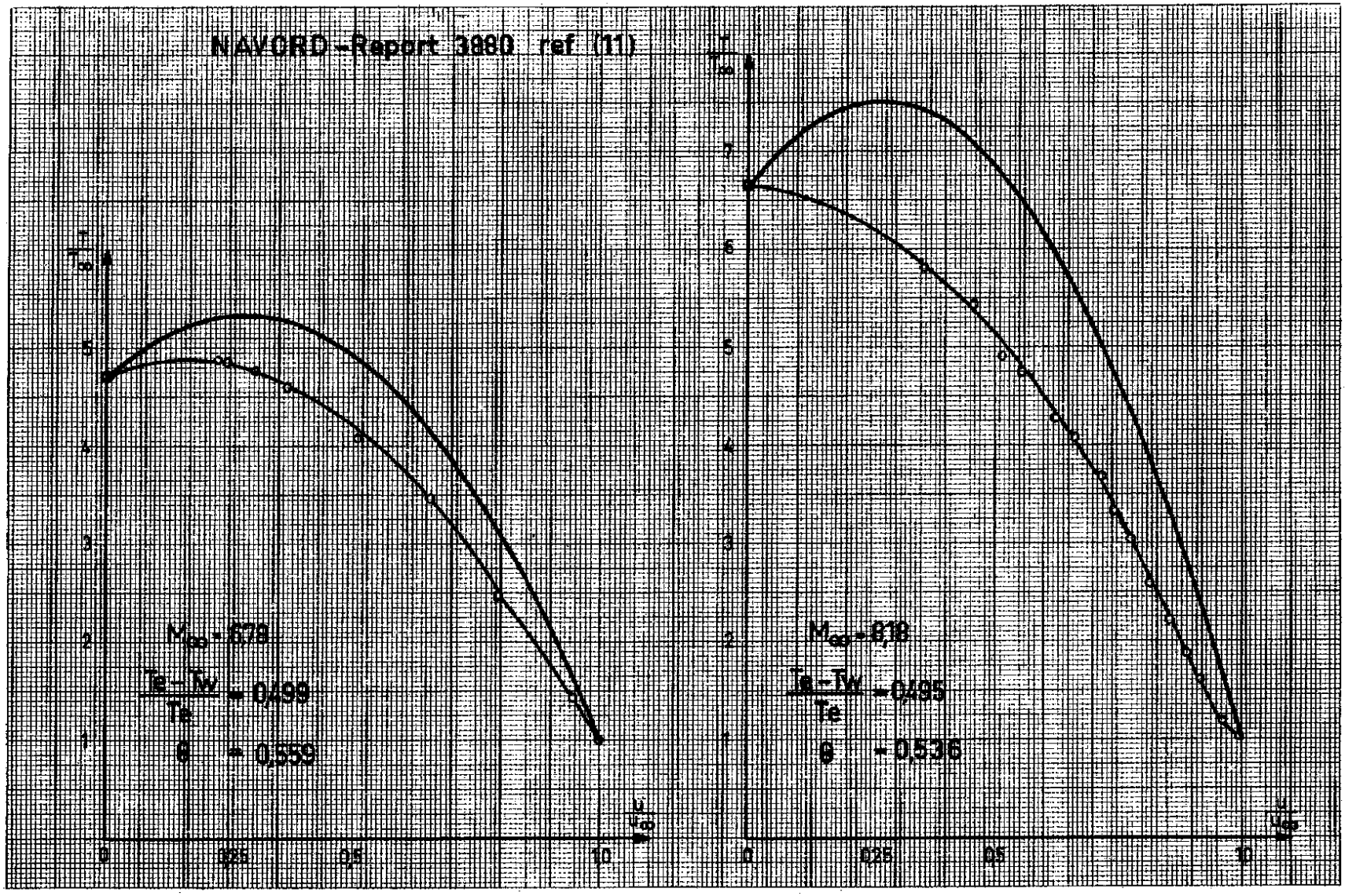

FIGURE 14

FIGURE 15

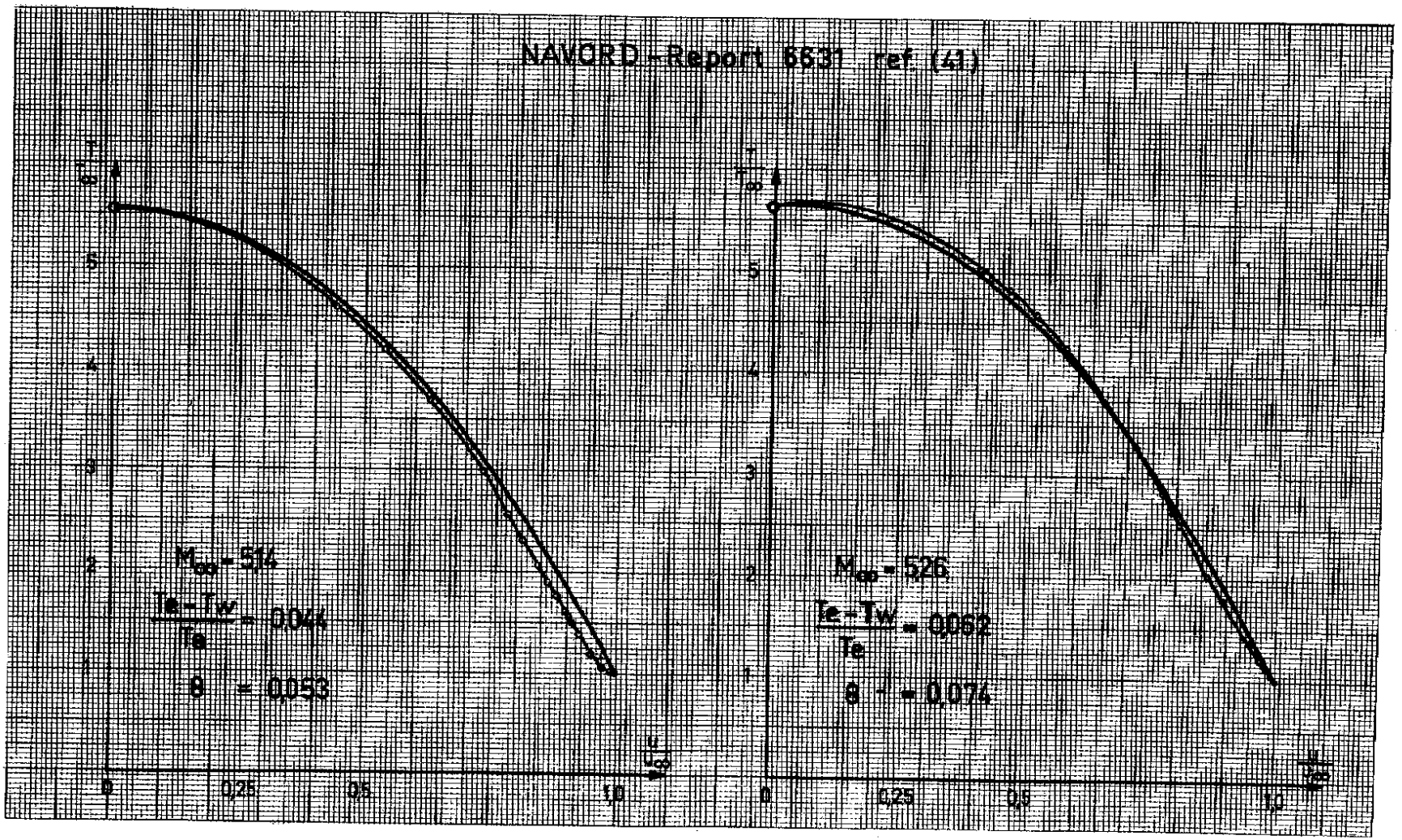

FIGURE 16

FIGURE 17

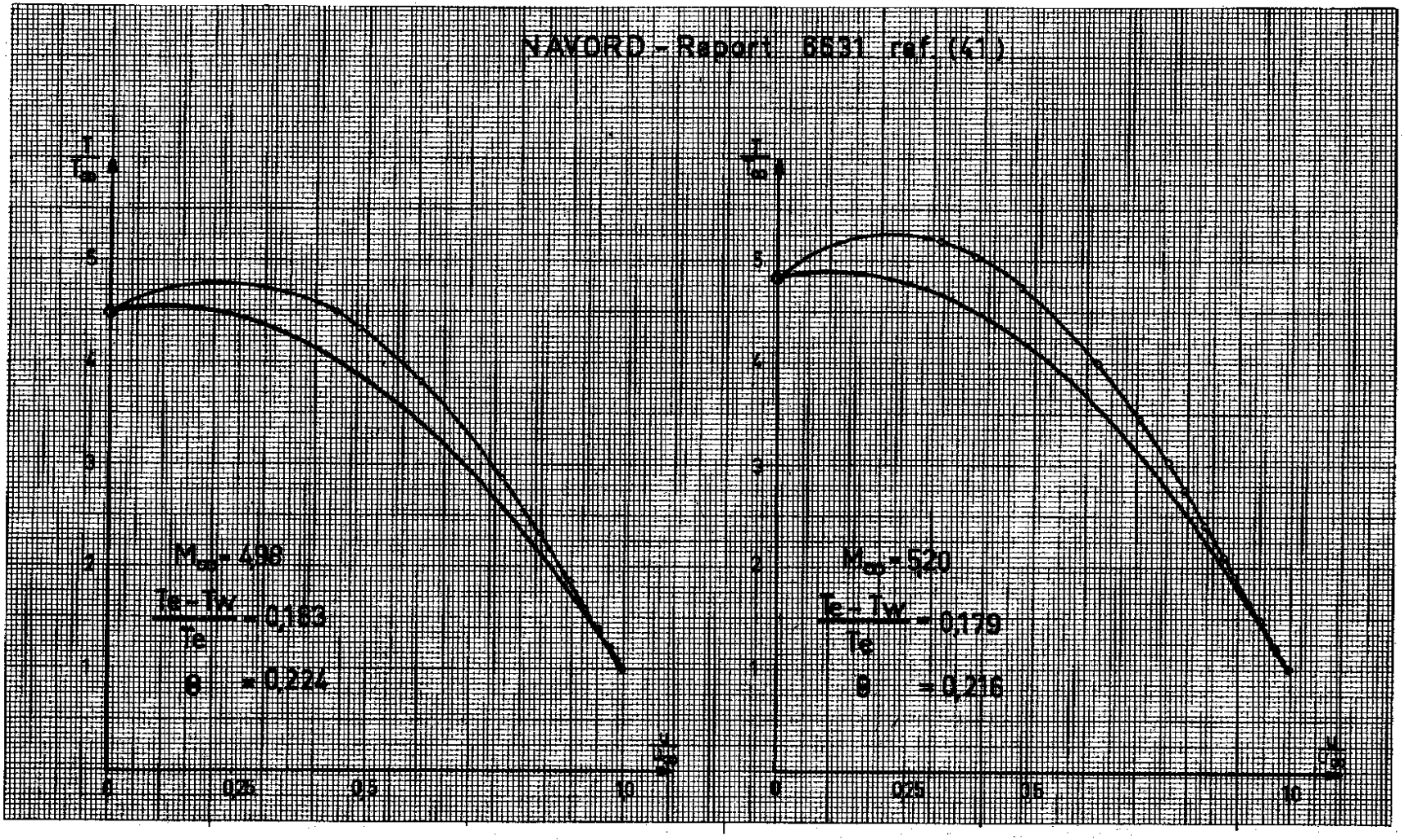

FIGURE 18

FIGURE 19

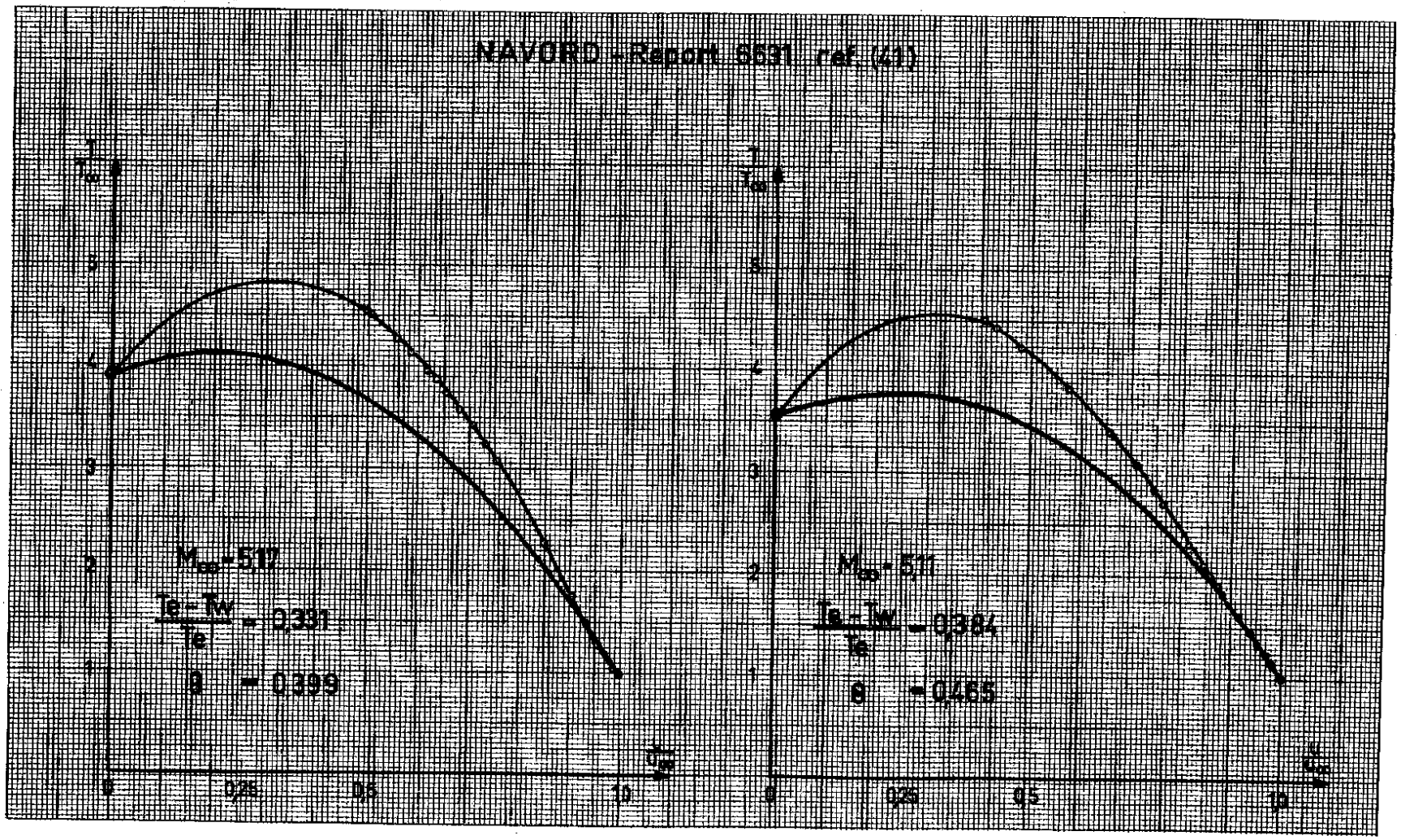

FIGURE 20

FIGURE 21

The present writer does not find a plausible explanation for these discrepancies. It is, however, clear that the integral terms δ_1, δ_2 (displacement and momentum-loss thickness) calculated from the curves $\frac{T}{T_\infty} = \frac{\rho_\infty}{\rho}$ with the relations (67) and (69), and Reynolds number formed with δ_2 may be noticeably incorrect.

6.3. ***On the determination of local friction coefficients by experimental slope evaluation.***

For evaluating the wall slope at the velocity profiles, it is usual to assume a straight line course of $u\,(y)$ within the laminar sublayer. The outer edge of the laminar sublayer is determined by the intersection point of a plot of $\frac{u_\tau}{u_\infty}$ against the logarithm of the wall distance $\frac{y}{\delta}$.

It is believed that this procedure of determining the wall slope involves remarkable uncertainties, as is evidenced by the fig. 22 through 26, related to ref. [11] and fig. 27 through 29, related to ref. [41]. A plot in physical coordinates is chosen, from which the accuracy of the experimental data and the fitting by a curve may be critically examinated in the best way.

In these figures, the slopes recalculated from the values c_f as listed in the summarizing tables of ref. [11] and [41] (using the SUTHERLAND formula for $\mu\,(T)$) are drawn as thin, ful lines. There exist, indeed, some difficulties to support these lines as an adequate evaluation of the physical feature.

Tentatively — inspite of the probable uncertainty in the values $\frac{T}{T_\infty}$, $\frac{\rho_\infty}{\rho}$, δ_2 and R_{δ_2} discussed under 6.2 — the wall slope was calculated from the relation (35), basing upon the measured values of δ_1, $(\delta_1)_u$, δ_2, $(\delta_2)_u$ R_{δ_2}, $\left(\frac{\delta_1}{\delta_2}\right)_u = H_{12}$ and $\frac{\delta_2}{(\delta_2)_u}$. This slope is drawn in the figures 22 through 29 as dashed-dotted line. Since, with regard to the fig. 10 through 21, δ_2 is obviously too small in the case of ref. [41] and too high in the case of ref. [11], the calculated c_f values may probably be incorrect by a factor about proportional to δ_2 with the same trends [see equ. (35)]. From the figures 27, 28, related to cases with small heat transfer and good agreement between experimental and theoretical curves $\frac{T}{T_\infty}\left(\frac{u}{u_\infty}\right)$, it turns out that the theoretical slope from equ. (35) may be regarded as a fairly good approximation to the real slope.

In all cases, however, the dashed-dotted slopes calculated from equ. (35) are much larger than the experimental slopes (order of 50 % and more, especially for values $\Theta \approx 0{,}5$). Higher c_f-values in the case of cooling of the wall ($\Theta > 0$) appear to be supported by the free flight experiments of SOMMER and SHORT [19] and by the prediction of some other theories, i. e. the T'-method, as is evidence by the figures 7 and 8 of the present report.

As to the experiments of ref. [11], the conceded (though small) favorable pressure gradient $\left(\frac{dp}{dx} < 0\right)$ causes, due to the « wall condition » $\left(\frac{\partial \tau}{dy}\right)_w = \frac{dp}{dx}$, a deviation

from the straight line in direction to a more convex course of $\frac{u}{u_\infty}\left(\frac{y}{\delta}\right)$. Thus, in the neighbourhood of the wall, there is in this case a reason more for the drawn theoretical course of the wall slope.

Another physical fact that may influence the present consideration must be kept in mind here. Wall cooling at high Mach numbers as applied in the above discussed measurements (and as case of most practical interest) causes a temperature maximum near the wall which in general lies within the laminar sublayer (see the figures 10 through 21). From (12) follows that this maximum $\left(\frac{T}{T_\infty}\right)_{max}$ occurs for $\frac{u}{u_\infty}=\frac{b}{2c}=\frac{\Theta}{2}$ and has the value

$$\left(\frac{T}{T_\infty}\right)_{max}=1+r\frac{K-1}{2}M_\infty^2\left(1-\Theta+\frac{\Theta}{4}\right) \tag{124}$$

In the case of fig. 15 with $M_\infty=8{,}18$, $\Theta=0{,}536$ (ref. [11]), evaluation of (124) yields $\left(\frac{T}{T_\infty}\right)_{max}=7{,}50$ and $\frac{T_w}{T_\infty}=6{,}65$.

Hence, the maximum temperature is about 13 % higher than the wall temperature. The related viscosity then varies within the sublayer about proportionally with the temperature. For stronger cooling, for instance such that holds $T_w=T_\infty\,(\Theta=1)$, as was present in some experiments of ref. [19], the maximum temperature for $M_\infty=5$ is about twice as high as the wall temperature. Now, when constant shearstress is assumed near the wall, the slope $\frac{\partial u}{\partial y}$ within the laminar sublayer varies reverse proportional with the viscosity, and $u\,(y)$ has a turning-point at the location of $T=T_{max}$. The theoretically predicted location of this turning-point is indicated in some figures

By this rough estimation it is evidenced that at strongly cooled walls, a straight-line course of $u\,(y)$ may be a poor approximation and the wall slope obtained from such an approximation may be noticeably wrong.

It is felt that a detailed theory on the laminar sublayer would be helpful in removing the present difficulties, as already suggested by Prof. Kestin.

Figure 22 to 29

Experimental velocity profiles $\frac{u}{u_\infty}(y)$ from the references [11] and [41]. Criticism of wall-slope evaluation $\left(\frac{\partial u}{\partial y}\right)_w$. Thin ful lines: wall-slope recalculated from c_f-value given in [11] and [41] respectively; thin dashed-dotted lines : wall slope calculated from equ. (35), using the values $\delta^*=\delta_1$ and $\theta=\delta_2$ from [11] [41] and evaluating $(\delta_1)_u$ and $(\delta_2)_u$ from $\frac{u}{u_\infty}(y)$. Thick dashed lines : estimated course of $\frac{u}{u_\infty}(y)$ near the wall. ⊕ calculated turning-points in the figures 24, 25, 26.

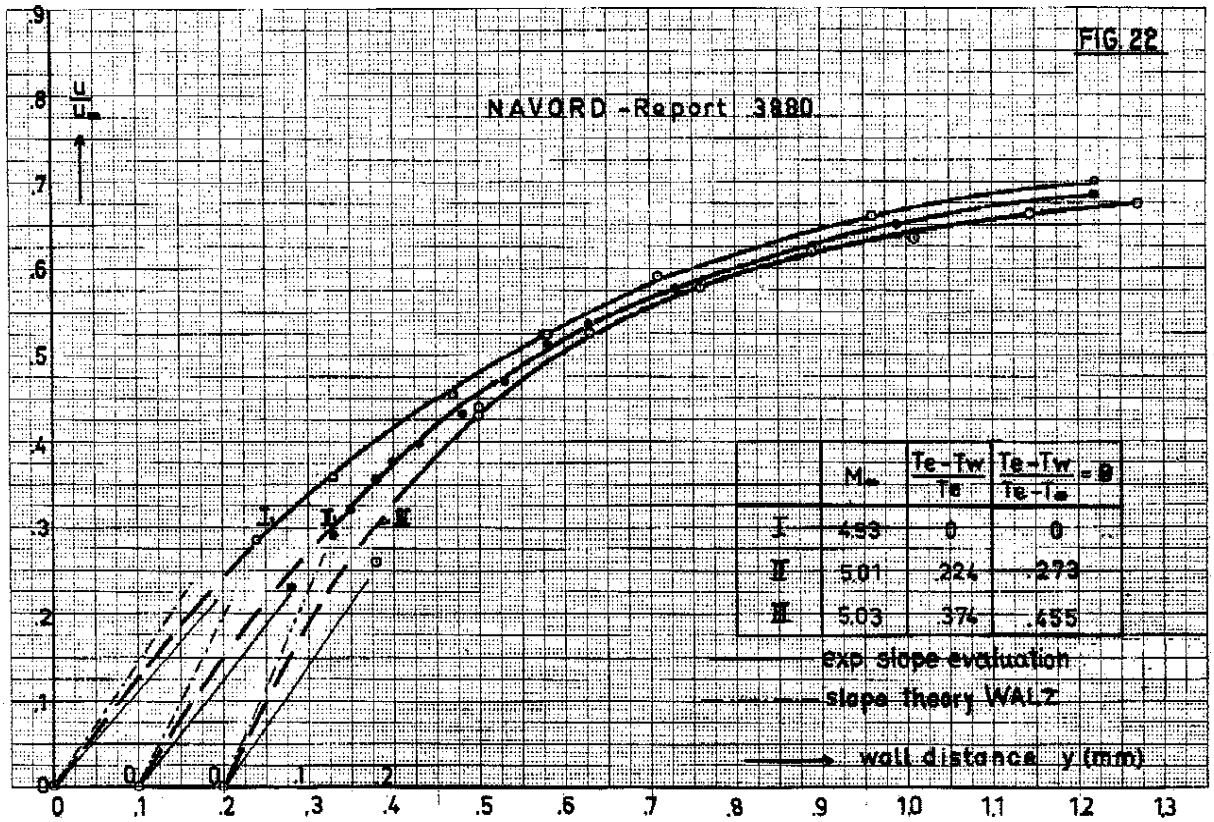

FIGURE 22

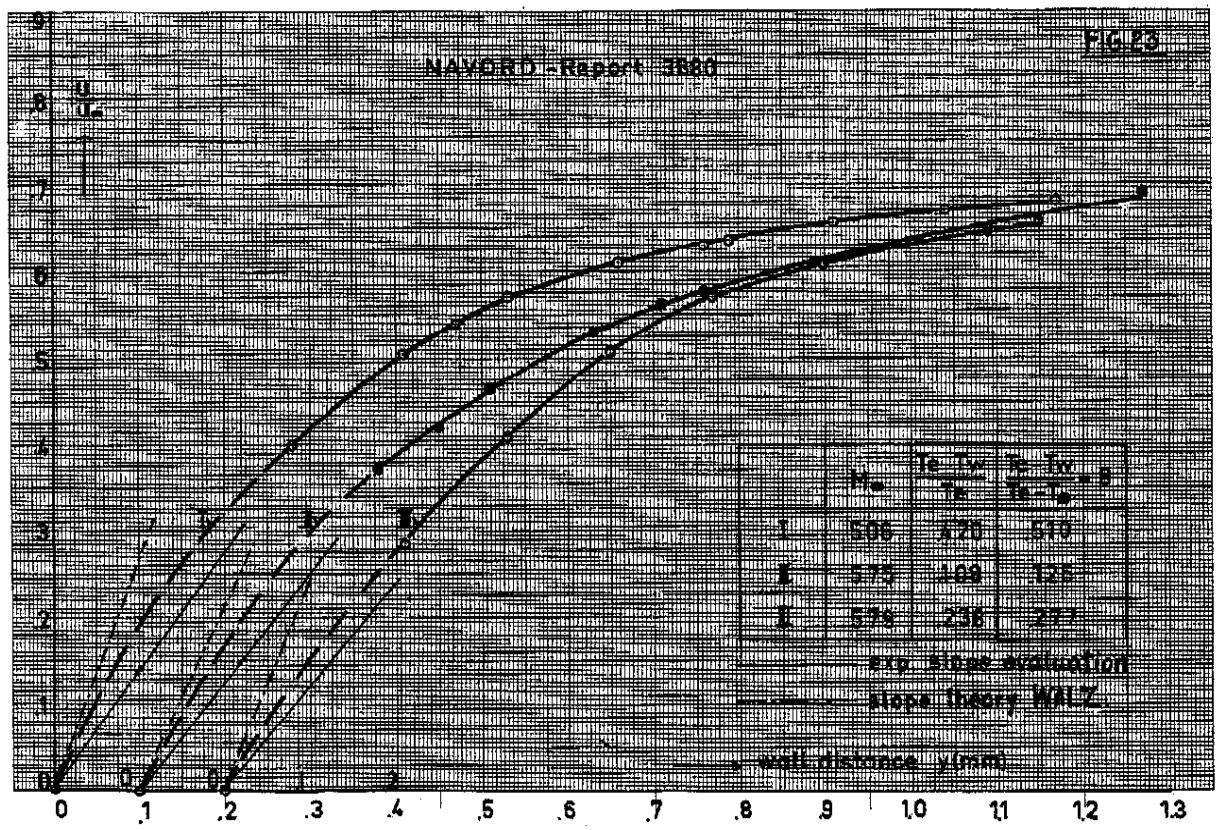

FIGURE 23

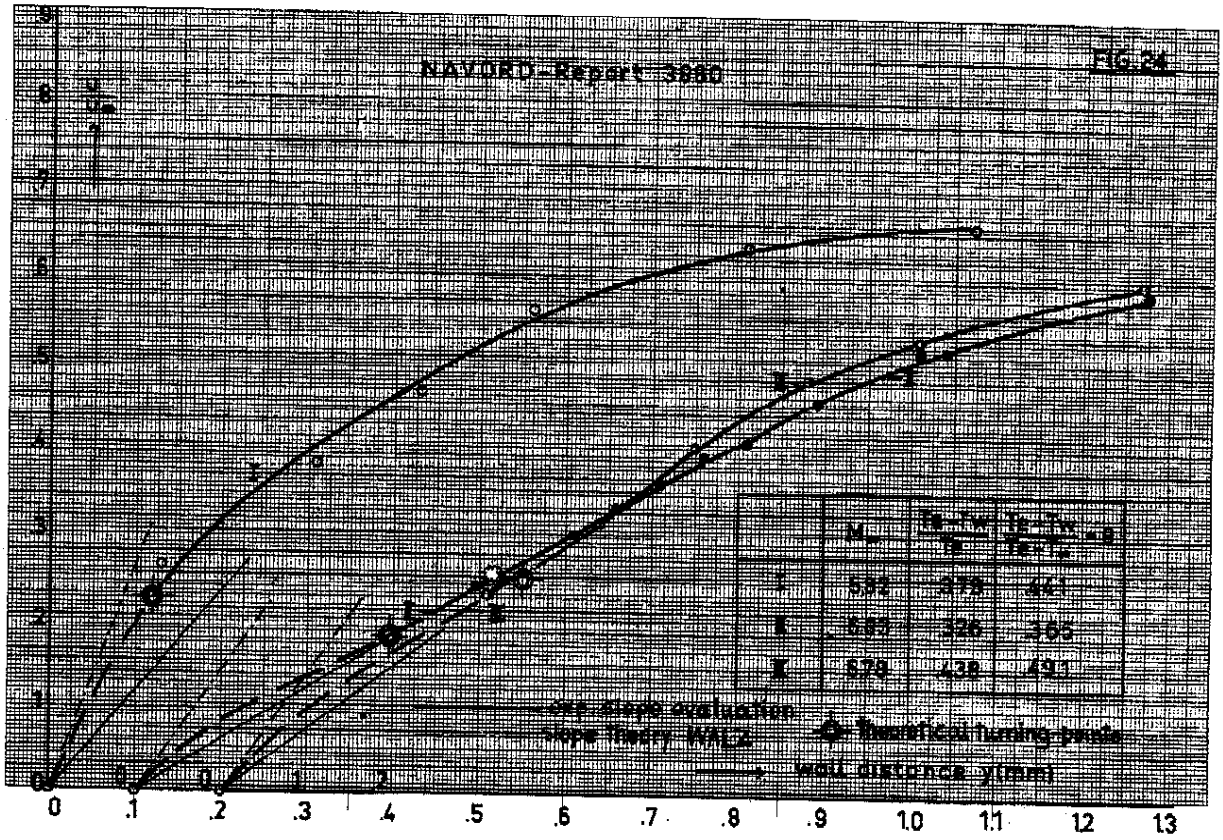

FIGURE 24

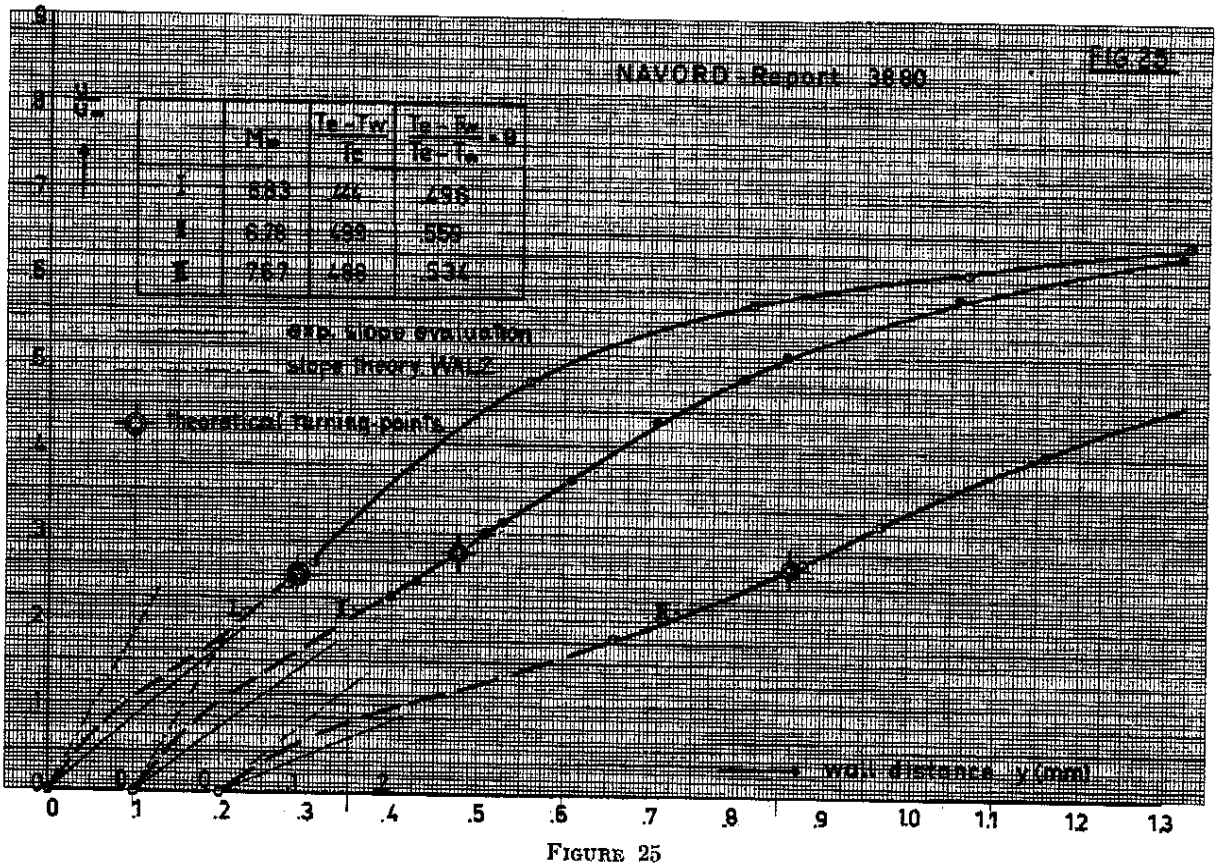

FIGURE 25

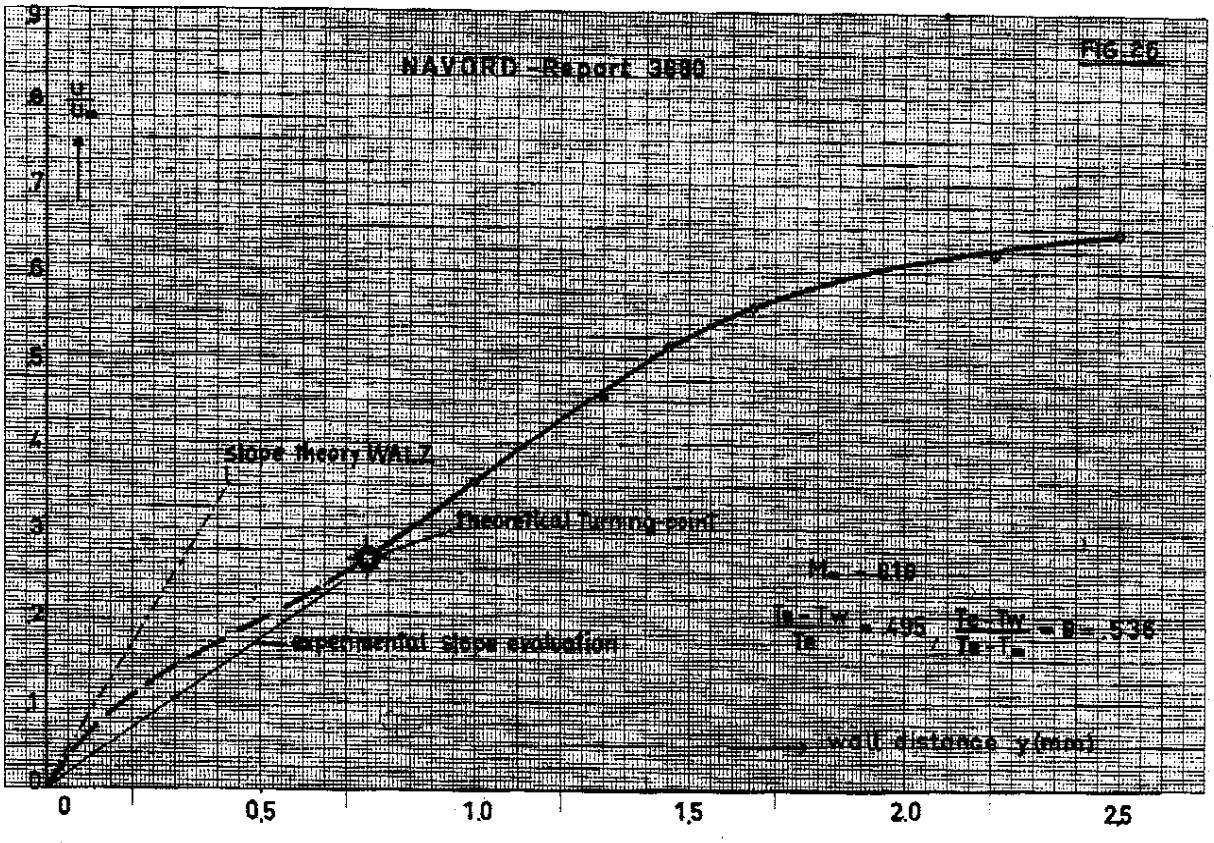

FIGURE 26

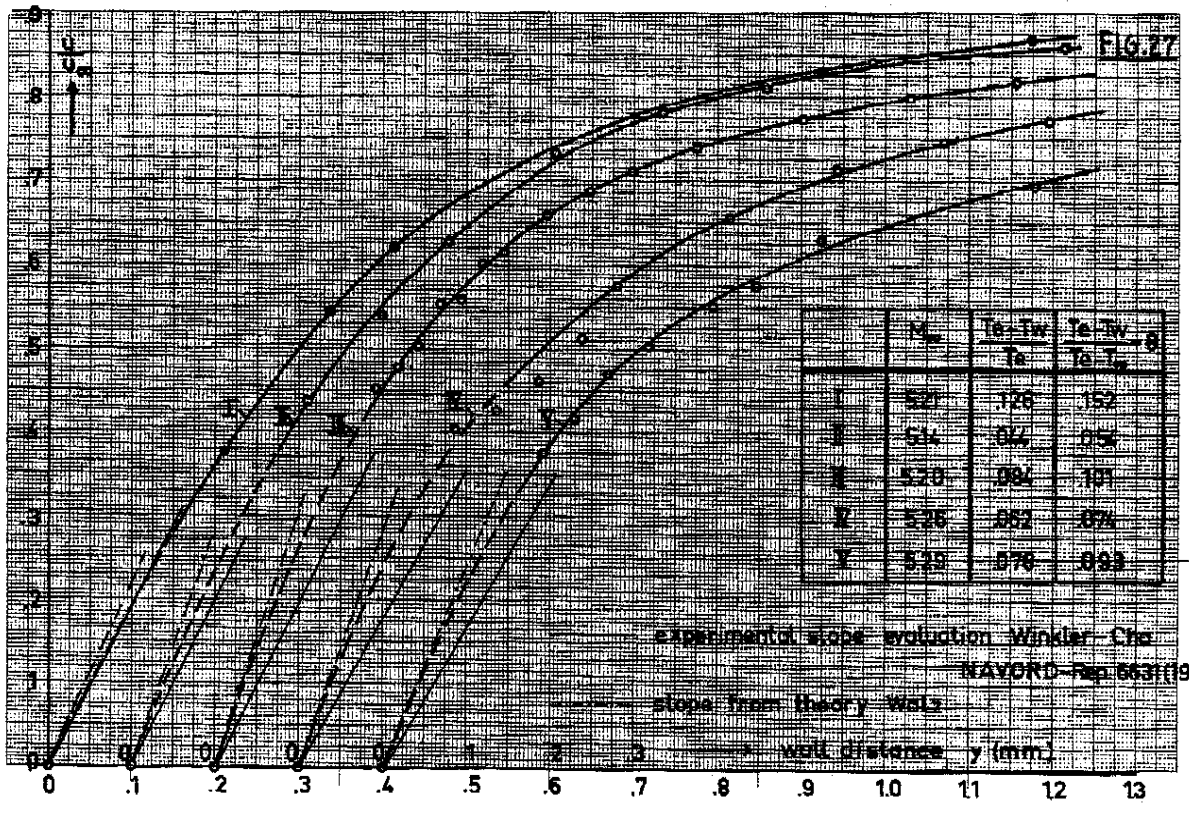

	M_∞	$\frac{T_e - T_w}{T_e}$	$\frac{T_e - T_w}{T_e - T_\infty}$
I	521	.126	.152
II	514	.042	.054
III	520	.094	.101
IV	526	.062	.074
V	519	.076	.093

FIGURE 27

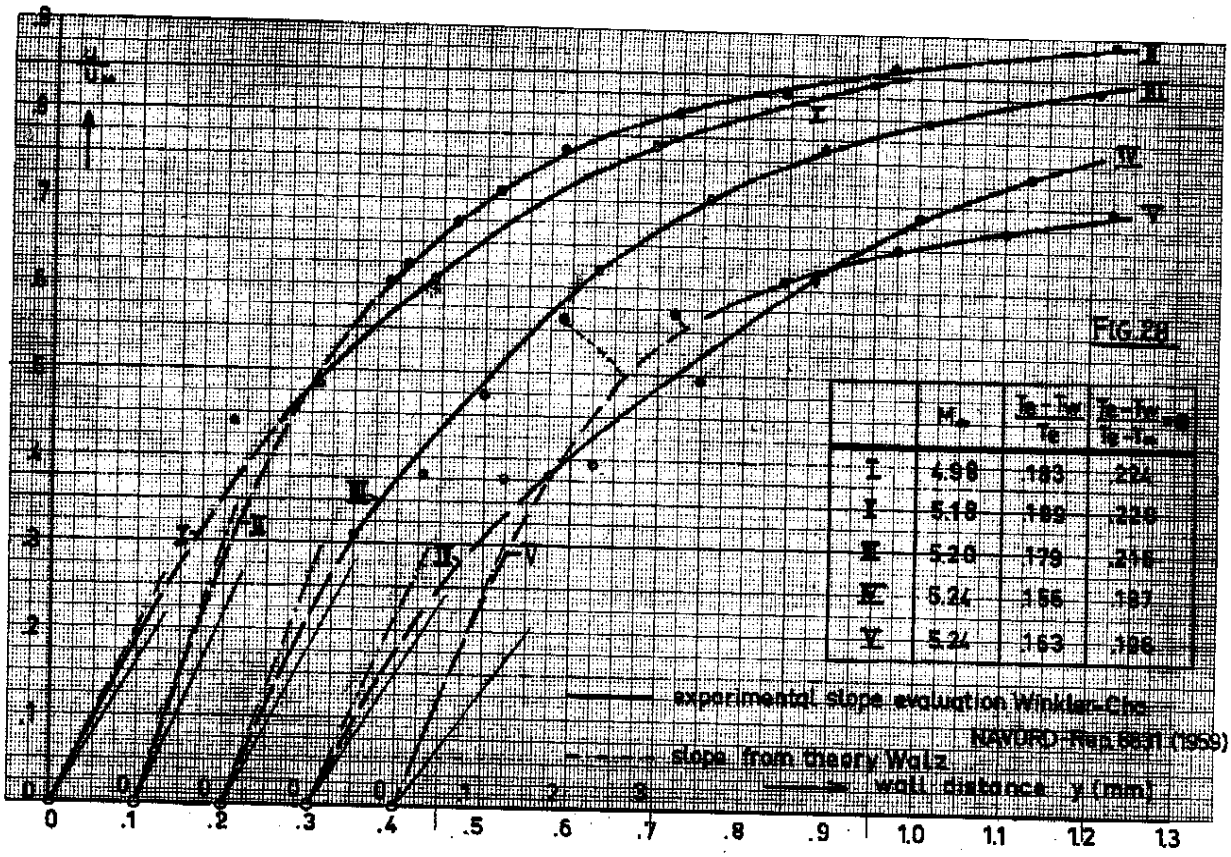

	M_∞	$\frac{T_e - T_w}{T_e}$	$\frac{T_e - T_{w_{ad}}}{T_e - T_\infty}$
I	4.98	.183	.294
II	5.18	.189	.326
III	5.20	.179	.316
IV	5.24	.156	.197
V	5.24	.163	.196

FIGURE 28

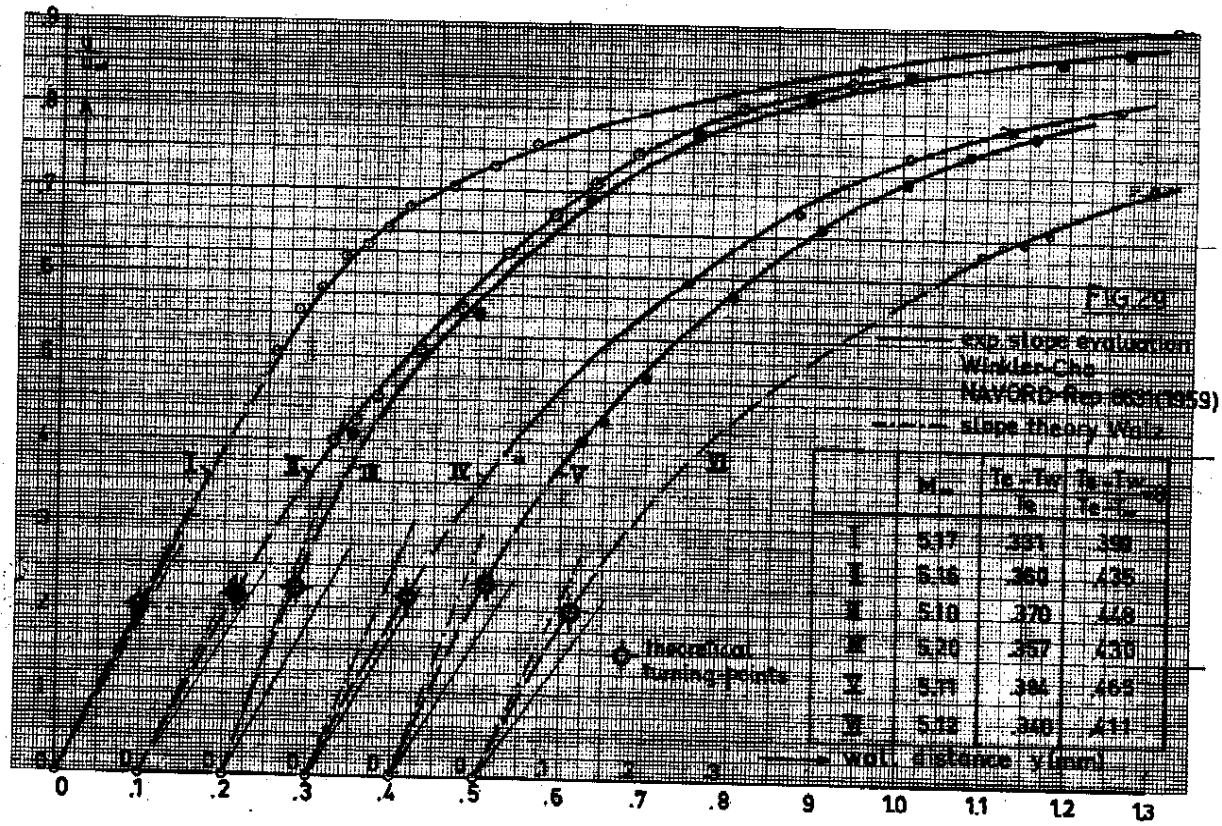

	M_∞	$\frac{T_e - T_w}{T_e}$	$\frac{T_e - T_{w_{ad}}}{T_e - T_\infty}$
I	5.17	.331	.398
II	5.16	.360	.435
III	5.18	.370	.448
IV	5.20	.357	.430
V	5.11	.384	.465
VI	5.12	.340	.411

FIGURE 29

6.4. *Note on the empirical wall-friction law of Winkled and Cha, ref. [41].*

From the foreoing discussion about the slope evaluation from boundary layer surveys, we must conclude that information about the wall friction obtained in this way must be regarded with caution. Nevertheless, a critical review on existing calculation methods for local wall friction data outlined in ref. [41] is noteworthy. WINKLER and CHA find that all known calculation methods are valid each one only in a certain range of Reynolds number, Mach number and/or heat transfer rate. Therefore, a new empirical method of data reduction from compressible flow with heat transfer to incompressible flow is suggested, which gives a fairly good fit of all available measurements, (which, as we now must believe, probably contain more or less systematic errors, when c_f is determined by wall slope evaluation). For incompressible turbulent wall friction coefficients c_{f_i} at a flat plate, the well-known law of SCHULTZ-GRUNON [23] is accepted as most convenient. It writes :

$$c_{f_i} = \frac{0{,}0246}{R_{(\delta_2)_u}^{1/4}}; \qquad R_{(\delta_2)_u} = \frac{\rho_\infty u_\infty (\delta_2)_u}{\mu_\infty} \quad (\mu_w = \mu_\infty) \tag{125) (126}$$

and is consistent with the law of LUDWIEG-TILLMANN [4], equ. (24), when flat plate conditions are introduced.

The values c_f observed in compressible flow with heat transfer then may be related to the values c_{f_i} by the following reduction formula :

$$c_f = c_{f_i} \left(\frac{T_\infty}{T_0} \right)^{1/2} \left(\frac{T_w}{T_r} \right)^{1/4} \tag{127}$$

The usefulness of this reduction formula turns out from fig. 30, which is a reproduction of the related figure in ref. [41].

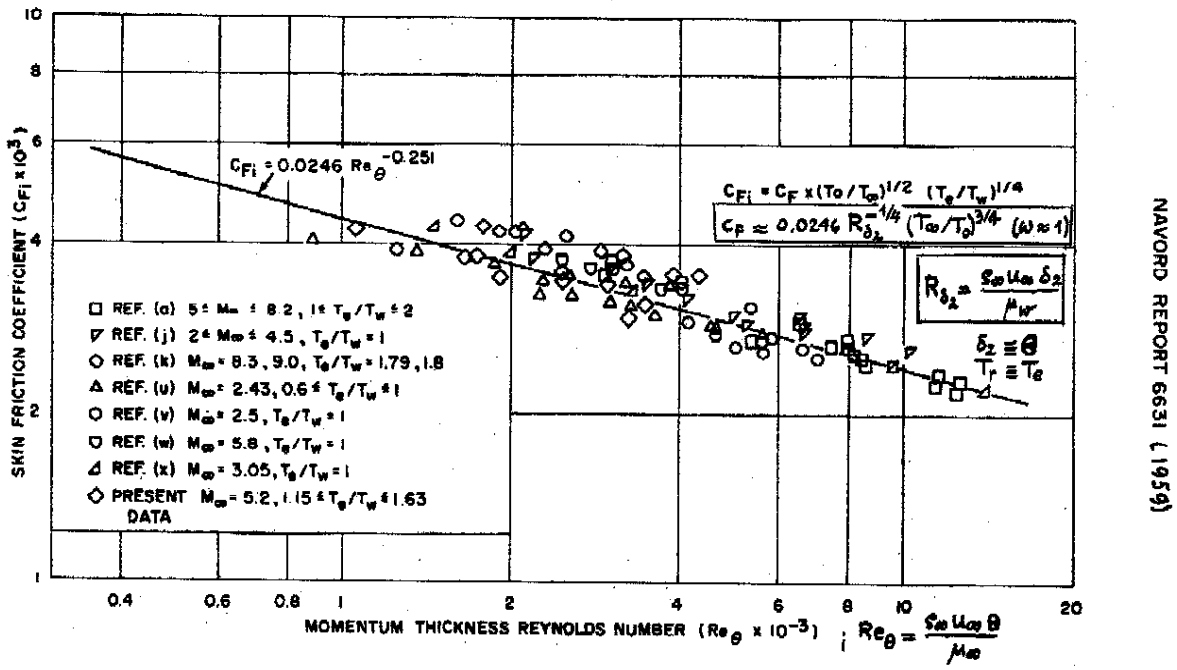

FIGURE 30
The new empiircal law of WINKLER-CHA [41] for the local wall-friction coefficient c_f reproduced from [41] and rewritten in terms of the present theory.

It may be interesting to compare equ. (127) with the generalized wall friction law (35), derived from (24). For this, we must introduce the REYNOLDS number R_{δ_2} defined with (32). In addition we may write :

$$\left(\frac{\mu_r}{\mu_w}\right)^{0,268} \approx \left(\frac{T_r}{T_w}\right)^{0,268\,\omega} \approx \left(\frac{T_r}{T_w}\right)^{1/4}; \qquad 0{,}8 < \omega < 1{,}0 \begin{cases} \text{for hypersonic tunnel experiments of ref. 11, [41], and} \\ \text{others with high wall cooling.} \end{cases} \tag{128}$$

With (125), (128), and (32), equ. (127) may be rewritten as :

$$c_f \approx \frac{0{,}0246}{R_{\delta_2}^{0.251}} \left(\frac{T_\infty}{T_0}\right)^{3/4} \qquad \left(\text{with } \frac{T_\infty}{T_r} \approx \frac{T_\infty}{T_0} \text{ because of } r \approx 0{,}9\right) \tag{129}$$

and

$$\left(\frac{T_\infty}{T_0}\right)^{3/4} = \frac{1}{\left(1 + r\,\frac{\kappa - 1}{2} M_\infty^2\right)^{3/4}} \tag{130}$$

This means that WINKLER and CHA have practically introduced the local REYNOLDS number R_{δ_2}, equ. (32) (indeed, but probably not being aware of), which was suggested by the considerations in chapter 3. The expression (130) may be compared with the analytical expression (90) for $\frac{\delta_2}{(\delta_2)_u}$. The difference between (130) and (90) is that $\frac{\delta_2}{(\delta_2)_u}$ depends also upon the heat transfer parameter Θ and the shape parameter H of the velocity profile, while (130) does not. The latter fact is comprehensible, since the increase of c_f with wall cooling ($\Theta > 0$) was not observed in the boundary layer surveys of [11], [41], and others.

We do not intend to conclude that the empirical relation (129) supports the definition (32) for R_{δ_2}. But it is believed that the relation (129) might be of interest, though not all experimental data fitted by it may be considered to be reliable.

7. Conclusions

Attempts to establish the similarity laws for turbulent boundary layers on the field of compressible flow with heat transfer are hampered by uncertainties, recently discovered in hypersonic boundary layer surveys. The present lack of reliable experimental information on this field stimulates engineering concepts about the behaviour of compressible turbulent boundary layers. Such concepts are supported by reliable direct measurements of gross boundary layer quantities like the averaged or local wall friction forces and integral terms over the velocity distribution. The application of integral conditions for momentum and energy, combined with generalized laws for the wall friction and dissipation (based upon approved laws from the incompressible field) then appear to be a trustworthy way for predicting the behaviour of compressible turbulent boundary layer with heat transfer and streamwise pressure gradient.

In agreement with the consideration of Prof. KESTIN, it is felt that for removing the present difficulties in understanding the discrepancies between experimental results and theoretical or semi-empirical predictions, more interest must be centered on what is happening within the laminar sublayer.

LIST OF SYMBOLS

List of Symbols

Lengths

x	coordinate along the surface
y	coordinate normal to the surface
L	reference length (for instance : length of a flat plate)
δ	total thickness of the boundary layer
δ_1	displacement thickness, equ. (67)
δ_2	momentum-loss thickness, equ. (69)
δ_3	energy-loss thickness, equ. (71)
δ_4	density-loss thickness, equ. (73)
$(\delta_1)_w$, $(\delta_2)_w$, $(\delta_3)_w$, $(\delta_4)_w$, $= 0$	quantities related to the pure velocity profile, equ. (68), (70), (72), 74).
Z	$= \delta_2(R_{\delta_2})^n$ thickness parameter of the two-parameter theory

Velocities

u	x-component of the velocity } time-averaged mean values
u_δ	x-component of the velocity at $y = \delta$ } time-averaged mean values
v	y-component of the velocity } time-averaged mean values
u_∞	free stream velocity
a_δ	sound velocity at local conditions (at $y = \delta$)

Forces

p	static pressure accross the boundary layer ($p_\delta \approx p$)
τ	shear-stress within the boundary layer
τ_w	wall shear-stress

Temperatures

T	temperature within the boudary layer (time averaged mean value)
T_δ	temperature at $y \geqq \delta$
T_w	temperature at $y = 0$
T_0	adiabatic stagnation temperature, equ. (12) for $\frac{u}{u_w} = 0$, $\Theta = 0$, $r = 1$
T_r	recovery temperature, equ. (19)

Medium properties

ϱ	density within the boundary layer (time averaged mean value)
ϱ_δ	density at $y \geqq \delta$
μ	effective viscosity within the boundary layer (= molecular + eddy viscosity)
μ_δ	effective viscosity at $y \geqq \delta$
μ_w	molecular viscosity at $y = 0$
λ	heat conductivity
c_p	specific heat at constant pressure
c_v	specific heat at constant volume
$\varkappa$	$= \frac{c_p}{c_v}$

Dimensionaless quantities

M_δ	$= \frac{u_\delta}{a_\delta}$ local MACH number
Θ	$= \frac{T_r - T_w}{T_r - T_\delta}$ heat transfer parameter

$R_{\delta 2} = \frac{\rho_\delta u_\delta \delta_2}{\mu_w}$ local REYNOLDS number formed with the local momentum-loss thickness δ_2 [equ. (69)], outeredge quantities ρ_δ, u_δ and wall viscosity μ_w

$R_{(\delta 2)u} = (R_{\delta_2})_{M_\delta = 0,\ \Theta = 0}$

$R_{(\delta 2)u} = \frac{\rho_\delta u_\delta (\delta_2)_4}{\mu_\delta}$

R_x REYNOLDS number formed with the flow length x and outeredge quantities

$R_L = \frac{\rho_\delta u_\delta L}{\mu_\delta}$ REYNOLDS number formed with the reference length L and outeredge quantities

$H = (\frac{\delta_3}{\delta_2})_u$ shape parameter of the velocity profile (second parameter, besides Z, the two-parameter theory)

$H_{12} = (\frac{\delta_1}{\delta_2})_u = H_{12}(H)$ other shape parameter of the velocity profile

$c_f = 2 \frac{\tau_w}{\rho_\delta u_\delta^2}$ local wall-friction coefficient

$C_F = \int_0^1 c_f \, d\frac{x}{L}$ averaged friction coefficient

$\alpha(H_{12})$ universal function in the wall friction law of LUDWIEG-TILLMANN, equ. (24)

$\beta(H_{12})$ universal function in the dissipation law of ROTTA-TRUCKENBRODT, equ. (39); $\beta(H_{12}) \approx \beta = 0{,}0056$ suggested by TRUCKENBRODT [25].

Subscripts

0	related to adiabatic stagnation conditions
∞	related to free stream conditions
δ	related to $y = \delta$ (outer edge of the boudary layer)
w	related to $y = 0$
i	related to incompressible case
u	related to the velocity profile

REFERENCES

[1] KOVASZNAY, L.S.G. (1953). Turbulence in supersonic flow. *J. Aero. Sci.*, Vol. 20, No. 10, 657-670.

[2] CHU, B.T. and KOVASZNAY, L.S.G. (1958). Non-linear interactions in a viscous heat-conducting compressible gas. *J. Fluid Mech.*, Vol. 3, 494-514.

[3] MORKOVIN, M.V. (April 1960). *AGARD-Symposium on Boundary layer Research*, London.

[4] WALZ, A. (1956). Näherungstheorie für kompressible turbulente Grenzschichten. *Zeitschr. f. Angew. Math. u. Mech.* (ZAMM), Vol. 36, Sonderheft, 50-56.

[5] COLES, D. (1954). Measurements of turbulent friction on a smooth flat plate in supersonic flow. *J. Aero. Sci.*, Vol. 21, No. 7, 433-448.

[6] HILL, F.K. (1956). Boundary-layer measurements in hypersonic flow. *J. Aero. Sci.*, Vol. 23, No. 1, 35-42.

[7] FENTER, F.W. and STALMACH, C.J.jr (1958). The measurement of turbulent boundary layer shear-stress by means of surface impact-pressure. *J. Aero. Space Sci.*, Vol. 25, 793-94.

[8] MATTING, F.W., CHAPMAN, D.R., NYHOLM, Y.R. and THOMAS, A.G. (1961). *Turbulent skin-friction at high* MACH *numbers and* REYNOLDS *number in air Helium.* NASA TR-R 82.

[9] ROTTA, J. (1959). Uber den Einfluß der MACH-Zahl und des Wärmeübergangs auf das Wandgesetz turbulenter Strömung. *Zeitschr. Flugwiss.*, Vol. 7, No. 9, 264-274.

[10] ROTTA, J. Turbulent boundary layers with heat transfer in compressible flow. AGARD *Symposium on Boundary layer Research*, London 1960 (Rep. 60-62 of AVA Göttingen).

[11] LOBB, R. K., WINKLER, E. M. and PERSH, J. (1955). *Experimental investigation of turbulent boundary layers in hypersonic flow.* NAVORD Rep. 3880, U.S. Naval Ord. Lab. (White Oak, Md.).

[12] LUDWIEG, H. and TILLMANN, W. (1949). Investigations of the wallshearing stress in turbulent boundary layers. NACA TM 1285 (1950). *Transl. of Ing. Arch.*, Vol. 17, 288-299.

[13] VAN DRIEST, E. R., *in* : C. C. LIN (1959). *Turbulent flows and heat transfer*, Sect. F, 379-427, Princeton Univ. Press, New Jersey.

[14] SPENCE, D. A. (1960). Some applications of CROCCO's integral for the turbulent boundary layer. Proc. 1960 Heat Transf. *Fluid Mech. Inst. Stanford Univ.*, 62-76.

[15] PRETSCH, J. (1942). Zur theoretischen Berechnung des Profilwiderstandes. Jahrb. d. deutsch. Luftfahrtforschung I, 61 (1938). *Transl. NACA*, TM 1009.

[16] CROCCO, L. (1941). Sullo strato limite laminare nei gas lungo una lamina plana. *Rend. Math. Univ.*, Roma, V. 2, 138.

[17] RUBESIN, M. W. and JOHNSON, H. A. (1949). A critical review of skin-friction and heat transfer solutions of the laminar boundary layer of a flat plate. *ASME Trans.*, Vol. 71, No. 4.

[18] FISCHER, W. W. and NORRIS, R. H. (1949). Supersonic convective heat transfer correlations from skin-temperature measurements on a V 2 - rocket in flight. *ASME Trans.*, vol. 71, No. 5.

[19] SOMMER, S. C. and SHORT, B. J. (1955). Free-flight measurements of turbulent-boundary-layer skin friction in the presence of severe aerodynamic heating at MACH numbers from 2.8 to 7.0. AMES Aeron. Lab. Moffet Field Calif. *NACA TN* 3391.

[20] PRANDTL, L. (1932). Uber den Reibungswiderstand strömender Luft. *AVA Göttingen* III. Liefg. (1927). Zur turbulenten Strömung in Rohren und längs Platten. *AVA Göttingen* IV. Liefg.

[21] v. KARMAN, Th. and SCHOENHERR, K. E. (1932). Resistance of flat surfaces moving through a fluid. *Trans. Soc. Nav. Arch. and mar. Eng.*, Vol. 40, 279.

[22] PRANDTL, L. and SCHLICHTING, H. (1934). Das Widerstandsgesetz rauher Platten. *Werft, Reederei*, Hafen 1-4.

[23] SCHULTZ-GRUNOW, F. (1941). Neues Widerstandsgesetz für glatte Platten. Luftf.-Forschg., Vol. 17, 239 (1940), Transl. *NACA TM* 986.

[24] ROTTA, J. (1951). 1) Beitrag zur Berechnung turbulenter Grenzschichten. Ing. Arch., Vol. 19, 31-41. Transl. *NACA TM* 1344.
(1952) 2) Schubspannungsverteilung und Energiedissipation bei turbulenten Grenzschichten. *Ing.-Arch.*, Vol. 20, 195-207.

[25] TRUCKENBRODT, E. (1952). Ein Quadraturverfahren zur Berechnung der laminaren und turbulenten Reibungsschicht bei ebener und rotationssymmetrischer Strömung. *Ing.-Arch.*, Vol. 20, 211-228.

[26] GRUSCHWITZ, E. (1931). Die turbulente Reibungsschicht in ebener Strömung bei Druckabfall und-Anstieg. *Ing.-Arch.*, Vol. 2, 321-346.

[27] v. DOENHOFF, A. E. and TETERVIN, N. (1943). Determination of general relations for the behaviour of turbulent boundary layers. *NACA Rep.* 772.

[28] ELSER, K. (1949). *Reibungstemperaturfelder in turbulenten Grenzschichten.* Mittl. a.d. Inst. f. Thermodyn. und Verbr. Mot. ETH Zürich, Ber. Nr. 8, Verlag Leemann, Zürich.

[29] v. KARMAN, Th. (1921). Uber laminare und turbulente Reibung. *ZAMM*, Vol. 1, 233.

[30] WALZ, A. (1960). Beitrag zur Näherungstheorie kompressibler turbulenter Grenzschichten. *Ber. d. Deutsch. Versuchs.-Anstalt f. Luftfahrt* (DVL), Nr. 84 (1959) and Nr. 136 (1960).

[31] STEWARTSON, K. (1949). Correlated incompressible and compressible boundary layers. *Proc. Roy. Soc.*, A, Vol. 200, 84.

[32] CULICK, F. E. C. and HILL, J. A. F. (1958). A turbulent analogue of the STEWARTSON-ILLINGWORTH transformation. *J. Aero Sci.*, Vol. 25, 259-262.

[33] SPENCE, D. A. (1959). The growth compressible turbulent boundary layers on isothermal and adiabatic walls. *Roy. Aircr. Est.* (Farnborough) Rep. No. Aero 2619.

[34] WALZ, A. (1957). Nouvelle méthode approchée de calcul des couches limites laminaires et turbulentes en écoulement compressible. *Publ. Sci. Techn. d. Min. d. l'Air*, No. 309 (1956), No. 336 (1957).

[35] FERNHOLZ, H. H. (1961). Theoretische Untersuchungen zur optimalen Druckumsetzung in Unterschall-Diffusoren. Diss., Lehrstuhl und Inst. f. Strömungslehre und Strömungsmech., *Techn. Hochsch. Karlsruhe.*

[36] CHAPMAN, D. R. and RUBESIN, M. W. (1949). Temperature and velocity profiles in the compressible laminar boundary layer with arbitrary distribution of surface temperature. *J. Aero. Sci.*, Vol. 16, 547-565.

[37] SCHLICHTING, H. (1951). Der Wärmeübergang an einer längs angeströmten Platte mit veränderlicher Wandtemperatur. Forschg. *Ing.-Wesens*, Vol. 17, 1.

[38] DIENEMANN, W. (1951). Berechnung des Wärmeübergangs an laminar umströmten Körpern mit konstanter und ortsveränderlicher Wandtemperatur. *ZAMM*, Vol. 33, 89-109 (1953), Diss. T.H. Braunschweig. *Summary J. Aero. Sci.*, Vol. 18, 64 (1951).

[39] COHEN, N. B. (1959). A method for computing turbulent heat transfer in the presence of streamwise pressure gradient for bodies in high speed flow. *NASA Memo.*, 1-2-59 L.

[40] WIEGHARDT, K. (1948). Ein Energiesatz zur Berechnung laminarer Grenzschichten. *Ing.-Arch.*, Vol. 16, 231-242.

[41] WINKLER, E. M. and CHA (1959). *Investigation of flat plate hypersonic turbulent boundary layers with heat transfer at a MACH number of 5.2.* NAVORD Rep. 6631.

[42] DEISSLER, R. G. and LOEFFLER, Jr. (1959). *Analysis of turbulent flow and heat transfer on a flat plate at high MACH numbers with variable fluid properties.* NASA TR R-17.

[43] KESTIN, J. and RICHARDSON, P. D. *Heat transfer across turbulent incompressible boundary layers.* Lecture presented at the Intern. Coll. on Turbulence 28 Aug.-2 Sept. 1961 at Marseille, France.

[44] ROTTA, J. *Incompressible turbulent boundary layers.* Lecture presented at the Intern. Coll. on Turbulence 28 Aug.-2 Sept. 1961 at Marseille, France.

ACKNOWLEDGMENTS

The author wishs to thank Professors A. FAVRE and H. SCHLICHTING for the invitation to prepare the present survey. Particular gratitude is due to Prof. H. GÖRTLER who sponsored this work in the " DVL-Institut für angewandte Mathematik und Mechanik ", Freiburg i.Br.

Emmendingen, August 7, 1961.

DISCUSSION DE LA COMMUNICATION DU Dr. WALZ

Itiro TANI, University of Tokyo

In Dr. WALZ's treatment [1] of compressible turbulent boundary layer problems, the empirical formulae of wall friction and energy dissipation for incompressible flows are used to obtain the generalized expressions for compressible flows. The dissipation formula for incompressible flows is that put forward by ROTTA [2] and TRUCKENBRODT [3], but the writer has felt some doubt about this formula in that the effect of the form parameter H (ratio of displacement and momentum thicknesses) is unexpectedly small, in marked contrast to the case of laminar boundary layers.

From analysis of a number of existing experimental data, RUBERT and PERSH [4] have obtained a dissipation formula showing the dependence on both REYNOLDS number and H. By assuming LUDWIEG-TILLMANN formula for wall friction and similarity of velocity profiles of the form of velocity defect law, the writer [5] has derived from the momentum and energy integrals the energy dissipation in a closed form, which indicated again the dependence on both REYNOLDS number and H and yielded results agreeing fairly well with those obtained by RUBERT and PERSH. It should be mentioned that the ROTTA-TRUCKENBRODT formula is based primarily on a single experiment of SCHUBAUER and KLEBANOFF [6] and that the wall friction as found in this experiment is known to be too high.

REFERENCES

[1] WALZ, A. : DVL Berichte 84 (1959) und 136 (1960).
[2] ROTTA, J. : Mitt. a. d. Max-Planck Inst. f. Strömungsforschung, 1 (1950).
[3] TRUCKENBRODT, E. : Ing. Arch., **20**, 211 (1952).
[4] RUBERT, K. F. and PERSH, J. : NACA TN 2478 (1951).
[5] TANI, I. : J. Aero Sci., **23**, 606 (1956).
[6] SCHUBAUER, G. B. and KLEBANOFF, P. S. : NACA TR 1030 (1951).

Dr. MICHEL, ONERA, Paris

Je désire seulement faire une remarque concernant l'évolution du coefficient de frottement avec la température de paroi.

Dans les théories c_f croît quand T_p décroît (cooled wall).

Dans les expériences de LOBB-WINKLER-PERSH et WINKLER-CHA Cf décroît quand T_p croît.

Le Dr. WALZ explique cette différence par une mauvaise détermination de la pente à l'origine du profil des vitesses, dans l'expérience.

Je veux faire observer que dans les expériences en question le flux de chaleur a également été mesuré; le résultat est qu'il décroît quand T_p diminue. Le coefficient de frottement augmenterait donc pendant que le coefficient de flux de chaleur diminue, ce qui nous éloigne dangereusement du concept d'analogue de REYNOLDS.

Des expériences ont été effectuées à l'O.N.E.R.A. pour déterminer le coefficient de frottement à partir de l'équation globale des quantités de mouvement. Elles ont comporté l'exploration détaillée de la couche limite sur un cylindre refroidi intérieurement, la détermination de δ_2 et de sa dérivée $\frac{d\delta_2}{dx}$ qui donne le c_f. Le résultat confirme au nombre de Mach 2,6 les résultats des expériences du NOL. Le problème de l'évolution du c_f avec la température de paroi ne nous semble pas encore résolu. Des expériences systématiques semblent encore nécessaires.

Réponse au Dr. WALZ à propos des résultats de mesure de frottement global

— Pour exploiter les mesures de frottement global, il est nécessaire d'estimer une origine fictive de la couche limite et pour cela d'admettre une certaine évolution en faisant appel à une certaine théorie. Or il n'est pas prouvé actuellement que toutes les théories semi-empiriques ne sont pas en défaut dans le cas d'un flux de chaleur à la paroi. Seuls nous semblent utilisables les mesures de frottement local, dont l'exploitation ne peut être effectuée que si la couche limite a pu y être caractérisée d'une façon précise, le seul nombre de Reynolds dont on puisse être sûr étant celui basé sur une épaisseur de la couche limite, comme l'épaisseur de quantité du mouvement.

COMMENTAIRE DE LA SECTION

COUCHES LIMITES TURBULENTES

Professeur Hans W. LIEPMANN, Président

Turbulent boundary layers share with free turbulence the intermittent surface between the turbulent and irrotational fluid. The outer part of the boundary layer thus shows many characteristics of free turbulence. The essential difference between free turbulent and boundary layer flow is the existence of the laminar sublayer in the latter. The sublayer is largely responsible for the dissipation as well as for the production of turbulent energy, and progress in the understanding of turbulent layers will depend to a large measure on future work on the sublayer. A promising beginning in sublayer work has been made.

Semi-empirical theories are successful in dealing with the overall behavior of turbulent boundary layers and appear to be sufficient for most problems of engineering interest except separation. Even in these semi-empirical approaches it is important to recognize the double structure of the flow in the layer. Attempts to extend the phenomenological theories without new physical ideas are valuable only if the result is a simplification of formalism and a clearer demonstration of the assumptions and limitations.

Experiments and theory show that compressibility effects in the turbulent boundary layers up to Mach numbers of the order of ten are due mainly to the temperature dependence of density, viscosity and heat conductivity. Compressible and incompressible boundary layers are thus qualitatively similar and it seems possible to relate the characteristics of high speed boundary layers to a corresponding one in incompressible flow. The energy in the acoustic radiation from the layer is too small to contribute markedly to the turbulent energy balance. Eventually, i.e. at a sufficiently high Mach number of the flow, acoustic radiation must become an essential feature of the turbulence of the layer and qualitatively different conditions will occur.

Here as in all other phases of turbulence research there exists a need for much more experimentation. However, anybody who intends to embark on experiments must recognize the difficulties involved. Experience has shown that it is by no means easy even to establish a well-defined turbulent boundary layer, in particular in an adverse pressure gradient. Experience has also shown that quick — hit and run — experiments under badly controlled conditions are worse than useless.

In an attempt to list a few more definite problems for future work one must recognize that practically all problems of free turbulent flow are present in the turbulent boundary layer and hence the list of free turbulent problems applies here as well. In addition the following may be mentioned :

a) Space-time correlation measurements of wall pressure fluctuations and of the velocity fluctuations within the layer have shown a characteristic propagation velocity of about 80 per cent of the free stream velocity. This characteristic velocity which is definitely associated with the motion of large eddies should be obtainable from a stability theory of the turbulent layer. Experiments with controlled disturbances appear very promising here.

b) Measurements of sublayer flow at high Reynolds number are possibly the single most important field for experimental work in turbulent boundary layers. The difficulties are obvious and a great deal of ingenuity is required to find suitable installation and measuring setups. At least a working hypothesis on sublayer flow has now been developed, and this should help very much in formulating experiments.

c) Most spectacular but of less immediate importance would be the demonstration of turbulent boundary layers with acoustic radiation sufficient to alter the energy balance. The question of the existence of truly supersonic turbulence is after all still open.